2017

Thermochemical conversion of organic and plastic waste materials through pyrolysis

Yuan Xue
Iowa State University

Thermochemical conversion of organic and plastic waste materials through pyrolysis

by

Yuan Xue

A dissertation submitted to the graduate faculty

in partial fulfillment of the requirements for the degree of

DOCTOR OF PHILOSOPHY

Co-Majors: Mechanical Engineering, and Biorenewable Resources and Technology

Program of Study Committee:
Xianglan Bai, Major Professor
Robert C. Brown
Atul G. Kelkar
Javier Vela-Becerra
Wenzhen Li

The student author, whose presentation of the scholarship herein was approved by the program of study committee, is solely responsible for the content of this dissertation. The Graduate College will ensure this dissertation is globally accessible and will not permit alterations after a degree is conferred.

Iowa State University

Ames, Iowa

2017

DEDICATION

The dissertation is dedicated to my family and many friends. My first and special feeling of gratitude to my parents, Hong Xue and Weifang Wang. Although we are mostly ten thousand miles away for the last four years, their words of wisdom and continuous encouragement are always in accompany with me during my hardest time and inspiring me to do my best.

The dissertation is also dedicated to my aunt, Xin Huang. Her excellence and persistence for perusing knowledge set an example for me to be a good researcher.

I also dedicate this dissertation to many friends and colleagues who have supported me during my PhD study. I will always appreciate all they have done.

TABLE OF CONTENTS

NOMENCLATURE

HDPE	High Density Polyethylene
PBM	Plastic-Biomass Mixture
HHV	Higher Heating Value
BET	Brunauer–Emmett–Teller
MSW	Municipal Solid Waste
WTE	Waste-To-Energy
ESP	Electro Static Precipitator
MW	Molecular Weight
NCG	Non-Condensable Gas
GC	Gas Chromatogram
EPA	Environmental Protection Agency
TGA	ThermoGravimetric Analysis
DSC	Differential Scanning Calorimetry
MAN	Modified Acid Number
MSD	Mass-Spectrometer Detector
FID	Flame Ion Detector
TCD	Thermal Conductivity Detector
FT-TR	Fourier Transform Infrared spectroscopy
SF	Stage Fraction
PE	Polyethylene
PP	Polypropylene

PS	Polystyrene
PET	Polyethylene Terephthalate
FCC	Fluid Catalytic Cracking
PAH	Polyaromatic Hydrocarbon
SEM	Scanning Electron Microscopy
AAEM	Alkali and Alkaline Earth Metal
CFP	Catalytic Fast Pyrolysis

ACKNOWLEDGMENTS

I would like to express my deepest gratitude to my major professor, Dr. Xianglan Bai, for the opportunities, guidance, mentorship, wisdom, and patience. Dr. Bai's curiosity and unstoppable pursuit for science always remind me what an excellent researcher should be like.

I would also like to thank my graduate committee members, Dr. Robert C. Brown, Dr. Atul Kelkar, Dr. Wenzhen Li and Dr. Javier Vela for their insightful discussions about research projects and valuable feedback provided during my qualifiers and preliminary exams to complete this work.

Special thanks to the Postdocs in Dr. Xianglan Bai's groups, Dr. Shuai Zhou and Dr. Ashokkumar Sharma for showing me the quality to be an efficient researcher, at the same time maintaining a good life-work balance. Thanks to the groups of Dr. Robert C. Brown, Dr. Mark Wright and Dr. Hui Hu for providing dynamic and excellent research environment helping my research career to thrive.

I am grateful to Iowa Energy Center (IEC), ExxonMobil and National Science Foundation (NSF) for their generous funding of my research projects. I am also thankful for all the discussions and feedback through the process of completing these meaningful projects.

I am very thankful for all the instruction, help, guidance and discussions with staff at the Bioeconomy Institute (BEI). Ryan Smith's management, Dr. Patrick Johnston's technology expertise, Dr. Marjorie Rover's consideration for maintaining a clean and safe research environment. I would also like to thank other BEI staff members, Lysle Whitmer, Patrick Hall, Preston Gable for all their help and guidance during my research career.

I would also like to thank the staff and faculty at Iowa State University who have offered me abundant resources throughout my PhD study. Particularly, the Directors of Graduate Education from both the Mechanical Engineering and Biorenewable Resources and Technology Program, Dr. Abhijit Chandra and Dr. Jackie Baughman. The staffs in the Department of Mechanical Engineering and Bioeconomy Institute have always been nice and warm to help on many occasions.

I would like to thank Dr. Mirka Deza, Dr. Xianglan Bai, and Dr. Joseph Schafer for the opportunity to assist with teaching of ME 231 Thermodynamics and EM 378 Fluid Mechanics. It was a pleasure for me to work with and learn to be an instructor from them.

I am grateful to all of my colleagues at BEI for all of the valuable discussions and help with completion of projects. When I came to BEI at 2013, I was fortunate to meet with many talented senior members, including Yanan Zhang, Kwang Ho Kim, Matthew Kieffer, Kaige Wang, Karl Broer, who have helped to lay the foundation of my early research. Special thanks to Tannon Daugaard for his teaching me the safety rules and instruction of running different reactors in the BEI lab. It is precious experience for me to meet and work during my time at BEI with Dr. Qi Dang, Dr. Fenglei Qi, Dr. Longwen Ou, Dr. Xuefei Zhao, Dr. Juan Proano, Wangda Qu, Yiwei Gao, Joel Braden, Wenqin Li, Wenqi Li, Arpa Ghosh, Ross Mazur.

My PhD could not have been achieved without the help from many talented and hardworking undergraduate research assistants. I would like to thank the help from Kyle Steen, Cyrus Lund, Dakota Even, Mitch Amundson, Benjamin Deininger, Nate Hamlett, Shaocheng Luan, Chaoyue Huang, Issac Lai, Xiangwei Niu, Junkai Wang.

The collaborations with many groups in and out of Iowa State University have boosted my learning process of different research fields, including Dr. Catie Brewer and Feng Cheng, Dr. Zhiyou Wen and Haoqin Zhou, Dr. Brent Shanks and Jiajie Huo, Dr. Laura Jarboe and Kirsten Davis, Dr. Jean-Philippe Tessonnier and Thomas Hoff.

I would also like to greatly thank all my family and friends. I am proud of and grateful to my parents. Their wisdom about life and work have helped me shape the work ethic and lead a meaningful life. The loving words from my grandmother, are always giving peacefulness when I feel homesick.

Lastly, I would like to thank Jonathan Lee for his never-fade away song “Shan Qiu (Mountains)”. “The life is like climbing mountains------fighting and growing up alone.”

ABSTRACT

Co-pyrolysis of biomass with plastic is a promising pathway to produce pyrolysis oil with improved quantity and quality. The technology can also provide guidance for processing Municipal Solid Waste consisting of plastic and organic wastes. However, the reaction pathway and chemistry behind co-pyrolysis of biomass and plastics are very complex and unclear. Research in this dissertation focuses on unravelling the cross-reactions between biomass and plastics during co-pyrolysis, and enhancement of these reaction for optimizing the yields of valuable chemicals and hydrocarbons.

First, co-pyrolysis of high density polyethylene and red oak was conducted in a bench-scale continuous fluidized bed reactor. Problems encountered previously including reactor clogging and defluidization were overcome by increasing the pyrolysis temperature over 525 °C. It was found that pyrolysis oil from co-pyrolysis had a significantly higher HHV compared to that from red oak pyrolysis. Synergetic effects were observed in terms of increased yields of furan, acids from read oak, and inhibited char yield.

Second, the co-conversions of polyethylene and cellulose, xylan, lignin were studied in a tandem micro-pyrolyzer. When co-pyolyzed with PE, cellulose and xylan were found to produce more anhydrosugars and light oxygenated compounds, and lignin with higher yield of phenolic monomers. Biomass also facilitated the depolymerization of polyethylene by increasing smaller hydrocarbon molecules. By changing the pyrolysis and catalyst bed temperatures, it was found both thermal synergy and catalytic synergy contribute to the synergetic effects between biomass and polyethylene.

Third, acid pretreated corn stover and polyethylene were co-pyrolyzed to investigate the possibility of boosting the quality of pyrolysis products through synergistic effects. It was discovered that acid infusion strongly catalyzes the cross-reaction between corn stover and polyethylene to improve the sugar yields (during non-catalytic pyrolysis) and hydrocarbon yields (during catalytic pyrolysis) due to enhanced hydrogen transfer from the plastic to biomass. Co-pyrolysis of the acid infused corn stover and polyethylene also demonstrated a potential for overcoming char agglomeration associated with pyrolysis of the acid infused corn stover.

Lastly, a systematic investigation of how carrier gases and feedstock-catalyst contact mode affecting the pyrolysis of different plastics was conducted. The product distribution from catalytic pyrolysis of plastics were highly dependent on the arrangements of feedstock and catalyst (*in-situ* VS. *ex-situ*). Pyrolysis of hydrogen deficient plastics (PS and PET) benefited from hydrogen as carrier gas in terms of reduced solid residue and increased selectivity of mono-ring aromatic.

CHAPTER I

GENERAL INTRODUCTION

Introduction

The concerns about energy supply, national security and environmental problems have drawn people's attention away from petroleum to renewable energy, such as solar, wind and biorenewable resources. Due to its abundance, sustainability and carbon-neutral emission, biomass has gained tremendous attention from the society. According to the Renewable Fuel Standard 2 (RFS 2), renewable fuels should reach 36 billion gallons in US at 2022, which has driven the production of cellulosic ethanol through biochemical pathway in recent years.

Thermochemical conversion of biomass consists of several pathways including gasification, pyrolysis, hydrothermal process and hydrolysis into sugars [1]. Pyrolysis is the thermal depolymerization process of biomass in the absence of air or inert condition at moderate temperatures. Among several thermochemical pathways, pyrolysis stands out since it can convert biomass into energy-dense liquid which is known as bio-oil and easy to transport. Together with the liquid products, char as well as non-condensable gases containing carbon oxides and light hydrocarbons are also produced from the process. Due to the high oxygen content presenting in biomass, the bio-oil are facing the problems of high moisture content, oxygenated compounds, viscosity and acidity, which exerts technical challenges for bio-oil's upgrading into drop-in fuel. To remove the oxygen in bio-oil, hydropyrolysis of biomass and hydro-upgrading of bio-oil are widely studied [2-6]. Recently, Marker et al. [7, 8] achieved an Integrated Hydropyrolysis and Hydroconversion (IH2) of biomass to directly produce gasoline and diesel. In addition to hydrodeoxygenation process, some acid catalysts are very effective for oxygen removal during catalytic pyrolysis of

biomass through introducing acid-catalyzed dehydration, decarboxylation and decarbonylation to produce aromatics hydrocarbons and light olefins [9]. Huber et al. [10-13] conducted a series of biomass conversion with zeolite, which is one of the most common used catalysts in petroleum industry, and found that HZSM-5 zeolite gives the best performance in terms of hydrocarbon production. However, the catalytic pyrolysis process still suffers from the heavy coke deposition and following catalyst deactivation due to biomass low $(H/C)_{eff}$ ratio.

Plastics wastes, which is a cheap hydrogen resource, are abundantly available in Municipal Solid Waste (MSW) and Municipal Plastic Wastes (MPW). Most plastics have higher $(H/C)_{eff}$ ratios than biomass does. Thus, co-pyrolysis and catalytic co-pyrolysis of biomass and plastics are considered as a potentially promising choice for producing liquid pyrolysis products with improved qualities. In addition, biomass-based organic wastes also present in MSW, which are comingled with plastic wastes. Separation of plastic waste and organic wastes in MSW is highly labor-intense work, which is almost impossible to achieve. Thus, understanding of co-pyrolysis of biomass and plastics could also be beneficial in utilizing MSW for energy products.. Many studies have focused on the co-pyrolysis of biomass, or biomass components with polyethylene or polypropylene. However, the conclusions from these studies are often quite controversial to each other. Several researchers reported that the co-pyrolysis can not only enhance the yield of liquid products, but also improve the carbon and hydrogen contents of it. These improved qualities are thought to be attributed to the hydrogen transfer from the plastic to biomass [14]. On the other hand, it was also observed that the yield of solid from co-pyrolysis was higher than that from independent pyrolysis of biomass or plastic with a decrease of liquid products at the same time [15].

Based on the types of products (gases, liquid, solid), different physicochemical properties are applied for analysis. For gases products, heating value is the mostly used. For liquid products, heating value, elemental composition, viscosity, acidity, moisture, and density are often mentioned. Properties, such as surface area, elemental composition and heating value, are used for solid products analysis.

Several types of reactors have been used to investigate the co-pyrolysis of biomass and plastics. Batch or semi batch reactors, including autoclave [16], self-designed glass reactor [17], packed-bed reactor [15] are quite often used to investigate the slow co-pyrolysis. Micro-pyrolyzer-GC/MS [18] is the only batch type reactor can achieve fast co-pyrolysis due to its small heat capacity. Continuous reactor, such as auger reactor [19] and fluidized bed reactor [20], are also chosen to study the synergy between biomass and plastics.

Literature Review

Heating rate of pyrolysis and whether the catalyst is used are two important criteria to categorize studies on co-pyrolysis of biomass and plastics. Thus the literature review is carried out following the two criteria. To evaluate the synergetic effects between biomass/biomass components and plastic polymers, one simple way is to compare the experiment yield and additive (calculated, theoretical) yield of specific products. Assuming that there is no synergetic effects between biomass and plastics, the additive (also denoted as expected, calculated, theoretical, predicted in other studies) yield of products is calculated by summing up the yield when biomass or plastic is individually converted. If the experiment yield of specific product is higher than the corresponding additive yield, this product is promoted due to the synergetic effects.

Non catalytic slow pyrolysis

Back to 2002, Sharypov et al. [16, 21, 22] conducted a series of studies for co-pyrolysis of biomass and plastics within a pressurized autoclave. The feedstock used were beech wood, pine wood, cellulose, hydrolytic lignin and medium density polyethylene, atactic polypropylene, isotactic polypropylene. The synergy between beech wood/cellulose and atactic polypropylene

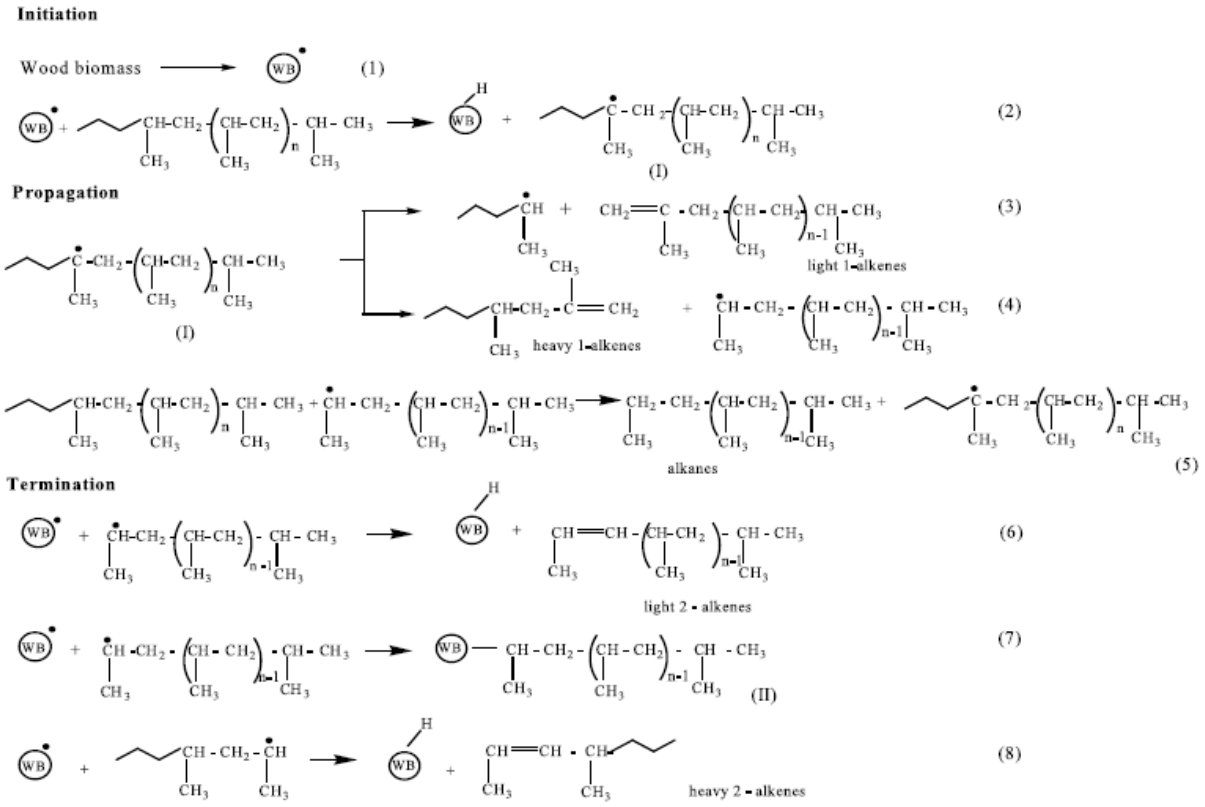

Figure 1. Reaction mechanism for slow co-pyrolysis of biomass and PP [22]

was the most prominent in terms of high light liquid yield when the mixing ratio of biomass and PP was 1:4. Most biomass components decomposed below 400 °C, while polypropylene decomposed above 400 °C. It thus indicated that the solid from biomass pyrolysis, which still contains oxygenated functionalities, could donate radicals to promote the hemolytic scission

of polyolefin chain. The degradation of polymer chain consists of three steps including initiation, propagation and termination. In the initiation step for polymer degradation, the chain scission could start with biomass derived radicals, in addition to self-generated radical. In the termination step, the biomass derived free radicals could be stabilized by grabbing hydrogen from the polymers.

Brebu et tal. [17] investigated a slow co-pyrolysis of pine cone with different synthetic polymers. Compared to the theoretical sum of product yield, adding PE, PP or PS to pine cone could largely increase the gas and liquid yield, and reduce char yield. As found by previous researches, if reactive compounds from biomass pyrolysis was not transported from reaction zone immediately after formation, they could further undergo secondary reaction, which include dehydration, repolymerization, recondensation reactions, to form char, light gas and water [23, 24]. With hydrogen from plastic, the secondary reaction leading to char could be inhibited. It was observed that in the liquid product, the amount of nC_5–nC_{15} compounds is smaller and that of the compounds above nC_{16}–nC_{18} is higher in the co-pyrolysis oils compared to the theoretical values, which could result from the biomass-derived radicals joining in the polymer radical terminations. Same test conditions were also applied to co-pyrolysis of lignin and PE, PP, PS, PC (polycarbonate) [25]. In the co-pyrolysis of PE, PP and lignin, it was found that the experimental yield of nC_7-nC_{10} hydrocarbons higher than calculated yield while that of nC_{11}-nC_{16} lower. Since abundant reactive radicals could be produced from lignin pyrolysis, the scission of PE and PP polymer chain is highly enhanced with these radicals. The interactions between lignin and PS/PC includes reactions with aromatic structure in PS and PC that interfere with degradation of oxygen-containing functional groups bonded to the aromatic structure in lignin. Specially, new polyaromatics

compounds were found with the co-pyrolysis of lignin and PS. Overall, the free radicals from biomass can be stabilized with hydrogen atoms from polymers. The cracking of polymers is highly dependent on which step of polymer degradation the biomass-derived free radicals participate in. If more radicals are involved in the initiation step rather than the termination step, the cracking of polymer chain could be improved.

By carefully quantifying chemicals from co-pyrolysis of polyethylene and beech wood in a tube reactor [26], it was found that the addition of PE into beech wood pyrolysis showed negligible effects on primary reaction, but inhibited the secondary reaction to produce char and light gases. With H-abstraction from PE in the vapor phase, the production of levoglucosan and methoxyphenols with unsaturated alkyl side chain from beech wood increased. However, the cracking of PE into lower molecular weight compounds is hindered due to the combination of PE radicals and hydrogen radicals from biomass char.

Except for common feedstocks/reactants mentioned above, materials including tyre and paper wastes are also gaining research interests for co-pyrolysis. Cao et al. [27] and Martínez et al. [19] conducted co-pyrolyzed waste tyres and biomass, and both reported synergistic effects. Interestingly, the evidenced positive synergistic effects between waste tyre and biomass is stronger in a continuous auger reactor than fixed bed reactor. Besides, the additives in waste tyre, possible Calcium Oxide, may promote the dehydration reaction of biomass, thus promoting the water formation during co-pyrolysis [19]. Waste paper containing mostly cellulose is one of the major components in MSW [28, 29]. Waste papers and plastics are always co-mingled in MSW, separation of which is almost impossible considering the high cost of this labor intensive work. According to Chen et al. [30], the co-pyrolysis of waste newspaper and HDPE generates higher yield of liquid and lower yields of

gas and solid, compared to their corresponding theoretical yields. The liquid product exhibits improved qualities as lower moisture, density, viscosity and higher pH, heating value. Chemical composition analysis of liquid product reveals that the synergistic effect were related to the quantity change of compounds in co-pyrolysis oil rather new chemical generated from cross reaction between waste paper and HDPE.

Generally, there exists a best mixing ratio of plastic and biomass to maximize the liquid production during co-pyrolysis. Increasing the plastic percentage in the mixture will increase the reaction time to fully pyrolyze biomass and plastics due to the high bond energy of plastic [31].

Although most aforementioned studies reported positive synergistic effects between biomass and plastics, some negative effects are also found. In a study conducting a slow co-pyrolysis of polystyrene and cellulose [32], the synergetic effects result in higher yields of solid and gases, and lower yield of liquid. However, the physical properties of the liquid products were improved in terms of lower density, moisture and acidity. Similar phenomenon was also observed in Meng's work [15]. Regular pyrolysis of PS and PP generally leaves no solid residue as final products, the co-pyrolysis solid products could be only from biomass side. Although most plastic decomposes in a higher temperature range than biomass does, their melting temperature is below 300 °C, which overlaps with the decomposition temperature range of biomass. It is probable the biomass particles either stick to or is enclosed by melting plastic, which suppresses the transport of pyrolysis vapors out of reaction zone. This limited mass transfer increases the possibility of secondary reaction including dehydration, decarboxylation, decarbonylation and repolymerization, resulting in the production of solid and light gas at the expense of liquid products. Thus, increasing the

mass transfer and product transport during co-pyrolysis of biomass and plastic could potentially minimize the negative synergistic effects.

Non catalytic fast pyrolysis

As summarized above, most co-pyrolysis work were conducted with slow rather than fast heating rate in which the cross-reactions between biomass and plastic could be totally different. Fast pyrolysis is preferred for biomass to maximize the liquid product yield since secondary reaction of products into light gases and char could be largely avoided due to the fast heating rate. To maximize the yield of hydrocarbons products with similar carbon number as gasoline and diesel, slow pyrolysis is preferred for deep cracking of the polymer chain in plastics. Otherwise, wax with high carbon number but low volatility and octane number could be obtained. In addition to the decomposition kinetics difference, another obvious difference between biomass and plastic pyrolysis is that plastics melt before decomposition, which is not observed for biomass pyrolysis except lignin.

Ojha and Vinu [18] studied the fast co-pyrolysis of cellulose and polypropylene with a pyroprobe 5200 micro-pyrolyzer. Different from slow pyrolysis, the experimental char yield from fast pyrolysis is higher than additive (theoretical) yield. This contrasting results were attributed to the reaction between PP derived hydrocarbon vapors with cellulose char to produce condensed ring aromatic compounds which are later retained together with char as solid residues. Another interesting observation, which is rarely reported before, is that alcohols covering a carbon number from C_8 to C_{20} were abundantly found in co-pyrolysis of PP and cellulose, with a corresponding decrease of anhydrosugars and ketones from cellulose. The observation indicates a hydroxyl groups abstraction by PP from cellulose derived

oxygenates. The hydroxyl groups not only combined with PP to form alcohols, but also catalyzes the cyclization of linear hydrocarbons to form cyclization products.

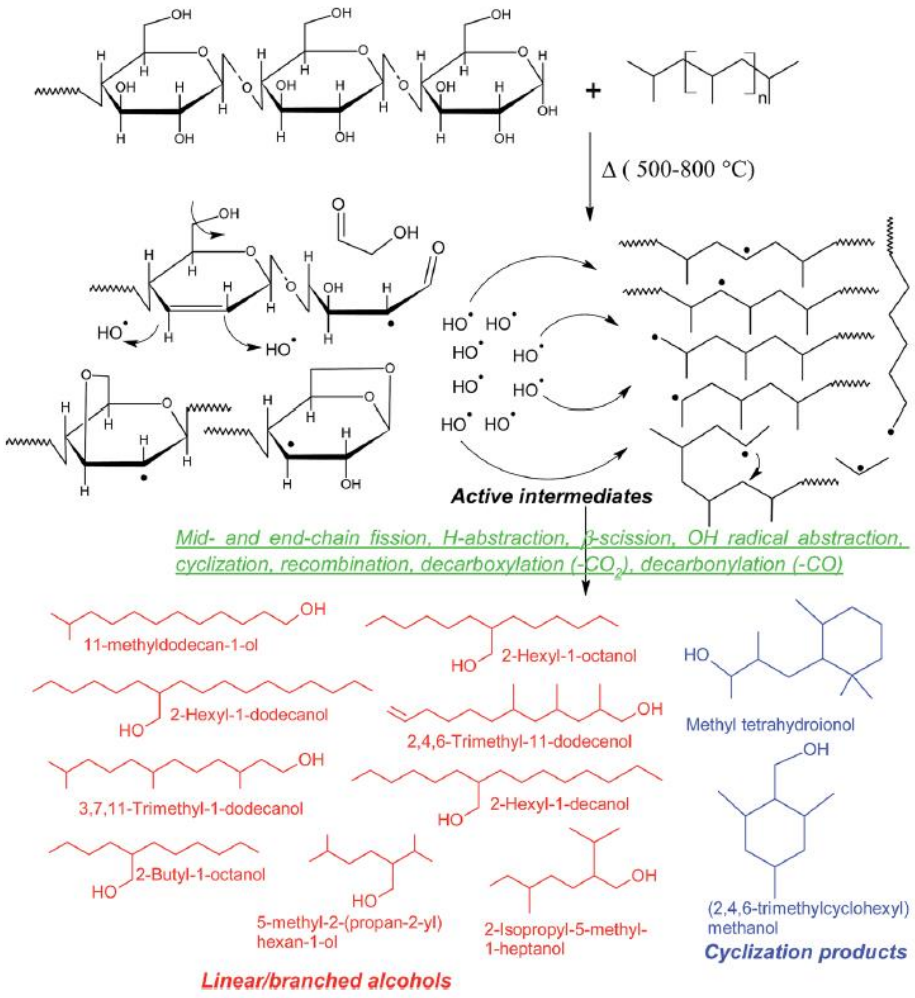

Figure 2. Reaction mechanism for fast co-pyrolysis of biomass and PP [18]

Additionally, Yang et al. [33] thereafter investigated the fast co-pyrolysis of LDPE and various biomass residue for oil production. The pyrolysis temperature was found to be an important factor affect the synergy between biomass and plastics. With the yields of gases, coke/char reduced at all temperature ranges, the synergy for promoting the production of tar/oil was obvious at higher temperature. During co-pyrolysis, most of the biomass derived light oxygenates were reduced, with only alcohols and esters being the major oxygenated

products. The production of aliphatic hydrocarbons from LDPE are quite enhanced, while the increasing or decreasing trend of aromatic hydrocarbons is not obvious. Notably, the inorganic components of biomass, mainly potassium and calcium, improved the decomposition of LDPE.

Dorado et al.[20] achieved a fast co-pyrolysis of waste polyethylene hay bale covers and switchgrass in a bubbling fluidized reactor. Due to the fast heating rate adopted in the fluidized bed, wax solids from partial depolymerization of polyethylene was found with nitrogen as the carrier gas, which interrupting the process with wax attached on the system. The problem was overcome with recycling part of the tail-gas as the carrier gas, which is denoted as Tail-Gas Reactive Pyrolysis (TGRP). Both the yields of pyrolysis oil and non-condensable gas increased with TGRP. The quality of pyrolysis oil was also improved in terms of lower oxygen content. By comparing hydrogen production and the oxygen content of pyrolysis oil, the author concluded that the deoxygenation is driven by H_2 releasing aromatization reaction, rather than hydrogen transfer from polyethylene to biomass.

Apart from PE, PP, PS and PET, PVC is the second most used plastic due to its low cost and stability. The chloride content of PVC make its pyrolysis quite distinct from other plastics. Thermal degradation of PVC contains two steps, the dehydrochlorination into a conjugated polyene followed by chain scission and aromatization to yield hydrocarbon products. The formation of polyaromatics hydrocarbons (PAH) and hydrochloride is an inevitable challenge for PVC pyrolysis, which is later found to be inhibited when PVC was fast co-pyrolyzed with biomass components [34]. The chloride is partly fixed into pyrolyzed residues. The tar yield from biomass components and PVC co-pyrolysis was higher than its corresponding calculated yield. HCl may function as the Lewis acid to catalyze the

depolymerization of cellulose into sugars and light oxygenates. On the other hand, the interaction between PVC and lignin pyrolysis char/residues is proved to increase the tar yield from PVC.

Catalytic pyrolysis

Aiming to address the disposal of agricultural plastics and produce drop-in fuel from biomass via co-pyrolysis, Dorado et al. [35] used HZSM-5 to catalyze co-pyrolysis of biomass and different plastics. Lignin, xylan, cellulose, switchgrass and HDPE, LDPE, PS, PET are adopted as the feedstock for pyrolysis. It was found that the plastic-biomass mixture with PE/PP/PET could produce higher amount of aromatic than theoretical yield. Among all the biomass components, the conversion of lignin into aromatic hydrocarbons profits most in co-pyrolyzing with plastics. The Diels-Alder type reaction is claimed as one of the major pathways, which consumes furans from biomass and olefins from plastic as the reactants. Later, the authors further co-pyrolyzed ^{13}C labelling cellulose and different plastics (PE, PP, PS and PET) [36]. Alkylated benzene is favored with the reaction between fragments from PE/PP and cellulose, while larger aromatic hydrocarbons are abundantly produced with the biomass-plastic mixture containing PS/PET. The distribution of $^{13}C_x{}^{12}C_y$ in various products, especially aromatic hydrocarbons, reveals that many more reactions beyond often mentioned hydrocarbon pool mechanism are quite active in the co-pyrolysis process.

Wang et al.[37-40] conducted a series of catalytic of plastic and biomass with different zeolites. The catalytic co-pyrolysis of LDPE and cellulose in the presence of HZSM-5 could enhance the aromatic yield and reduce coke formation. Three reason are proposed to explain the positive synergistic effects: the dehydration and other deoxygenation reaction of cellulose derived oxygenates into coke are suppressed with the hydrogen from

LDPE, LDPE-derived olefins may also react with cellulose derived oxygenates similar to methanol-to-olefin (MTO) reactions, initially formed aromatic from LDPE could catalyze the aromatization reaction of cellulose derived oxygenates [37]. The increase of aromatic hydrocarbons were in accompany with the decrease of carbon oxides and alkanes. More carbons are preserved since oxygen is removed by grabbing the hydrogen from alkanes. There exists an optimum mixing ratio of cellulose and LDPE for maximizing aromatic yield and the synergistic effects [38]. During catalytic co-pyrolysis of LDPE and biomass, one of the limiting step for alkane aromatization is the conversion of alkane into olefins. By adding Ga into conventional HZSM-5, the dehydrogenation reaction of alkanes is enhanced, which in turn helps increase the yield of mono-ring aromatic. The production of polyaromatic hydrocarbons is also suppressed, possibly due to the pore narrowing down with Ga treatment [39]. Similar product improvement was found with the modified P-ZSM-5 and P/Ni-ZSM-5. By comparing the product distribution, P-ZSM-5 and P/Ni-ZSM-5 is found to have higher hydrothermal stability than conventional ZSM-5 does [40]. Besides modifying the zeolites with both metal and non-metal elements, the change of its physical structure also improved the conversion for co-pyrolysis of biomass and plastics. For example, expanding the zeolite channel could enable more diffusion of compounds with larger molecular size from both biomass and plastic to participate in the co-pyrolysis process, thus improving the yield of aromatics [41].

Zhang et al.[42, 43] accomplished a catalytic co-pyrolysis of plastic and pine sawdust/black-liquor lignin in a continuous lab-scale fluidized bed reactor. Due to the presence of acid catalyst including LOSA-1, spent FCC and γ-Al_2O_3, problems reported previously with plastic pyrolysis and co-pyrolysis in fluidized bed reactor did not happen in

this study [20, 44, 45]. When pine sawdust was co-pyrolyzed with PE, rising the pyrolysis temperature helped increase the yield of olefins, while the yield of aromatic was the highest at 600 °C. By comparing the performance of different catalysts, LOSA-1, a microporous catalyst mainly consisting of ZSM-5, favors the monoaromatic compounds production. The mesoporous catalysts has little shape selectivity for aromatic and olefins. Although it was claimed by the author that the Diels-Alder reaction of plastic-derived olefins and biomass-derived furans is one of the reaction pathways when lignin and PE was co-pyrolyzed, it seems not to be true since lignin pyrolysis rarely generates furans.

Recently, there are several papers published focusing on co-pyrolysis of torrefied biomass and plastics [46-48]. Lee et al. [47] found that after the cellulose being torrefied, both the aromatic hydrocarbon yield and synergy between cellulose and PP were enhanced during co-pyrolysis with HZSM-5 zeolite. With torrefaction, the crystallinity and structure of cellulose were changed. The enhanced synergy by torrefaction were attributed to the easier decomposition of torrefied cellulose into small oxygenates and the formation of aliphatic intermediates. In another study carried out by Lee et al. [48], an enhancement of aromatic hydrocarbons were also observed with the co-pyrolysis of torrefied cork oak and HDPE. Specially, it was found that the mesoporous HY zeolite performs better in terms of mono-aromatics, olefins and paraffins production in comparison of microporous HY zeolite, which contradicts the findings by Zhang [43].

In addition to using zeolites, alumina, ceria and alumina-ceria supported cobalt catalysts were adopted for the catalytic co-pyrolysis of waste paper and plastic mixture (HDPE, PP and PET) [49]. The yield of liquid product is positively related to the plastic percentage in the feedstock. Due to the high pyrolysis temperature (700-800°C), gas rich in

hydrogen, carbon oxides and methane was the major product. One interesting observation is that with the increase of temperature, the yield of carbon monoxide decrease, with a corresponding increase of carbon dioxide and hydrogen. This observation is quite different from previous research focusing on biomass catalytic pyrolysis has showing that the yield of carbon monoxide increases with temperature while that of carbon dioxide is slight enhanced [50], which could be the results from the synergy between waste paper and plastics.

Dissertation organization

The dissertation is composed of six chapters in total. As introduced in *Chapter 1*, co-pyrolysis of biomass and plastics offers an optional technique to produce high-grade products, especially pyrolysis oil. The process, however, needs further investigation and understanding of the underlying mechanisms for both non-catalytic and catalytic co-pyrolysis of biomass and plastics to facilitate large-scale production. The Waste-To-Energy (WTE) technology of Municipal Solid Waste (MSW) is also highly relevant to the research work of co-pyrolysis of biomass and plastic since the MSW mostly consists of organic and plastic wastes. Non-catalytic co-pyrolysis can produce a product mixture of oxygenated compounds from biomass and hydrocarbons from plastics, and catalytic co-pyrolysis can generate a product stream that has been fully deoxygenated.

Apart from general introduction and conclusion, work is summarized into four chapters. *Chapter 2* focuses on the feasibility test for fast co-pyrolyzing waste HDPE and red oak biomass in a fluidized bed reactor, aiming to address the previously encountered problems including reactor clogging and defluidization in continuous reactor. The cross-

reactions between biomass and HDPE are systematically investigated by analyzing the physiochemical properties of products.

Chapter 3 explores the reaction mechanisms for co-pyrolysis of biomass/biomass components with PE in a micro-pyrolyzer. In this part, by co-pyrolyzing biomass/biomass components (cellulose, hemicellulose, lignin) and polyethylene in both absence and presence of catalyst, the thermal and catalytic synergies were extensively studied. Temperature, which is an important variable affecting the outcome of co-pyrolysis, is heavily focused in *Chapter 2*.

Acid pretreatment (infusion or leaching) of biomass prior to pyrolysis is previously found to improve the performance of biomass pyrolysis. Combining the idea with the findings from *Chapter 3*, *Chapter 4* is dedicated to the effects of acid pretreatments to co-pyrolysis of biomass and polyethylene. This leads to the hypothesis that acid pretreatments, either acid infusion or leaching, could enhance the cross-reaction, in terms of hydrogen transfer and Diels-Alder reactions.

Chapter 5 is trying to understand the effects of carrier gas type and feedstock-catalyst contact mode to catalytic pyrolysis of four major waste plastics (polyethylene, polypropylene, polystyrene, polyethylene terephthalate). Although there have been many previous works on plastic recycling by pyrolysis, few studies have focused on the effects of carrier gases and feedstock-catalyst contact mode to catalytic pyrolysis of plastics. It is believed that the work presented in this part could give insightful discussions about the chemistry of plastic pyrolysis and useful guidance for recycling municipal plastic wastes (MPW).

Chapter 6 summarizes the conclusions from each chapter and provides some suggestions for future work.

References

[1] R.C. Brown, T.R. Brown. Biorenewable resources: engineering new products from agriculture. John Wiley & Sons2013.

[2] D.C. Dayton, J. Carpenter, J. Farmer, B. Turk, R. Gupta. Biomass hydropyrolysis in a pressurized fluidized bed reactor. Energy & Fuels. 27 (2013) 3778-85.

[3] O. Jan, R. Marchand, L.C. Anjos, G.V. Seufitelli, E. Nikolla, F.L. Resende. Hydropyrolysis of Lignin Using Pd/HZSM-5. Energy & Fuels. 29 (2015) 1793-800.

[4] D. Meier, R. Ante, O. Faix. Catalytic hydropyrolysis of lignin: influence of reaction conditions on the formation and composition of liquid products. Bioresource Technology. 40 (1992) 171-7.

[5] F. Melligan, M. Hayes, W. Kwapinski, J. Leahy. Hydro-pyrolysis of biomass and online catalytic vapor upgrading with Ni-ZSM-5 and Ni-MCM-41. Energy & Fuels. 26 (2012) 6080-90.

[6] M.W. Nolte, J. Zhang, B.H. Shanks. Ex situ hydrodeoxygenation in biomass pyrolysis using molybdenum oxide and low pressure hydrogen. Green Chemistry. 18 (2016) 134-8.

[7] T.L. Marker, L.G. Felix, M.B. Linck, M.J. Roberts. Integrated hydropyrolysis and hydroconversion (IH2) for the direct production of gasoline and diesel fuels or blending components from biomass, part 1: Proof of principle testing. Environmental Progress & Sustainable Energy. 31 (2012) 191-9.

[8] T.L. Marker, L.G. Felix, M.B. Linck, M.J. Roberts, P. Ortiz‐Toral, J. Wangerow. Integrated hydropyrolysis and hydroconversion (IH2®) for the direct production of gasoline and diesel fuels or blending components from biomass, Part 2: continuous testing. Environmental Progress & Sustainable Energy. 33 (2014) 762-8.

[9] K. Wang, K.H. Kim, R.C. Brown. Catalytic pyrolysis of individual components of lignocellulosic biomass. Green Chemistry. 16 (2014) 727-35.

[10] T.R. Carlson, J. Jae, G.W. Huber. Mechanistic Insights from Isotopic Studies of Glucose Conversion to Aromatics Over ZSM‐5. ChemCatChem. 1 (2009) 107-10.

[11] T.R. Carlson, J. Jae, Y.-C. Lin, G.A. Tompsett, G.W. Huber. Catalytic fast pyrolysis of glucose with HZSM-5: the combined homogeneous and heterogeneous reactions. Journal of Catalysis. 270 (2010) 110-24.

[12] T.R. Carlson, G.A. Tompsett, W.C. Conner, G.W. Huber. Aromatic production from catalytic fast pyrolysis of biomass-derived feedstocks. Topics in Catalysis. 52 (2009) 241-52.

[13] T.R. Carlson, T.P. Vispute, G.W. Huber. Green gasoline by catalytic fast pyrolysis of solid biomass derived compounds. ChemSusChem. 1 (2008) 397-400.

[14] I. Boumanchar, Y. Chhiti, F.E.M.h. Alaoui, A. El Ouinani, A. Sahibed-Dine, F. Bentiss, et al. Effect of materials mixture on the higher heating value: Case of biomass, biochar and municipal solid waste. Waste Management. (2016).

[15] Q.M. Meng, X.P. Chen, Y.M. Zhuang, C. Liang. Effect of Temperature on Controlled Air Oxidation of Plastic and Biomass in a Packed‐Bed Reactor. Chemical Engineering & Technology. 36 (2013) 220-7.

[16] V. Sharypov, N. Marin, N. Beregovtsova, S. Baryshnikov, B. Kuznetsov, V. Cebolla, et al. Co-pyrolysis of wood biomass and synthetic polymer mixtures. Part I: influence of experimental conditions on the evolution of solids, liquids and gases. Journal of Analytical and Applied Pyrolysis. 64 (2002) 15-28.

[17] M. Brebu, S. Ucar, C. Vasile, J. Yanik. Co-pyrolysis of pine cone with synthetic polymers. Fuel. 89 (2010) 1911-8.

[18] D.K. Ojha, R. Vinu. Fast co-pyrolysis of cellulose and polypropylene using Py-GC/MS and Py-FT-IR. RSC Advances. 5 (2015) 66861-70.

[19] J.D. Martínez, A. Veses, A.M. Mastral, R. Murillo, M.V. Navarro, N. Puy, et al. Co-pyrolysis of biomass with waste tyres: upgrading of liquid bio-fuel. Fuel Processing Technology. 119 (2014) 263-71.

[20] C. Dorado, C.A. Mullen, A.A. Boateng. Coprocessing of Agricultural Plastic Waste and Switchgrass via Tail Gas Reactive Pyrolysis. Industrial & Engineering Chemistry Research. 54 (2015) 9887-93.

[21] N. Marin, S. Collura, V. Sharypov, N. Beregovtsova, S. Baryshnikov, B. Kutnetzov, et al. Copyrolysis of wood biomass and synthetic polymers mixtures. Part II: characterisation of the liquid phases. Journal of Analytical and Applied pyrolysis. 65 (2002) 41-55.

[22] V. Sharypov, N. Beregovtsova, B. Kuznetsov, L. Membrado, V. Cebolla, N. Marin, et al. Co-pyrolysis of wood biomass and synthetic polymers mixtures. Part III: Characterisation of heavy products. Journal of Analytical and Applied pyrolysis. 67 (2003) 325-40.

[23] P.R. Patwardhan, D.L. Dalluge, B.H. Shanks, R.C. Brown. Distinguishing primary and secondary reactions of cellulose pyrolysis. Bioresource technology. 102 (2011) 5265-9.

[24] T. Hosoya, H. Kawamoto, S. Saka. Secondary reactions of lignin-derived primary tar components. Journal of Analytical and Applied Pyrolysis. 83 (2008) 78-87.

[25] M. Brebu, I. Spiridon. Co-pyrolysis of LignoBoost® lignin with synthetic polymers. Polymer Degradation and Stability. 97 (2012) 2104-9.

[26] S. Kumagai, K. Fujita, T. Kameda, T. Yoshioka. Interactions of beech wood–polyethylene mixtures during co-pyrolysis. Journal of Analytical and Applied Pyrolysis. 122 (2016) 531-40.

[27] Q. Cao, L.e. Jin, W. Bao, Y. Lv. Investigations into the characteristics of oils produced from co-pyrolysis of biomass and tire. Fuel Processing Technology. 90 (2009) 337-42.

[28] M.E. Edjabou, M.B. Jensen, R. Götze, K. Pivnenko, C. Petersen, C. Scheutz, et al. Municipal solid waste composition: Sampling methodology, statistical analyses, and case study evaluation. Waste Management. 36 (2015) 12-23.

[29] H. Zhou, A. Meng, Y. Long, Q. Li, Y. Zhang. An overview of characteristics of municipal solid waste fuel in China: physical, chemical composition and heating value. Renewable and Sustainable Energy Reviews. 36 (2014) 107-22.

[30] W. Chen, S. Shi, J. Zhang, M. Chen, X. Zhou. Co-pyrolysis of waste newspaper with high-density polyethylene: Synergistic effect and oil characterization. Energy Conversion and Management. 112 (2016) 41-8.

[31] A. Dewangan, D. Pradhan, R.K. Singh. Co-pyrolysis of sugarcane bagasse and low-density polyethylene: Influence of plastic on pyrolysis product yield. Fuel. 185 (2016) 508-16.

[32] P. Rutkowski, A. Kubacki. Influence of polystyrene addition to cellulose on chemical structure and properties of bio-oil obtained during pyrolysis. Energy conversion and management. 47 (2006) 716-31.

[33] J. Yang, J. Rizkiana, W.B. Widayatno, S. Karnjanakom, M. Kaewpanha, X. Hao, et al. Fast co-pyrolysis of low density polyethylene and biomass residue for oil production. Energy Conversion and Management. 120 (2016) 422-9.

[34] H. Zhou, C. Wu, J.A. Onwudili, A. Meng, Y. Zhang, P.T. Williams. Effect of interactions of PVC and biomass components on the formation of polycyclic aromatic hydrocarbons (PAH) during fast co-pyrolysis. RSC Advances. 5 (2015) 11371-7.

[35] C. Dorado, C.A. Mullen, A.A. Boateng. H-ZSM5 Catalyzed Co-Pyrolysis of Biomass and Plastics. ACS Sustainable Chemistry & Engineering. 2 (2014) 301-11.

[36] C. Dorado, C.A. Mullen, A.A. Boateng. Origin of carbon in aromatic and olefin products derived from HZSM-5 catalyzed co-pyrolysis of cellulose and plastics via isotopic labeling. Applied Catalysis B: Environmental. 162 (2015) 338-45.

[37] X. Li, H. Zhang, J. Li, L. Su, J. Zuo, S. Komarneni, et al. Improving the aromatic production in catalytic fast pyrolysis of cellulose by co-feeding low-density polyethylene. Applied Catalysis A: General. 455 (2013) 114-21.

[38] X. Li, J. Li, G. Zhou, Y. Feng, Y. Wang, G. Yu, et al. Enhancing the production of renewable petrochemicals by co-feeding of biomass with plastics in catalytic fast pyrolysis with ZSM-5 zeolites. Applied Catalysis A: General. 481 (2014) 173-82.

[39] J. Li, Y. Yu, X. Li, W. Wang, G. Yu, S. Deng, et al. Maximizing carbon efficiency of petrochemical production from catalytic co-pyrolysis of biomass and plastics using gallium-containing MFI zeolites. Applied Catalysis B: Environmental. 172 (2015) 154-64.

[40] W. Yao, J. Li, Y. Feng, W. Wang, X. Zhang, Q. Chen, et al. Thermally stable phosphorus and nickel modified ZSM-5 zeolites for catalytic co-pyrolysis of biomass and plastics. RSC Advances. 5 (2015) 30485-94.

[41] Y. Hong, Y. Lee, P.S. Rezaei, B.S. Kim, J.-K. Jeon, J. Jae, et al. In-situ catalytic copyrolysis of cellulose and polypropylene over desilicated ZSM-5. Catalysis Today. (2016).

[42] H. Zhang, J. Nie, R. Xiao, B. Jin, C. Dong, G. Xiao. Catalytic co-pyrolysis of biomass and different plastics (polyethylene, polypropylene, and polystyrene) to improve hydrocarbon yield in a fluidized-bed reactor. Energy & Fuels. 28 (2014) 1940-7.

[43] H. Zhang, R. Xiao, J. Nie, B. Jin, S. Shao, G. Xiao. Catalytic pyrolysis of black-liquor lignin by co-feeding with different plastics in a fluidized bed reactor. Bioresource technology. 192 (2015) 68-74.

[44] R. Aguado, R. Prieto, M.J. San José, S. Alvarez, M.n. Olazar, J. Bilbao. Defluidization modelling of pyrolysis of plastics in a conical spouted bed reactor. Chemical Engineering and Processing: Process Intensification. 44 (2005) 231-5.

[45] U. Arena, M.L. Mastellone. Defluidization phenomena during the pyrolysis of two plastic wastes. Chemical Engineering Science. 55 (2000) 2849-60.

[46] I. Elsayed, A. Eseyin. Production high yields of aromatic hydrocarbons through catalytic fast pyrolysis of torrefied wood and polystyrene. Fuel. 174 (2016) 317-24.

[47] H.W. Lee, Y.-M. Kim, J. Jae, J.-K. Jeon, S.-C. Jung, S.C. Kim, et al. Production of aromatic hydrocarbons via catalytic co-pyrolysis of torrefied cellulose and polypropylene. Energy Conversion and Management. 129 (2016) 81-8.

[48] H.W. Lee, Y.-M. Kim, B. Lee, S. Kim, J. Jae, S.-C. Jung, et al. Catalytic copyrolysis of torrefied cork oak and high density polyethylene over a mesoporous HY catalyst. Catalysis Today. (2017).

[49] J. Chattopadhyay, T.S. Pathak, R. Srivastava, A.C. Singh. Catalytic co-pyrolysis of paper biomass and plastic mixtures (HDPE (high density polyethylene), PP (polypropylene) and PET (polyethylene terephthalate)) and product analysis. Energy. 103 (2016) 513-21.

[50] K. Wang, P.A. Johnston, R.C. Brown. Comparison of in-situ and ex-situ catalytic pyrolysis in a micro-reactor system. Bioresource Technology. 173 (2014) 124-31.

CHAPTER 2

FAST PYROLYSIS OF BIOMASS AND WASTE PLASTIC IN A FLUIDIZED BED REACTOR

A paper published to the journal *Fuel*

Yuan Xue[1], Shuai Zhou[2], Robert C. Brown[1,2], Atul Kelkar[1], Xianglan Bai[1*]

Abstract

Co-pyrolysis of red oak and high density polyethylene (HDPE) was conducted in a laboratory-scale, continuous fluidized bed reactor in a temperature range from 525 to 675 °C. Pyrolysis products, including two fractions of pyrolysis-oil, non-condensable gases and char were analyzed to assess the influence of pyrolysis temperature and co-feeding of biomass with HDPE. It was found that increasing pyrolysis temperature up to 625 °C promoted the production of pyrolysis-oil and its yield reached 57.6 wt%. Further increase in pyrolysis temperature caused the cracking of pyrolysis-oil to form light gases rich in hydrocarbons. Organic phase of pyrolysis-oil produced from plastic-biomass mixture (PBM) had a higher heating value (HHV) up to 36.6 MJ/kg contributed by the additive effect of HDPE-derived aliphatic hydrocarbons. A significant synergetic effect was also observed during co-pyrolysis. Co-pyrolysis with HDPE increased the production of furan, acids and water from red oak. Co-presence of HDPE also inhibited char formation from red oak and improved the HHV of the resulting char. The char produced from co-pyrolysis had a significantly lower BET surface area than red oak biochar. Not only did HDPE-derived particulate matter blocks the pores, the synergetic interaction also resulted in the formation of large and shallow micro-pores on the char surface.

Keywords: biomass; plastic; fast pyrolysis; pyrolysis-oil; char

[1] Department of Mechanical Engineering, Iowa State University, Ames, IA 50011, USA
[2] Bioeconomy Institute, Iowa State University, Ames, Iowa USA, 50011
* Corresponding author. Postal address: Iowa State University, 2070 Black Engineering Building, Ames, IA 50011; Tel: +1 515 294 6886; Fax: +1 515 294 3261; E-mail address: bxl9801@iastate.edu (X. Bai)

Introduction

Each year the US alone produces 250 million tons of municipal solid waste (MSW). Among it, over 50 % of the non-recyclable MSW ends up in landfill sites [1]. The landfilled MSW takes away valuable land and creates numerous potential environmental problems. In fact, the discarded MSW represents a tremendous energy source. Waste-to-energy (WTE) technologies can mitigate negative impacts of MSW and provide sustainable energy from low-cost feedstock. Examples of these technologies include incineration, gasification, anaerobic digestion, and pyrolysis [2, 3]. Pyrolysis depolymerizes dry feedstock under an oxygen free environment. When the pyrolysis temperature is moderately high (450 to 550 °C) [4], the volatiles arise from pyrolysis process can be condensed to become liquid product, called pyrolysis-oil [5]. Unlike other technologies that produce heat or gases, pyrolysis-oil is transportable liquid and can be upgraded to transportation fuels or other platform chemicals [6]. Another advantage of the pyrolysis process is that it has low requirements for the feedstock type and reactor design, thus technology is relatively easy to scale up.

While MSW consists of many different types of materials, biomass and plastics make up a majority of the composition [1]. When biomass is pyrolyzed alone, it produces a number of oxygenated products, such as sugars, aldehydes, ketones, acids and phenols. The presence of oxygen in the pyrolysis-oil (resulting from an abundance in the biomass feedstock) lowers the heating value and also causes thermal instability and corrosiveness [7]. On the other hand, plastic wastes are rich in hydrogen and contain much less oxygen than biomass. High density polyethylene (HDPE), the most commonly used plastic for example, has virtually no oxygen. Thus, compared to pyrolyzing biomass alone, co-pyrolyzing biomass and waste

plastics increases carbon and hydrogen contents in the feedstock and could be beneficial in improving the quality of pyrolysis-oil. As a result, higher quality pyrolysis-oil could potentially reduce the costs associated with catalytic hydro-deoxygenation, which is required to process it into hydrocarbon fuels [8].

Co-pyrolysis of biomass with different plastics has been investigated extensively [8-22]. Biomass and the plastics were often placed inside of batch reactors or fixed bed reactors prior to heating and slowly pyrolyzed at a discontinuous mode [8]. For example, Costa et al. [9] co-pyrolyzed rice husk and polyethylene in a batch reactor at 350-430 °C for up to 60 minutes and reported that the thermal conversions of both biomass and PE are facilitated by the presence of each other. Martinez et al. [12] also slowly pyrolyzed biomass and synthetic polymers and found that the viscosity and acidity of pyrolysis-oil decreased whereas the heating value increased compared to that of pyrolysis-oil obtained when pyrolyzing biomass alone. It was also reported that the yield of pyrolysis-oil was much higher than the theoretical sum of pyrolysis oils produced from biomass and plastics when they are independently pyrolyzed [13]. Recently, Sajdak et al. [19-21] thoroughly investigated co-pyrolysis of biomass and polypropylene and concluded that co-pyrolysis has a significant synergistic effect. In their study, the mixed feedstock was pyrolyzed in a batch reactor for 50 min. at a heating rate of 5 °C/min.

It is noteworthy that in general, maximum yield of pyrolysis-oil is achieved from biomass upon fast pyrolysis [23] since slow pyrolysis of biomass usually promotes the formation of char and light gases instead of pyrolysis-oil [24]. During fast pyrolysis, the feedstock is rapidly heated (>100 ºC/s) and pyrolysis vapor is instantly swept away from the reactor zone and quenched. The vapor retention time is usually less than 2 s in fast pyrolysis

to limit secondary reactions that decreasing the amount of the condensable vapor. Although fast pyrolysis of biomass alone was extensively studied, very few investigated fast co-pyrolysis of biomass and plastics [10, 15, 16, 18, 22, 24] in continuous mode. It was reported that the synergetic effect among biomass and plastics is negligible during fast pyrolysis due to the short reaction time in the reactor [10, 22]. A contradictory result, however, is reported by Martinez et al. at a study using an auger reactor [12].

It should also be noted that fast co-pyrolysis of biomass and plastics was mostly conducted at the optimum temperature for fast pyrolyzing biomass (450- 500 °C). However, the optimum pyrolysis temperature of biomass is often too low for completely decomposing plastics during fast pyrolysis since some plastics, such as HDPE, degrade at much higher temperatures than biomass does [25].

In this study, red oak and HDPE pellets are co-pyrolyzed in a lab-scale, continuous fluidized bed reactor. The estimated heating rate in the fluidized bed is 600 °C/s, which is typical for fast pyrolysis. Pyrolysis temperatures were ranged from 525 to 675 °C. Fast pyrolysis at below 500 °C in the reactor is not sufficient to completely depolymerize HDPE to volatiles due to the short reaction time. As a result, the melted plastic either forms agglomerates with the fluidizing sand or biomass thus developing defluidization inside of the fluidized reactors. Thus it was determined that the fast co-pyrolysis of biomass and HDPE has to be conducted in a higher temperature range than the optimal temperature of biomass pyrolysis. In this work, pyrolysis products, including two fractions of pyrolysis-oil, non-condensable gases and pyrolysis char are analyzed using comprehensive analytical methods and the results are compared with the products produced from pyrolysis of red oak alone.

Material and methods

Feedstock

High density polyethylene (HDPE) pellets were obtained from USI Corporation, Taipei. The pellets, 4 mm in diameter and 2 mm in thickness, are made from recycled plastics. Northern red oak (Quercus Rubra) was purchased from Wood Residues Solutions (Montello, WI). The bark free chips were first ground by a mill cut and then sieved to a constant size range between 250 and 400 μm. Proximate and ultimate analyses of the feedstock are given in Table S1.

Pyrolysis

Co-pyrolysis of red oak and HDPE was conducted using a laboratory-scale continuous fluidized bed reactor. The schematic diagram of the reactor system and its specification can be found elsewhere [26]. Specifically, the reactor system consists of a feeder, an injection auger, and a stainless steel reactor that is 0.34 m in height and 38.1 mm in inner diameter. Silica sand from 410 to 600 μm was used as the heat carrier in the reactor and nitrogen gas was used as the sweep gas. The feed rate of material was 60 g/h and the estimated vapor residence time in the reactor was 1.1 s [27].

The separation and collection of pyrolysis products were conducted by two cyclones, an electrostatic precipitator (ESP) and condensers that are located downstream of the reactor. Char and ash particles were removed by two cyclones connected in series. Liquid nitrogen was sprayed to the pyrolysis vapor prior to the vapor stream entering the ESP to reduce the temperature of the vapor steam to 90 ºC. The aerosols of relatively high molecular-weight (MW) compounds in the vapor were collected at a collection bottle attached to the end of the ESP. This fraction of pyrolysis-oil is referred as organic phase in this study. The light MW

compounds in the pyrolysis vapor were condensed and recovered at further downstream using a condenser chilled to -10 ºC. This light MW fraction of pyrolysis-oil is referred as aqueous phase.

Pyrolysis char was collected in the cyclones. The yield of char was determined by weighing the sand bed and two cyclones before and after each experiment. The yield of pyrolysis-oil was determined by measuring the weight difference of the pyrolysis-oil collection system including pipes, vessels and containers. The composition of non-condensable gases (NCGs) in the exhaust stream was measured with a micro-Gas Chromatogram (GC) (Varian CP-4900) calibrated for nitrogen (N_2), hydrogen (H_2), carbon oxides (CO_2, CO), and hydrocarbon gases up to C_3 which include ethylene (C_2H_4), ethane (C_2H_6), and propane (C_3H_8). A drum-type gas meter (Ritter, Germany) and the ideal gas law were used to determine the volume of NCG. Since the hydrocarbon gases with C_4+ were not calibrated in this study, the total yield of NCGs was reported by subtracting the yields of pyrolysis-oil and char from 100 %.

According to the EPA report, the ratio of plastics to biomass is 1:4 in general MSW. [23] Thus, a mixture of the feedstock consisting of 20 % HDPE and 80 % red oak was prepared and pyrolyzed at 525, 575, 625 and 675 ºC, respectively. Red oak alone was also pyrolyzed at 575 ºC for the comparison. All the pyrolysis tests were duplicated and average mass yields were reported in this study. The standard errors between two runs at the same conditions were all below 5 %.

Characterization of pyrolysis products

The pyrolysis-oil and char were characterized using the analytical methods described next. The CHNS elemental analysis of pyrolysis-oil and char were conducted using

Elementar (vario MICRO cube) elemental analyzer. Based on the elemental composition, a theoretical equation developed by Demirbas [28] was used to determine the higher heating value (HHV) of pyrolysis-oil and char. Water content of the aqueous phase was measured using a Karl-Fischer Titrator (KEM, MKS-500) with Hydranal-composite 5K solution. Since solubility of the organic phase in the Hydranal-composite 5K solution is very low, water content in the organic phase was measured using a Mettler Toledo Thermogravimetry/Differential Scanning Calorimetry system (TGA/DSC). During the TGA test, the temperature of the organic phase sample was increased from 25 to 105 ºC with a ramp of 10 ºC/min and then was kept at the final temperature for additional 40 minutes. Modified acid number (MAN) of the pyrolysis-oil was measured with a titrator (Metrohm, 798 MPT Titrino) using N,N-dimethyl formamide and methanol as the solvents. MAN value was expressed as mg KOH/g of pyrolysis-oil.

An Agilent 7890B gas chromatography with Agilent 5977A mass-selective-detector (MSD) and flame ionization detector (FID) system was used to identify and quantify the chemical compounds in pyrolysis oils. The capillary column used in the GC was a ZB-1701 (60 m × 250 μm × 0.25 μm). The injection temperature was 250 ºC and the oven temperature was kept at 35 ºC for 1 minute and then ramped to 280 ºC with 3 ºC /min. A total of 8 carbohydrates derivatives, 14 lignin derivatives, and aliphatic hydrocarbons with C_8-C_{20} were identified and quantified using authentic chemicals. The hydrocarbon compounds with C_8-C_{12} were calibrated by using n-Decane, C_{13}-C_{17} hydrocarbons were using n-Hexadecane, and C_{18}-C_{20} compounds were calibrated using n-Octadecane, respectively. All the calibration curves had regression coefficients at least 0.99.

A NOVA 4200e surface analyzer (Quantachrome Instruments) was used to measure Brunauer-Emmet-Teller (BET) surface area of char. Prior to the measurement, the char was degassed at 300 ºC under vacuum for 5 hours.

Char was also analyzed for Fourier transform infrared spectroscopy (FT-IR) using a Nicolet iS10 (Thermo Scientific) instrument. Each sample was scanned 32 times at a resolution of 4 cm^{-1} and interval of 1 cm^{-1}. The normalized spectra were obtained in the region of wave number ranging from 500 to 4000 cm^{-1}. In addition, the micro-structure of char was observed with scanning electron microscope (FEI Quanta-250 SEM).

Results and discussion

Products distribution

The products distribution from co-pyrolysis of PBM is given in Fig. 1. The pyrolysis-oil yield (the sum of the organic and aqueous phases) from co-pyrolysis increased from 49.0 wt% at 525 ºC to 57.6 wt% at 625 ºC before leveling off to 44.5 wt% at 675 ºC. Char yield was found to decrease monotonically from 14.0 to 5.7 wt% when the temperature increased to 675 ºC. It is noteworthy that the yield of pyrolysis-oil decreased from 57.6 to 44.5 wt% whereas char yield only decreased slightly when increasing pyrolysis temperature above 625 ºC. On the other hand, the yields of NCG remained nearly constant up to 625 ºC then increased significantly at the higher temperature. The results suggest that the decreased char mainly converted to pyrolysis oil during pyrolysis at temperatures up to 625 ºC. However, pyrolysis at even higher temperatures caused the cracking of pyrolysis-oil to NCG. Compared to pyrolysis of red oak alone at 575 ºC, co-pyrolyzing PBM improved pyrolysis-oil yield from 50.3 to 55.2 wt%. No significant changes in the yields of NCG were found

when red oak was co-pyrolyzed with HDPE at the same temperature. In a previous study, pyrolysis of red oak at 500 ºC using the same reactor system resulted in 63.3 wt% of pyrolysis-oil [26], which is much higher than 50.3 wt% at 575 ºC. Thus, for red oak alone, increasing pyrolysis temperature above 500 ºC would reduce pyrolysis-oil yield. Nevertheless pyrolysis-oil yield from PBM increased until the temperature reaches 625 ºC. On the other hand, the char yield was 12.5 wt% from pyrolyzing red oak alone and it reduced to 8.4 wt% from co-pyrolysis of PBM. Pyrolysis of HDPE alone at 575 ºC does not produce char. Since red oak accounts for 80 wt% of total mass in PBM, 12.5 wt% char produced from pyrolysis of red oak alone equivalents to 10.0 wt% char when the mixture was pyrolyzed (i.e., 12.5 wt% × 80%). Thus the result suggests that co-pyrolysis of PBM reduced the amount of char originating from red oak (8.4 wt% from pyrolyzing the mixture) due to synergetic effect between red oak and HDPE.

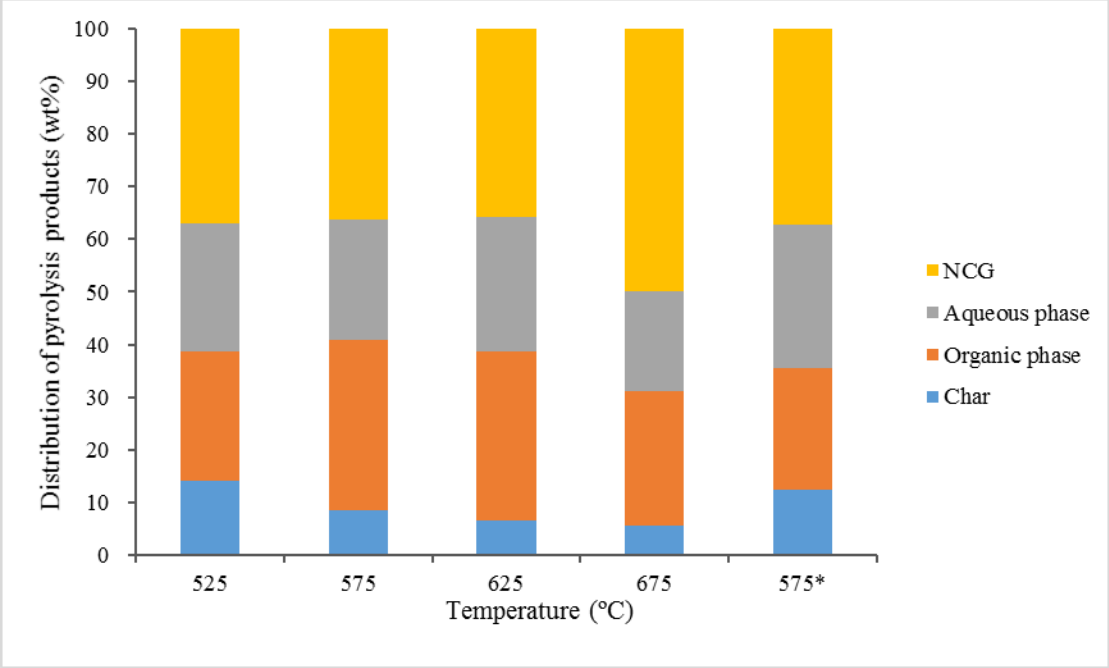

Figure 1. Distribution of pyrolysis products (*pyrolysis of only red oak)

The yields of two fractions of pyrolysis-oil produced are given in Fig. S1. The organic phase produced from co-pyrolysis of PBM was highly viscous and had waxy texture, especially for the pyrolysis oils produced at the lower end of the temperature range. The yield of the organic phase oil was 32.1 wt% at 625 ºC and then decreased to 25.4 wt% at 675 ºC. The maximum yield of aqueous phase was 25.5 wt% at 625 ºC. However, the change in the yield across the entire temperature range was rather small. The results indicate that increasing pyrolysis-oil yield up to 625 ºC was mainly contributed by the increase in the yield of the organic phase. When pyrolysis temperature further increased, the yields of the organic and aqueous phase both decreased.

Compared to pyrolyzing red oak alone, co-pyrolysis of PBM increased the yield of organic phase from 23.1 to 32.5 wt% whereas it decreased the yield of aqueous phase from 27.2 to 22.7 wt%. This result suggests that HDPE-derived products are mostly collected in organic phase.

The carbon balance among pyrolysis products was also calculated and given in Fig. 2. As temperature increased, the carbon content of char decreased from 20.1% to 7.9%. The carbon content in NCG remained similar (34 ~ 36%) up to 625 ºC before it increased to 48.46% at 675 ºC. Among the pyrolysis products, pyrolysis-oil contained 43.7 ~ 56.3% of carbon in the original feedstocks. The organic phase contained a significantly higher amount of carbon compared to other pyrolysis products. At 625 ºC, the organic phase alone contained 43.0% of total carbon. When pyrolysis temperature exceeds 625 ºC, the shift in carbon from organic and aqueous phase to NCG was observed due to cracking. Compared with pyrolysis of red oak alone, less carbon remained in char when PBM was co-pyrolyzed both at 575 ºC (19.6 vs. 12.1%) and increased amount of carbon ends up in the organic phase and NCG.

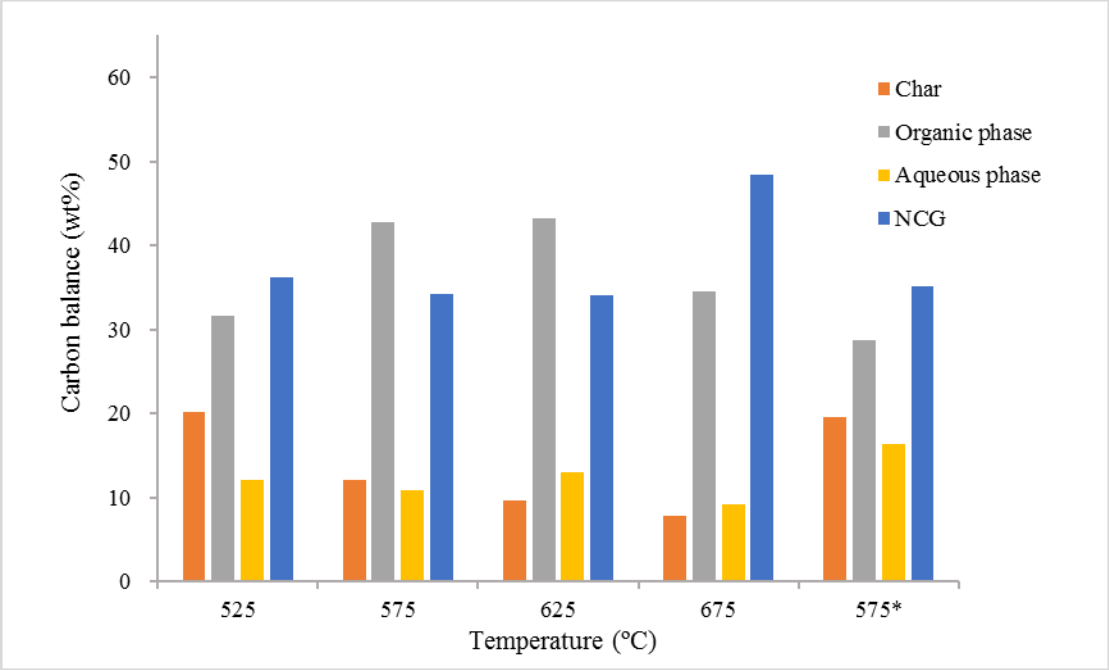

Figure 2. Carbon balance analysis of pyrolysis products (*pyrolysis of only red oak)

Characterization of pyrolysis-oil

Moisture content, modified acid number (MAN), elemental composition and higher heating value (HHV) of the organic and aqueous phases are listed in Table 1. The organic phase oil is nearly free of moisture attributed to the unique pyrolysis-oil collection system. Raising pyrolysis temperature increased carbon and hydrogen contents in the organic phase whereas it significantly reduced oxygen content. Oxygen content in the organic phase was only 13.77% at 675 ºC. Decreasing oxygen content improved HHV of the organic phase to 36.66 MJ/kg at the same temperature. Water produced from dehydration reaction of red oak was mostly collected in the aqueous phase as water content in this fraction was 40.44 - 44.57%. The change in CHO content was insignificant among the aqueous phase products of PBM. Due to the high water content, the HHVs of the aqueous phase were only 8.89 ~ 9.73 MJ/kg. MAN of aqueous phase decreased from 135.35mg KOH/g pyrolysis-oil to 105.95mg

KOH/g pyrolysis-oil when temperature increased, possibly due to decomposition of acids into NCG.

Table 1. Properties of pyrolysis-oil obtained from co-pyrolysis of PBM

Temperature (ºC)		525	575	625	675	575*
	Organic phase					
Elemental composition (wt%)	**C**	59.99	73.61	74.77	76.98	58.85
	H	5.71	9.23	9.33	9.14	6.24
	O[1)]	34.14	17.08	15.82	13.77	34.75
	N	0.13	0.08	0.08	0.10	0.11
	S	0.04	0.00	0.01	0.01	0.05
Higher heating value		22.95	35.16	35.87	36.66	23.23
Moisture (wt%)		0.79	1.56	1.60	1.20	3.90
	Aqueous phase					
Elemental composition (wt%)	**C**	26.84	26.94	28.42	27.17	28.47
	H	7.24	7.20	7.11	6.97	7.04
	O[1)]	64.93	64.91	64.11	65.24	63.26
	N	0.84	0.88	0.27	0.61	1.10
	S	0.16	0.08	0.09	0.01	0.14
Higher heating value[2)]		9.17	9.14	9.73	8.89	9.65
Moisture (wt%)		44.43	43.68	40.44	44.57	40.38
MAN (mg KOH/g)		135.35	123.09	113.94	105.95	111.52
Total moisture (wt%)[3)]		10.96	10.89	11.14	9.47	9.50

*Pyrolysis of red oak only

1) Determined by difference

2) Determined by theoretical calculation

3) Based on the total feedstock weight

Compared to pyrolysis-oil produced from red oak alone at 575 ºC, the HHV of the organic phase was much higher for co-pyrolysis of PBM (23.23 vs. 35.16 MJ/kg) mostly due to the additive effect of HDPE. However, the properties of the aqueous phase were less affected by co-pyrolyzing with HDPE. In fact, the aqueous phase produced from co-pyrolysis has slightly inferior properties compared to the aqueous phase produced from pyrolysis of only red oak, such as higher water content and MAN number. The result of increasing water from biomass during co-pyrolysis with a synthetic polymer was also found in the work of

Onal et.al [11]. This could be that hydrogen-transfer from decomposition of HDPE to red oak-derivatives enhanced water formation reactions by hydrodeoxygenation.

Table 2. Compositional analysis of pyrolysis-oils determined by GC/MSD-FID

Yield (wt%)	*Temperature (°C)*				
	525	***575***	***625***	***675***	***575[1)]***
Furfural	0.234	0.333	0.311	0.226	0.247
Acetol	0.922	1.005	1.328	1.035	0.851
2(5H)Furanone	0.125	0.138	0.129	0.081	0.141
Levoglucosan	2.238	2.470	2.196	1.770	2.433
Acetic acid	1.490	2.349	2.641	1.985	1.709
Dimethoxytetrahydrofuran	0.668	0.229	0.094	0.479	0.130
5-HMF	0.068	0.090	0.068	0.031	0.096
1,4:3,6-Dianhydro-α-d-glucopyranose	0.031	0.033	0.023	0.016	0.023
Sum of carbohydrate derivatives	***5.776***	***6.648***	***6.789***	***5.622***	***5.632***
phenol	0.010	0.019	0.032	0.043	0.019
guaiacol	0.042	0.036	0.027	0.020	0.035
2,6-dimethoxy phenol	0.065	0.069	0.035	0.019	0.070
2,6-methoxy 4-propenyl phenol	0.081	0.157	0.079	0.050	0.147
3,5-dimethoxy 4-hydroxy acetonphenone	0.030	0.041	0.038	0.023	0.041
3,5-dimethoxy 4-hydroxy benzenaldehyde	0.046	0.063	0.062	0.037	0.056
hydroquinone	0.018	0.025	0.027	0.018	0.020
3,5-dimethoxy acetophenone	0.037	0.047	0.035	0.025	0.047
vanillin	0.053	0.049	0.045	0.029	0.082
o-cresol	0.011	0.016	0.023	0.025	0.014
3(4)-methyl phenol	0.012	0.021	0.031	0.037	0.018
2-methoxy-p-cresol	0.029	0.026	0.023	0.021	0.026
4-ethyl,3-methyl phenol	0.005	0.008	0.013	0.011	0.007
2,4-dimethyl phenol	0.006	0.010	0.014	0.015	0.008
Sum of lignin derivatives	***0.445***	***0.587***	***0.486***	***0.373***	***0.588***
C8~C12	0.148	0.161	0.179	0.182	-
C13~C17	0.668	0.634	0.509	0.350	-
C18~C20	0.512	0.498	0.451	0.402	-
Sum of hydrocarbons	***1.327***	***1.293***	***1.140***	***0.933***	***-***

1) Pyrolysis of red oak only; The amount of carbohydrate derivatives and lignin derivatives were multiplied by 0.8 to obtain equivalence yield from red oak during co-pyrolysis.

The peaks of more than 50 oxygenated compounds and 60 aliphatic hydrocarbons were identified in the GC/MS chromatograms of pyrolysis-oils. Since the intensities of many

peaks were very low, only major peaks were quantified in this study. The yields of 22 oxygenates and HDPE-derived C_8-C_{20} hydrocarbons are given in Table 2. Since the HDPE pellets contain a negligible amount of oxygen, oxygenated products are assumed to originate from red oak. The oxygenated products were further grouped into carbohydrates-derived oxygenates (sugars, furans and acids) and lignin-derived oxygenates (phenols). Since PBM contains 80% red oak by weight, the product yields of red oak when it was pyrolyzed alone at 575 ºC was multiplied by 0.8 and reported in Table 2 in order to evaluate the synergistic effect of HDPE on the pyrolysis products of red oak during co-pyrolysis.

The yields of carbohydrate derived compounds first increased and then decreased as the pyrolysis temperature further increased. For example, the amount of levoglucosan, the major product from the depolymerization of cellulose, reached the maximum of 2.47% at 575 ºC then decreased to 1.77% at 675 ºC. It was previously reported that levoglucosan could decompose to light oxygenates in the vapor phase at relatively high temperatures (i.e., the temperature is higher than 600 °C) [29]. It is noteworthy that pyrolyzing red oak alone at temperatures higher than 500 ºC reduces the amount of carbohydrate derived compounds as the temperature increases. Thus, the above result suggests that optimum temperature for volatilizing pyrolysis products of red oak shifted to a temperature higher than 500 °C when red oak was co-pyrolyzed with HDPE. It was also found that the (equivalence) yield of carbohydrate-derived compounds in pyrolysis-oil was 5.63% when red oak alone was pyrolyzed (the red oak mass equivalence yield) whereas the yield increased to 6.65% by co-pyrolyzing PBM. As shown in the table 2, the yields of furans and acids improved by co-pyrolyzing PBM. Among the products, acetic acid was affected most by co-pyrolysis as the yield increased from 1.71% to 2.35%. In comparison, the yield of levoglucosan was not

affected by the presence of HDPE. While acetic acid is mainly produced from hemicellulose, it is also produced from decomposition of cellulose due to the dehydration reaction. Furans are also dehydration products of cellulose and hemicellulose. As it was reported in Table 1, co-pyrolysis increased the water content in pyrolysis-oil, suggesting the presence of HDPE promoted the dehydration reaction of carbohydrates in red oak whereas it did not influence the depolymerization reaction. Increased acids in pyrolysis-oil also explains higher MAN of aqueous phase obtained from co-pyrolysis compared to the pyrolysis-oil produced from pyrolysis of red oak alone.

The yields of phenolic monomers derived from the lignin fraction of red oak are also given in Table 2. Similar to carbohydrate-derived products, the total yield of phenols also first increased and then decreased with increasing pyrolysis temperature. The yield of most phenolic monomers, especially the phenols with longer side chains such as 3,5-dimethoxy 4-hydroxy acetonphenone, 3,5-dimethoxy 4-hydroxy benzenaldehyde, vanillin, 3,5-dimethoxy acetophenone, decreased with increasing temperature. It is likely that higher temperature promotes the cleavage of ketone and aldehyde functionalities from benzene rings. In return, the yields of phenol and methyl phenols monotonically increased with increasing temperature. While more phenol is formed due to the cracking of benzene ring-side chains at higher temperatures, the increased amount of methyl phenols is likely attributed to the hydrogen atoms donated by HDPE depolymeirzation. The total amount of quantified phenolic monomers produced in co-pyrolysis of PBM is similar to that of phenolic monomers evolved from pyrolysis of red oak alone at the same temperature. However, the amount of vanillin significantly decreased and in return methyl and propenyl phenols

increased during co-pyrolysis. This result also suggests that the interaction among phenolic radicals and HDPE-derived hydrogen or aliphatic radicals occurs during co-pyrolysis.

Depolymerization of plastics is commonly explained by free radical mechanisms [30, 31]. It was also suggested that the free radical generation from plastics decomposition is facilitated by free radicals generated by biomass [32]. Ates [33] stated that the radicals generated at the initial stage at lower temperatures from biomass pyrolysis were responsible for further decomposition of plastic polymer chains, e.g. by β-scission. They also speculated that the further transformation of radicals give different alkanes, carbonyl and hydroxyl groups or even aromatics. Furthermore, biomass-derived radicals can combine with plastic-derived radicals in a termination step to stabilize their structure [34]. High temperature favors these reactions since more of free radicals are produced.

Aliphatic hydrocarbons are derived from pyrolysis of HDPE. The hydrocarbons with C_{20}+ were also present but not quantified due to low solubility of these chemicals in both polar and non-polar solvents for GC/MSD-FID analysis. The total amount of quantified hydrocarbons decreased with increasing pyrolysis temperature. However, the amount of C_8~C_{12} increased with temperature at the expense of decreasing the amount of C_{13}+ hydrocarbons. This trend suggests that high pyrolysis temperature promoted the shift of the hydrocarbons with longer chains to shorter chain products.

Composition of non-condensable gases

Fig. S2 shows the yield of calibrated non-condensable gases. For all the experimental cases, carbon monoxide and carbon dioxide were two major gases in NCG. While both CO and CO_2 increased as pyrolysis temperature increased, the increase in the yield of CO was

much faster than that of CO_2. This indicates that higher temperature promotes decarbonylation more than decarboxylation. Higher temperature also promoted the increase in hydrogen and light hydrocarbon gases. The hydrocarbons (methane, ethane, ethylene and propane) yield was 1.8 wt% at 525 ºC and increased to 11.2 wt% at 675 ºC. Depolymerization of HDPE contributes to the high yield of light hydrocarbons since pyrolysis of red oak produces only a limited amount of hydrocarbon gases. It should be noted that the sum of the yields of the quantified NCGs are lower than the yield of total NCG calculated by the difference (100 % - pyrolysis oil % - char %). Light hydrocarbon gases with C_4+ that were not calibrated are expected to make up the difference in NCG yields.

Characterization of char

Properties of char, including the elemental composition, higher heating value and BET surface area, are listed in Table 3. Temperature dependence of elemental composition of char produced co-pyrolysis displayed an interesting trend. Increasing pyrolysis temperature increased carbon content and decreased oxygen content in char up to 625 ºC. Further increase in temperature decreased carbon content whereas increasing oxygen content of the char. In comparison, hydrogen content decreased monotonically along with increasing temperatures. The HHV of char reached its maximum of 29.11 MJ/kg at 625 ºC. Recall that the optimum yield of pyrolysis oil was also obtained at the given temperature. Also shown in Table 3, BET surface area of char monotonically increased from 3.074 to 7.569 m^2/g with increasing temperature. It is somehow expected since high temperature promotes the products volatilization and the reaction between C and CO_2 to form CO, thus making more porous char. Compared to pyrolysis of red oak alone, the char produced from co-pyrolysis of PBM

was higher in carbon content and lower in hydrogen and oxygen contents. As a result, the HHV of the char produced from co-pyrolysis was about 10% higher than that obtained from pyrolysis of red oak at the same temperature. It was also found that BET surface area of the char produced from co-pyrolysis was much lower than that of the char produced from red oak alone (3.80 vs. 6.75m^2/g).

Table 3. Properties of char

Temperature (ºC)		**525**	**575**	**625**	**675**	**575***
	char					
Elemental composition (wt%)	**C**	77.85	80.42	81.57	78.48	74.27
	H	3.08	2.96	2.92	2.83	3.22
	O[1)]	18.71	16.27	15.15	18.30	22.06
	N	0.31	0.31	0.32	0.38	0.31
	S	0.05	0.05	0.05	0.02	0.13
Higher heating value (MJ/kg)[2)]		27.53	28.59	29.11	27.44	26.02
BET surface area (m^2/g)		3.074	3.798	5.263	7.569	6.745

*Pyrolysis of red oak only

1) Determined by difference
2) Determined by theoretical calculation

The results of FT-IR analysis of the chars are shown in Fig.3. For all the spectra, aliphatic hydrocarbons such as alkanes and alkenes were detected at 3000-2860 cm^{-1}, and C-C, C-O stretching in aromatics were detected at 1200-1300 cm^{-1}. The intensities of these peaks were found to decrease with increasing temperature. This trend is in agreement with the decrease of phenols with ketone and aldehyde functionalities in the pyrolysis-oil produced at higher temperatures. The peaks at 1600 cm^{-1} and 1712 cm^{-1} were assigned to aromatic C=O and aromatic COOH/C=O stretching, respectively. These bands showed great intensity in samples, which are characterizations of highly condensed aromatic structure in char [26]. Some other peaks at 2100 cm^{-1} and 1900 cm^{-1} are assigned to Si-O and Si-H stretching [35]. These peaks showed relatively constant intensity, which could be attributed

to the ash content of char and small sand particles that traveled with char out the reactor. As shown in Fig. 3, co-pyrolysis char showed very strong intensity of aliphatic compounds whereas the corresponding intensity was very weak for the red oak char.

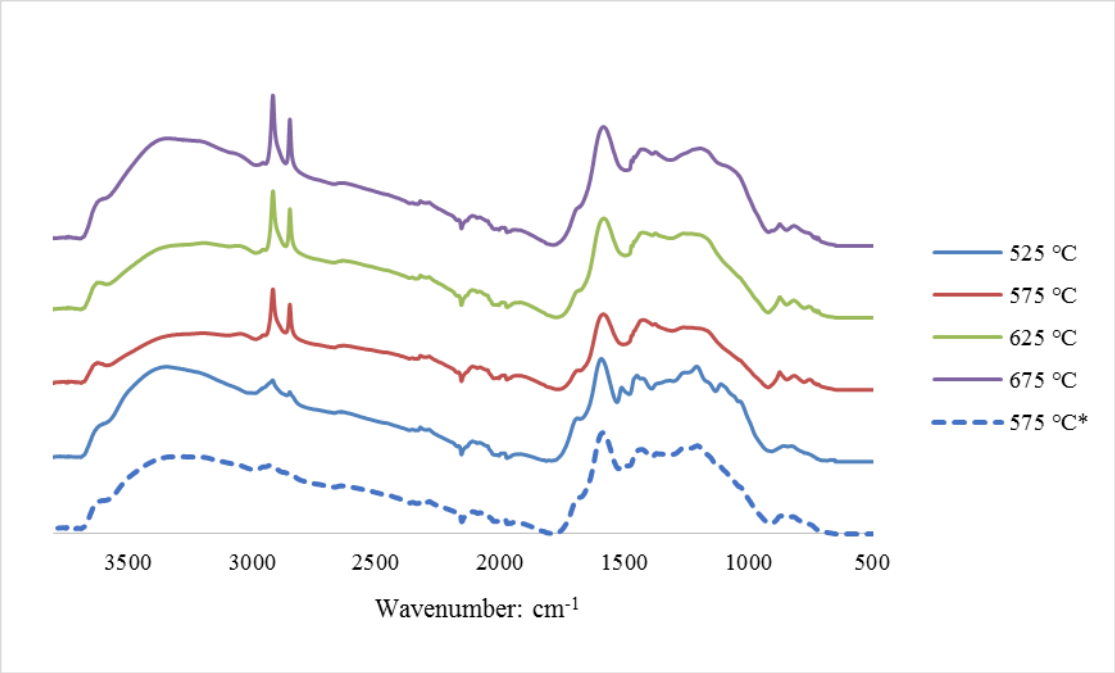

Figure 3. FT-IR spectra of char samples (*Char from pyrolysis of only red oak)

Fig.4 shows the microstructures of the chars produced from co-pyrolysis of PBM and pyrolysis of red oak (biochar), both at 575 ºC. The chars had no apparent difference in visual observation: both were fine powders that retaining the shape of raw red oak particles. However, the SEM images showed that the two chars have a distinct difference in their microstructures. The surface of the char produced from co-pyrolysis of PBM was covered by small particulate matter, some of the particulates were even embedded into the pores of the char. This phenomenon was not found in the char produced from red oak biochar. The pores of the char obtained from co-pyrolysis of PBM have larger diameters but are shallower compared to that of red oak biochar. HDPE melts at about 200 ºC but does not volatilize until it reaches higher temperatures (≥450 ºC). As a result, red oak particles that already started to

decompose would be covered by melted HDPE on its surface at lower the temperature region. The unique pore shapes suggest that during co-pyrolysis, the synergetic interaction between red oak particles and melted HDPE enhances decomposition of red oak at the interface of the contact to form large pores. However, the shell effect of melted HDPE also prevents pyrolysis products of red oak escaping from the interior of the particles, and thus creates shallow pores. The small particulate matter is likely HDPE-derived long chain hydrocarbons. Due to low volatility and a short reaction time inside the reactor, the hydrocarbons with long chains remain on the surface of red oak char after pyrolysis. These particulates could increase the carbon and hydrogen contents in char and therefore increase its HHV. The BET area of the char decreased for co-pyrolysis due to the blockages of the pores by the particulate matter and the formation of shallow pores that do not allow nitrogen gas to pass through during the BET absorption test.

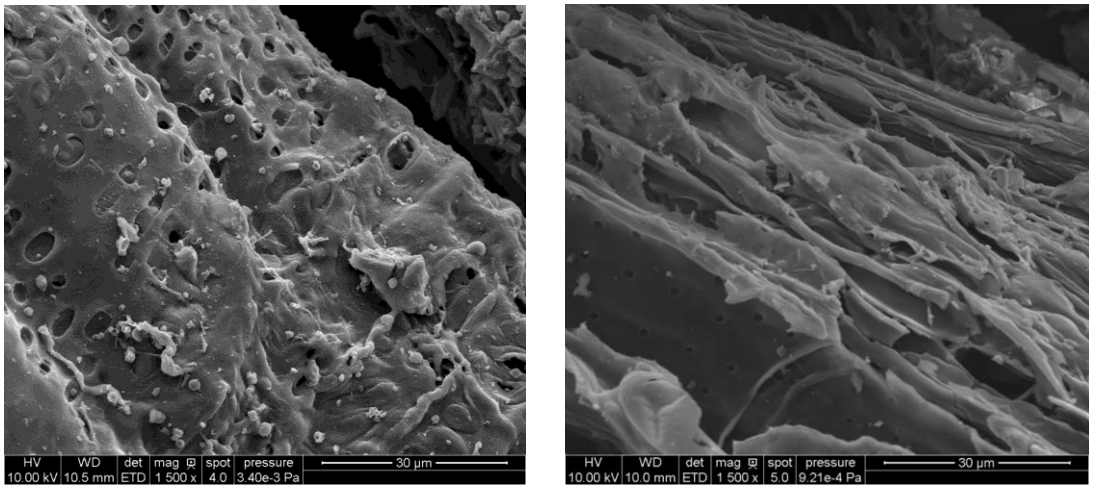

(a) **(b)**

Figure 4. SEM images of pyrolysis char obtained at 575 °C; (a) Char produced from co-pyrolysis of PBM; (b) Char produced from pyrolysis of red oak.

Conclusion

Fast co-pyrolysis of red oak and HDPE was conducted in a fluidized bed reactor with temperatures ranging from 525 ºC to 675 ºC. The maximum pyrolysis-oil yield of 57.6 wt%

was achieved at 625 ºC, at a temperature significantly higher than the optimum temperature of biomass. The synergetic effect among red oak and HDPE is evaluated by comparing the yields and properties of oxygenated products generated when red oak or PBM is pyrolyzed both at 575 °C. A significant synergetic effect was found during co-pyrolysis. The presence of HDPE increased the formation of furans and acids, decreased the amount of vanillin, and in return increased the amount of methyl or propenyl phenols. The total water content produced from red oak was also increased by the addition of HDPE, suggesting the dehydration reaction was enhanced by hydrogen transfer from HDPE. It was also found that co-pyrolysis of PBM not only reduces the amount of char produced from red oak, but also changes the properties of char. The synergetic interaction among red oak and melted HDPE resulted in the formation of large and shallow micropores on the surface of red oak. It was also found that the BET surface of char was largely reduced by co-pyrolyzing red oak with HDPE.

Acknowledgements

The research was supported by Iowa Energy center. The authors would like to thank Tannon Dauggard and Kyle Steen for assistance in operating fluidized bed reactor. Authors also thank Bernardo del Campo for instructions and assistance in conducting the experiment and processing the data of the char BET surface area.

References

[1] B.F. Staley, M.A. Barlaz, Composition of Municipal Solid Waste in the United States and Implications for Carbon Sequestration and Methane Yield, Journal of Environmental Engineering, 135 (2009) 901-909.

[2] J. Mata-Alvarez, S. Macé, P. Llabrés, Anaerobic digestion of organic solid wastes. An overview of research achievements and perspectives, Bioresource Technology, 74 (2000) 3-16.

[3] T. Malkow, Novel and innovative pyrolysis and gasification technologies for energy efficient and environmentally sound MSW disposal, Waste Management, 24 (2004) 53-79.

[4] G.W. Huber, S. Iborra, A. Corma, Synthesis of transportation fuels from biomass: chemistry, catalysts, and engineering, Chemical reviews, 106 (2006) 4044.

[5] F. Shafizadeh, Introduction to pyrolysis of biomass, Journal of Analytical and Applied Pyrolysis, 3 (1982) 283-305.

[6] T.P. Vispute, H. Zhang, A. Sanna, R. Xiao, G.W. Huber, Renewable chemical commodity feedstocks from integrated catalytic processing of pyrolysis oils, Science (New York, N.Y.), 330 (2010) 1222.

[7] Q. Zhang, J. Chang, T. Wang, Y. Xu, Review of biomass pyrolysis oil properties and upgrading research, Energy Conversion and Management, 48 (2007) 87-92.

[8] F. Abnisa, W.M.A. Wan Daud, A review on co-pyrolysis of biomass: An optional technique to obtain a high-grade pyrolysis oil, Energy Conversion and Management, 87 (2014) 71-85.

[9] P. Costa, F. Pinto, M. Miranda, R. André, M. Rodrigues, Study of the Experimental Conditions of the Co-pyrolysis of Rice Husk and Plastic Wastes, CHEMICAL ENGINEERING, 39 (2014).

[10] Y. Matsuzawa, M. Ayabe, J. Nishino, Acceleration of cellulose co-pyrolysis with polymer, Polymer Degradation and Stability, 71 (2001) 435-444.

[11] E. Önal, B.B. Uzun, A.E. Pütün, Bio- oil production via co- pyrolysis of almond shell as biomass and high density polyethylene, Energy Conversion and Management, 78 (2013) 704-710.

[12] J.D. Martínez, A. Veses, A.M. Mastral, R. Murillo, M.V. Navarro, N. Puy, A. Artigues, J. Bartrolí, T. García, Co- pyrolysis of biomass with waste tyres: Upgrading of liquid bio-fuel, Fuel Processing Technology, 119 (2013) 263-271.

[13] M. Brebu, S. Ucar, C. Vasile, J. Yanik, Co- pyrolysis of pine cone with synthetic polymers, Fuel, 89 (2010) 1911-1918.

[14] V.I. Sharypov, N. Marin, N.G. Beregovtsova, S.V. Baryshnikov, B.N. Kuznetsov, V.L. Cebolla, J.V. Weber, Co- pyrolysis of wood biomass and synthetic polymer mixtures. Part I: influence of experimental conditions on the evolution of solids, liquids and gases, Journal of Analytical and Applied Pyrolysis, 64 (2002) 15-28.

[15] T. Cornelissen, M. Jans, J. Yperman, G. Reggers, S. Schreurs, R. Carleer, Flash co-pyrolysis of biomass with polyhydroxybutyrate: Part 1. Influence on bio-oil yield, water content, heating value and the production of chemicals, Fuel, 87 (2008) 2523-2532.

[16] J. Zheng, Y.-q. Jin, Y. Chi, J.-m. Wen, X.-g. Jiang, M.-j. Ni, Pyrolysis characteristics of organic components of municipal solid waste at high heating rates, Waste Management, 29 (2009) 1089-1094.

[17] F. Paradela, F. Pinto, A.M. Ramos, I. Gulyurtlu, I. Cabrita, Study of the slow batch pyrolysis of mixtures of plastics, tyres and forestry biomass wastes, Journal of Analytical and Applied Pyrolysis, 85 (2009) 392-398.

[18] E. Jakab, M. Blazsó, O. Faix, Thermal decomposition of mixtures of vinyl polymers and lignocellulosic materials, Journal of Analytical and Applied Pyrolysis, 58 (2001) 49-62.

[19] M. Sajdak, R. Muzyka, Use of plastic waste as a fuel in the co-pyrolysis of biomass. Part I: The effect of the addition of plastic waste on the process and products, Journal of Analytical and Applied Pyrolysis, 107 (2014) 267-275.

[20] M. Sajdak, K. Słowik, Use of plastic waste as a fuel in the co-pyrolysis of biomass: Part II. Variance analysis of the co-pyrolysis process, Journal of Analytical and Applied Pyrolysis, 109 (2014) 152-158.

[21] M. Sajdak, R. Muzyka, J. Hrabak, K. Słowik, Use of plastic waste as a fuel in the co-pyrolysis of biomass: Part III: Optimisation of the co-pyrolysis process: Part III: Optimisation of the co-pyrolysis process, Journal of Analytical and Applied Pyrolysis, 112 (2015) 298-305.

[22] P. Bhattacharya, P.H. Steele, E.B.M. Hassan, B. Mitchell, L. Ingram, C.U. Pittman, Wood/ plastic copyrolysis in an auger reactor: Chemical and physical analysis of the products, Fuel, 88 (2009) 1251-1260.

[23] S. Czernik, A.V. Bridgwater, Overview of Applications of Biomass Fast Pyrolysis Oil, Energy & Fuels, 18 (2004) 590-598.

[24] P.T. Williams, S. Besler, The influence of temperature and heating rate on the slow pyrolysis of biomass, Renewable Energy, 7 (1996) 233-250.

[25] G. Elordi, M. Olazar, G. Lopez, M. Artetxe, J. Bilbao, Product Yields and Compositions in the Continuous Pyrolysis of High-Density Polyethylene in a Conical Spouted Bed Reactor, Industrial & Engineering Chemistry Research, 50 (2011) 6650-6659.

[26] K.H. Kim, X. Bai, M. Rover, R.C. Brown, The effect of low- concentration oxygen in sweep gas during pyrolysis of red oak using a fluidized bed reactor, Fuel, 124 (2014) 49-56.

[27] D. Kunii, Fluidization engineering / Daizō Kunii, Octave Levenspiel, Huntington, N.Y. : R. E. Krieger Pub. Co., Huntington, N.Y., 1977.

[28] A. Demirbaş, Calculation of higher heating values of biomass fuels, Fuel, 76 (1997) 431-434.

[29] P.R. Patwardhan, J.A. Satrio, R.C. Brown, B.H. Shanks, Influence of inorganic salts on the primary pyrolysis products of cellulose, Bioresource Technology, 101 (2010) 4646-4655.

[30] P.E. Savage, Mechanisms and kinetics models for hydrocarbon pyrolysis, Journal of Analytical and Applied Pyrolysis, 54 (2000) 109-126.

[31] J.F. Mastral, C. Berrueco, J. Ceamanos, Theoretical prediction of product distribution of the pyrolysis of high density polyethylene, Journal of Analytical and Applied Pyrolysis, 80 (2007) 427-438.

[32] J.A. Conesa, A. Marcilla, R. Font, J.A. Caballero, Thermogravimetric studies on the thermal decomposition of polyethylene, Journal of Analytical and Applied Pyrolysis, 36 (1996) 1-15.

[33] F. Ateş, N. Miskolczi, N. Borsodi, Comparision of real waste (MSW and MPW) pyrolysis in batch reactor over different catalysts. Part I: Product yields, gas and pyrolysis oil properties, Bioresource Technology, 133 (2013) 443-454.

[34] F. Ateş, M.A. Işıkdağ, Influence of temperature and alumina catalyst on pyrolysis of corncob, Fuel, 88 (2009) 1991-1997.

[35] E. Pretsch, Structure determination of organic compounds : tables of spectral data / Ernö Pretsch, Philippe Bühlmann, Martin Badertscher, Berlin : Springer, Berlin, 2009.

SUPPLEMENTAL INFORMATION FOR CHAPTER 2

Table S1. Ultimate and proximate analysis of red oak and HDPE

Red Oak		***High density polyethylene***	
Ultimate analysis (wt%)		***Ultimate analysis (wt%)***	
Carbon	47.16	Carbon	84.59
Hydrogen	5.39	Hydrogen	14.10
Oxygen[1)]	47.24	Oxygen[1)]	1.02
Nitrogen	0.12	Nitrogen	0.29
Proximate analysis (wt%)[2)]		***Proximate analysis (wt%)***[2)]	
Moisture content	7.74	Moisture content	0
Volatile	80.39	Volatile	99.80
Fixed carbon	11.46	Fixed carbon	0
Ash	0.64	Ash	0.20

1) Determined by difference
2) Determined by TGA analysis

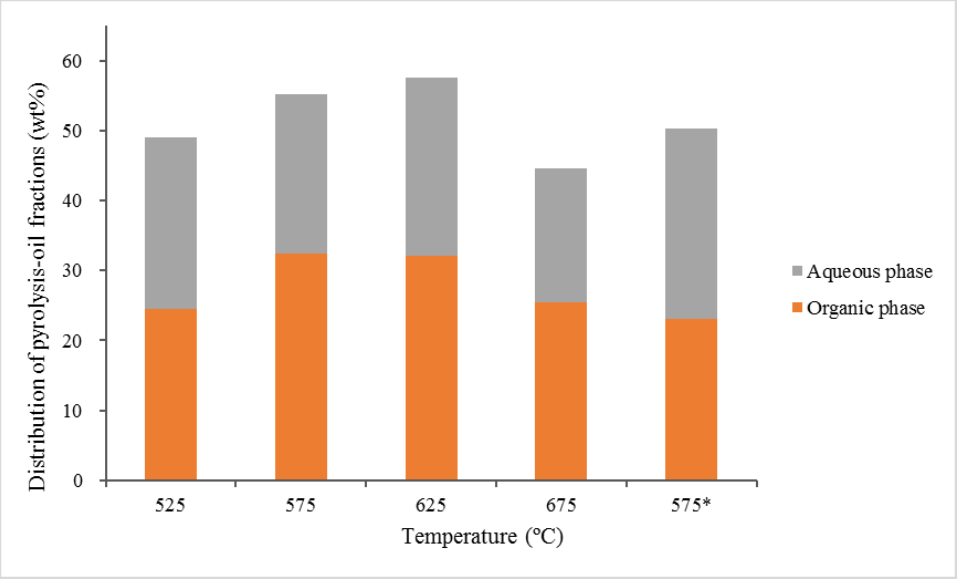

Figure S1. Distribution of organic and aqueous phases from co-pyrolysis (*pyrolysis of only red oak)

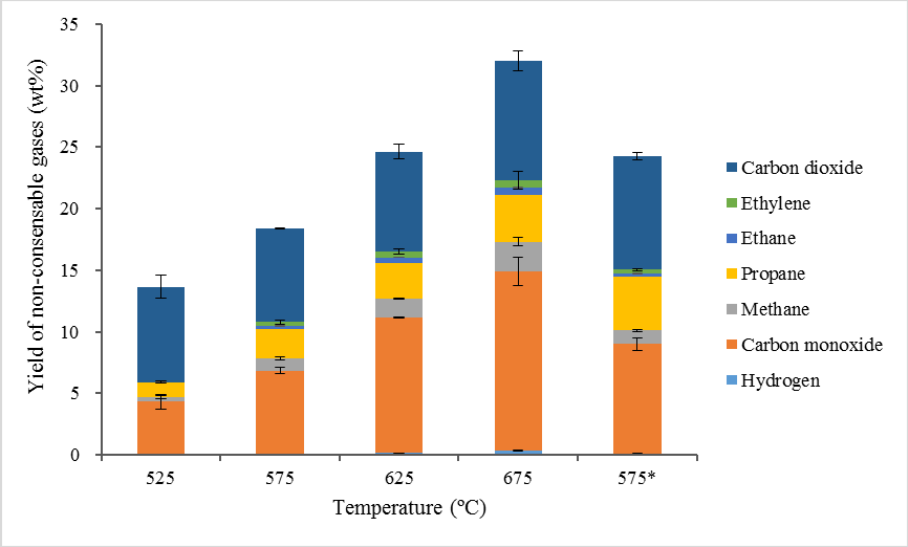

Figure S2. Composition of non-condensable gases (*pyrolysis of only red oak)

CHAPTER 3

CATALYTIC CO-PYROLYSIS OF BIOMASS AND POLYETHYLENE IN A TANDEM MICROPYROLYZER

A paper published to the journal *Fuel*

Yuan Xue[3], Atul Kelkar[1], Xianglan Bai[1*]

Abstract

In the present study, catalytic fast co-pyrolysis of biomass and polyethylene (PE) was studied in a tandem micro-pyrolyzer using ZSM-5 as the catalyst. Cellulose, xylan and milled wood lignin were co-pyrolyzed with PE in both the presence and absence of catalyst to investigate the interaction between biomass and PE during thermal depolymerization and the following catalytic upgrade of the pyrolysis vapor. Co-pyrolysis with PE was found to increase the yields of furans and double anhydrosugar from cellulose up to 45%. Co-pyrolysis of xylan and PE increased not only the yields of furans and double anhydrosugar, but also the yield of acetic acid by 45%. Depolymerization of lignin was strongly promoted by PE as the yields of various phenolic monomers increased up to 43%. It was also found that the amounts of pyrolysis char and carbon oxides produced from biomass compounds decrease when co-pyrolyzed with PE. The presence of cellulose, xylan or lignin, on the other hand, facilitated depolymerization of PE by increasing the yields of olefins and alkanes with shorter carbon chain. When the pyrolysis vapor was upgraded by HZSM-5 zeolite catalyst, synergy increased the yields of hydrocarbons and suppressed the formation of catalytic coke, compared to when biomass compounds and PE were independently converted. During

[3] Department of Mechanical Engineering, Iowa State University, Ames, Iowa 5001
* Corresponding author. Postal address: Iowa State University, 2070 Black Engineering Building, Ames, IA 50011; Tel: +1 515 294 6886; Fax: +1 515 294 3261; E-mail address: bxl9801@iastate.edu (X. Bai)

catalytic co-pyrolysis of cellulose and PE, the increase of the aromatic hydrocarbon yield was accompanied by the decrease in the selectivity of ethylene and propylene and no significant increase of total aliphatic hydrocarbons (i. e., the sum of olefins and alkanes), suggesting Diels-Alder reaction as the dominant reaction. On the other hand, catalytic co-pyrolysis of PE with xylan or lignin increased both the yields of aromatic and aliphatic hydrocarbons. The yield of alkanes decreased most significantly in the mixture of lignin and PE, suggesting that phenolic compounds act as strong hydrogen acceptors when they deoxygenate. In the present study, red oak and PE were also catalytically co-pyrolyzed and the effects of pyrolysis temperature and catalyst temperature on product distribution and the extent of synergy were investigated. Both higher pyrolysis temperature and catalyst temperature were able to reduce the formation of catalytic coke and increase the yield of aromatic hydrocarbons monotonically. However, the maximum yield of aliphatic hydrocarbons was obtained at the intermediate pyrolysis temperature or catalyst temperature. Synergy between biomass and PE was consistent, regardless of changing pyrolysis temperatures. In comparison, the synergy became less significant when catalytic temperature was increased.

Keywords: Biomass; Polyethylene; Catalytic pyrolysis; Zeolite catalyst; Hydrocarbons

Introduction

Lignocellulosic biomass is a carbon neutral and renewable substitute for fossil fuels in the production of hydrocarbons and other platform chemicals. Pyrolysis of biomass has been widely studied in different scales due to its simple process and economic advantages [1, 2]. When it is fast pyrolyzed and the pyrolysis vapor is rapidly quenched, up to 75% of

biomass converts to bio-oil that has higher energy density than biomass and can be easily transported [3]. Bio-oil is a mixture of oxygenated compounds; thus, it has to be catalytically deoxygenated before becoming biofuels. Catalytic pyrolysis is an approach that deoxygenates biomass during pyrolysis, before the vapor condenses. Compared to upgrading condensed bio-oil, catalytic pyrolysis eliminates the secondary reactions of bio-oil during storage and re-heating. Catalytic pyrolysis can be a simple and cost-effective way to produce hydrocarbons in a single process. However, similarly to the problems also found in the catalytic upgrading of bio-oil, catalytic pyrolysis of biomass usually produces low yields of hydrocarbons and large amounts of solid residues. Rapid deactivation of catalyst caused by catalyst coke reduces the lifetime of the catalyst and the need for frequent catalyst regeneration could make the process impractical. The aforementioned problems are mostly attributed to the intrinsically high oxygen content and hydrogen deficiency of biomass. Catalytic hydropyrolysis using hydrogen gas at elevated pressures removes oxygen in biomass by forming water and therefore enhances hydrocarbon yields and reduces solid residues [4, 5]. However, continuously feeding dry biomass into high-pressure reactors could be challenging. Alternatively, hydrogen can also be supplied externally, by co-pyrolyzing biomass and hydrogen rich materials at atmospheric pressure [6]. Co-pyrolysis with plastics is particularly attractive since waste plastics are abundantly available at low-cost. Many plastic materials are rich in hydrogen and contain less oxygen. For example, polyethylene (PE) is a hydrocarbon-based polymer containing virtually no oxygen, and also accounts for up to 40% of total plastic waste [7]. Although some are recycled, a significant portion of the waste plastics eventually ends up in landfill sites, creating a number of environmental

problems. Thus, co-pyrolysis of biomass and plastics also has the additional benefits of promoting a cleaner environment and energy recapture.

While co-pyrolysis of biomass and different forms of plastics were frequently studied, it should be noted that most studies were conducted in fixed reactors [8]. Although slowly pyrolyzing the mixed feedstock for extended reaction time could enhance the decomposition of plastic polymers to smaller molecular units, this pyrolysis method is detrimental to biomass conversion. When slowly pyrolyzed, biomass is preferentially decomposed into less valuable char and light oxygenated gases, as opposed to bio-oil. In recent years, catalytic fast co-pyrolysis of biomass and plastics was studied by a few research groups using micro-pyrolysis reactors [9-13]. The studies showed that positive synergy between biomass and plastics increases hydrocarbon yields and reduces solid residues. It was also suggested that the Diels-Alder reaction among carbohydrate-derived furans and plastic derived olefins in the catalytic site improves hydrocarbon yields during co-pyrolysis. Nevertheless, significantly varied results were observed among the literature. For example, the yields of aromatic hydrocarbons were varied from less than 10% to over 35%, despite that cellulose and PE were co-pyrolyzed using the same catalyst (ZSM-5) [9, 11]. The reaction mechanism between biomass compounds and plastics can be very complex [10] and requires further investigation. For example, Diels-Alder reaction does not occur between lignin and plastics. Catalytic co-pyrolysis of biomass and plastics involves two different types of interaction: the interaction among biomass and plastics during thermal decomposition by pyrolysis (i.e., thermal interaction) and the interaction between the decomposition products at the catalyst site (i.e., catalytic interaction). Thermal interaction is often ignored when the synergy of catalytic co-pyrolysis is described, since it is assumed that the reaction time during fast

pyrolysis is too short (i.e., within seconds) for biomass and plastics to thermally interact [14]. On the other hand, we recently conducted fast pyrolysis of biomass and plastic in a fluidized bed reactor without catalyst and found that the co-pyrolysis products were not a mixture of the pyrolysis products of biomass and plastics by simple addition [15]. This suggests that catalytic co-pyrolysis could proceed in a much more complex reaction pathway than it was previously proposed by others [9-12].

In the present study, biomass model compounds and PE were co-pyrolyzed using a tandem micropyrolyzer system with and without downstream catalytic bed to determine thermal interaction and catalytic interaction between the different feedstock materials. PE was selected since it is the most abundant plastic in the waste stream and also has been reported to have the strongest synergy with biomass during co-pyrolysis when compared to other types of plastics [9, 11]. In this study, red oak and PE were also co-pyrolyzed. Pyrolysis and catalyst temperatures were changed independently and the product distribution and synergy at varied reaction conditions were investigated.

Materials and Methods

Materials

Northern red oak (Quercus Rubra) was purchased from Wood Residues Solutions (Montello, WI). The bark free chips were first ground by a mill cut and then sieved to a particle size under 75μm. Cellulose, xylan, and PE were purchased from Sigma Aldrich. The particle sizes of PE were between 53-75 μm. Milled wood lignin was extracted from red oak following the procedure described by Bjorkman [16]. The elemental composition of red oak and its model compounds is given in Table 1.

HZSM-5 zeolite (CBV 3024 E, SiO_2/Al_2O_3=30:1) was purchased from Zeolyst International. The catalyst was first activated in a muffle furnace at 550 °C for 4 hours and then pelletized and screened to 50-70 mesh size before being used.

Table 1. Elemental composition of feedstock

Feedstock	Elemental analysis (wt%)			
	C	H	N	O[a]
Red oak	47.16	5.39	0.12	47.24
Cellulose	43.87	5.61	1.95	48.57
Xylan	42.02	5.17	0.11	52.7
Milled wood lignin	58.3	6.01	0.06	35.6
PE	85.71	14.29	0	0

[a] Determined by difference

Pyrolysis experiment

Fast pyrolysis was conducted in a Tandem micro-pyrolyzer system (Rx-3050 TR, Frontier Laboratories, Japan). The schematic setup of the system can be found elsewhere [17]. The Tandem micro-pyrolyzer consists of two stage reactors; a pyrolysis reactor and a catalytic bed. The temperature of each reactor can be controlled independently and the maximum allowed temperature is 900 °C.

For catalytic pyrolysis, an approximately 0.5mg sample was placed in a deactivated stainless steel cup, and then dropped into a preheated oven in the first reactor. The pyrolysis vapors were then carried by helium gas to the catalyst bed loaded with 10mg of catalyst. During co-pyrolysis tests, the mixture of 0.25mg PE and either 0.25mg red oak or its model compounds (i. e., cellulose, xylan or milled wood lignin) was placed inside of the cup. For non-catalytic pyrolysis, the catalyst bed was replaced with an empty quartz tube and the above tests were repeated.

Characterization of pyrolysis products

An Agilent 7890A gas chromatography (GC) with a three-way splitter was used to separate the volatile products from the micro-pyrolyzer. The GC oven temperature was kept at 40 °C for 3 minutes, then ramped to 250 °C with a heating rate of 10 °C/min, where it stayed for an additional 6 minutes. The front inlet temperature was kept at 280 °C to prevent the condensation of the products. Two ZB-1701 (60 m × 250 μm × 0.25 μm) capillary columns were connected to mass spectrometer (MS, 5975C, Agilent, USA) and flame ionization detector (FID), respectively. The volatile compounds were first identified in MS and then quantified using FID. The hydrocarbon compounds were calibrated with the authentic chemicals purchased from Sigma Aldrich. Depending on the solubility, the authentic chemicals were first dissolved in methanol or hexane with five different concentrations and then injected into GC/MS-FID prior to experiments. The regression coefficient of the calibration curve is no less than 0.99. A Porous Layer Open Tubular column (60 m × 0.320 mm) (GS-GasPro, Agilent, USA) was connected to a thermal conductivity detector (TCD), which is used to measure the oxygenated gas (CO and CO_2) and light hydrocarbons (CH_4, C_2H_6, C_2H_4, C_3H_6, C_3H_8, C_4H_8 and C_5H_{10}). The gas standard used for calibration was a mixture of the above mentioned gases diluted in helium (Praxair, USA). The yield of pyrolysis char was quantified by weighing the sample cup before and after the test. The catalytic coke accumulated on the catalyst was analyzed using CHNS elemental analyzer (vario MICRO cube).

All the tests were triplicated to ensure reproducibility, and the standard derivations of the experimental results are reported. The yields of pyrolysis products were reported based

on molar carbon yields. It was calculated by dividing the mole of carbon in a product by total carbon mole in the feedstock.

Results and discussions

Co-pyrolysis of biomass model compounds with PE

Non-catalytic co-pyrolysis

Cellulose, xylan and lignin were used as model compounds of biomass and co-pyrolyzed with PE to determine thermal interaction during co-pyrolysis of biomass and PE. In this study, milled wood lignin extracted from red oak was used to better represent natural lignin in biomass [16, 18]. Xylan is derived from birch wood.

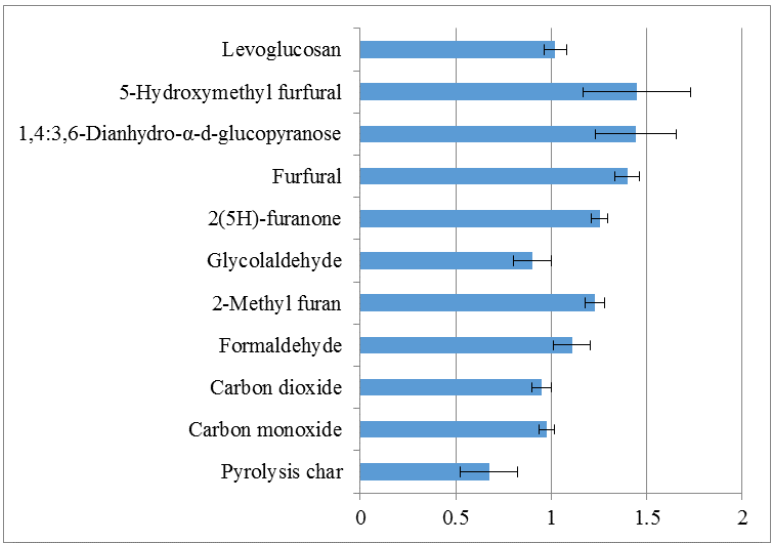

(a)

Figure 1. Ratios of product yields during co-pyrolysis of biomass model compounds and PE to pyrolysis of individual feedstock determined by GC/MS peak area (except the ratio of char is determined by weight). (a)-(c) are oxygenated compounds; (a) Cellulose-derived products; (b) Xylan-derived products; (c) Lignin-derived products; (d)-(f) are PE-derived aliphatic hydrocarbons when PE is co-pyrolyzed with (d) Cellulose; (e) Xylan; (f) Lignin; (g) is C_1-C_4 hydrocarbons when PE was co-pyrolyzed with different biomass model compounds. (C_n includes both alkanes and olefins containing n carbon atoms in (d)-(g))

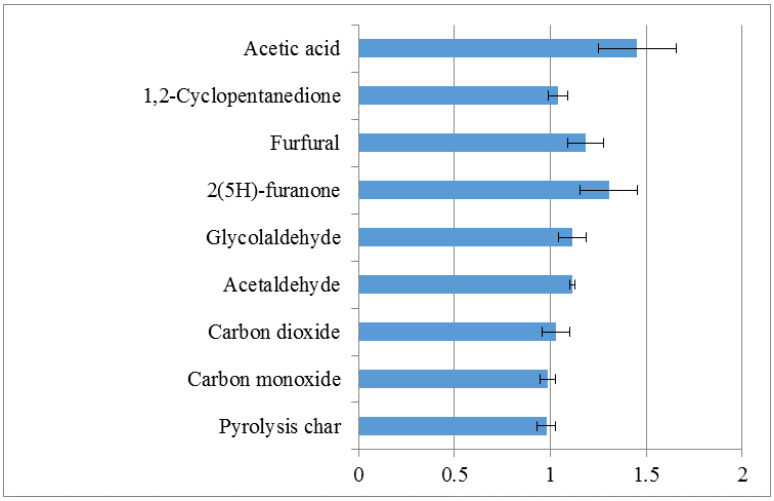

(b)

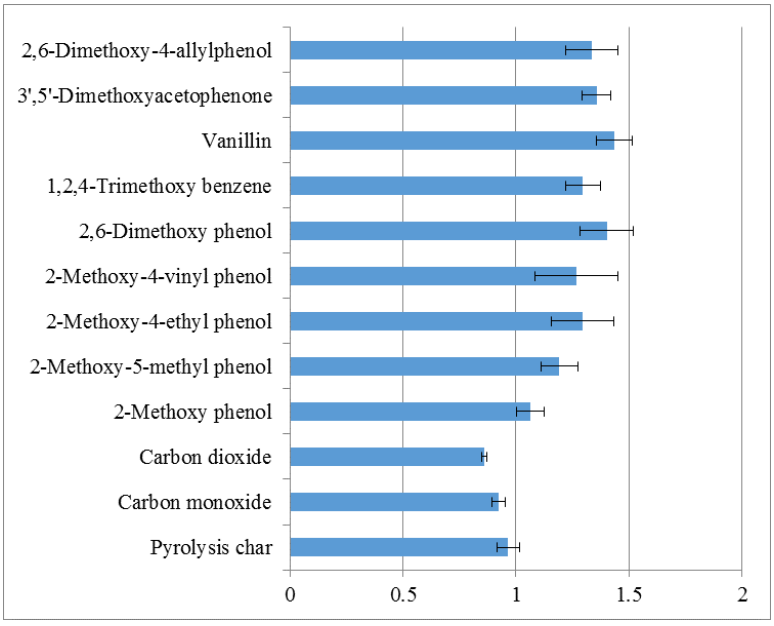

(c)

Figure 1. Continued

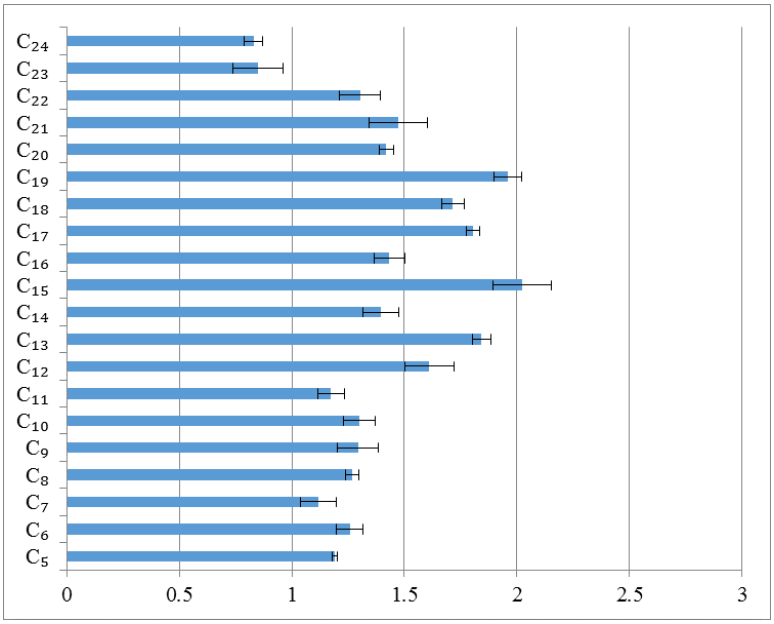

(d)

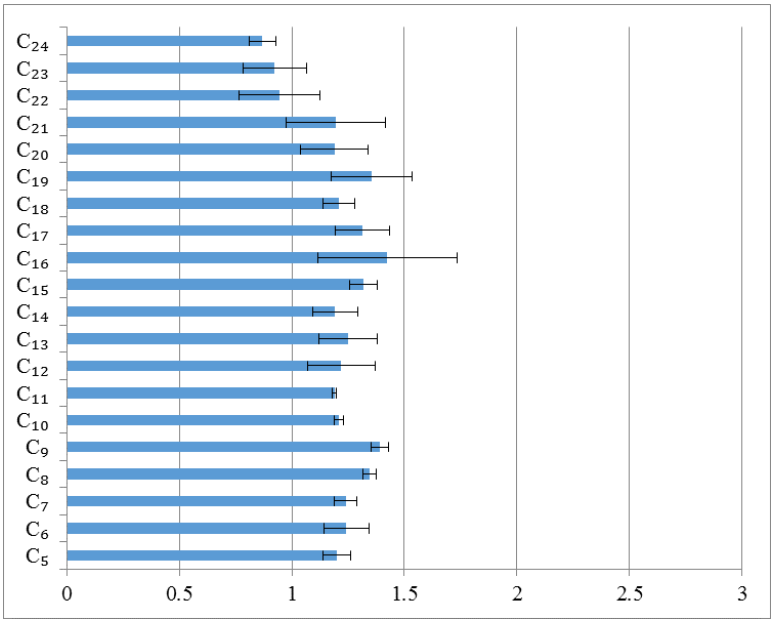

(e)

Figure 1. Continued

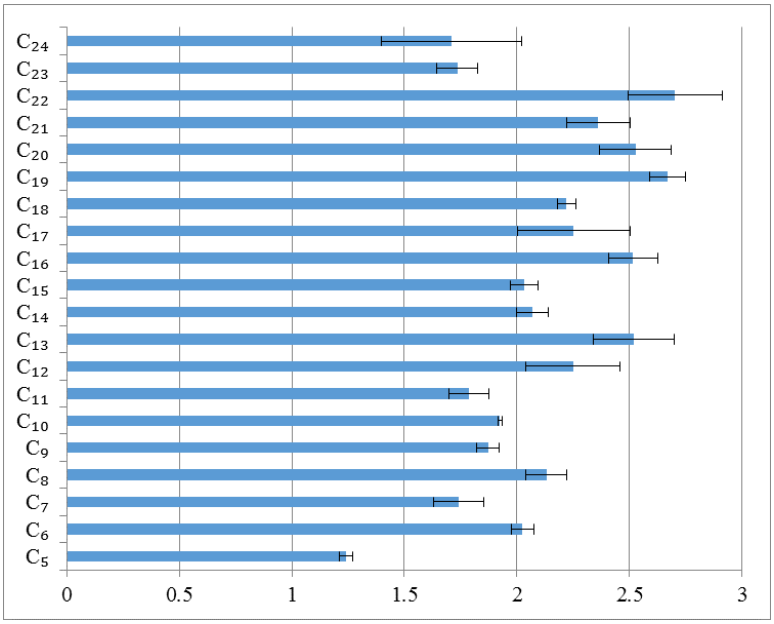

(f)

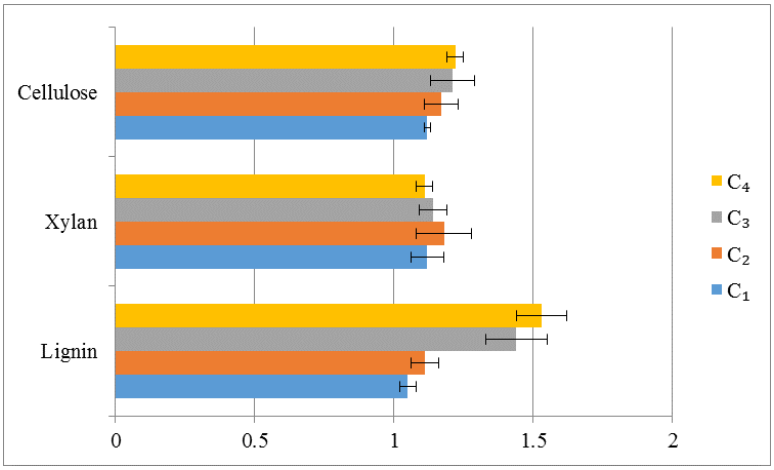

(g)

Figure 1. Continued

Typical pyrolysis products of biomass model compounds and PE were reported elsewhere [19, 20]. The major pyrolysis products of cellulose include levoglucosan, 5-hydroxylmethyl-furfural, 1,4:3,6-Dianhydro-α-d-glucopyranose (double anhydrosugar) and other furans. Xylan depolymerizes to xylose, furans, acetic acid and also double anhydrosugar. Lignin produces phenolic monomers and oligomers with various side chains

and functionalities [21-23]. Upon pyrolysis, PE is depolymerized to olefins and alkanes (together defined as aliphatics) with various chain lengths [24]. To assess synergetic thermal interaction, a ratio was calculated by dividing the GC/MS peak area of a pyrolysis product (which is proportional to the yield) during co-pyrolysis of a biomass compound and PE by the peak area of the same product when the model compound or PE was independently pyrolyzed. Among hydrocarbon products, C_1 to C_4 aliphatic-hydrocarbon gases can be produced from both biomass and PE. Thus, the ratios were calculated by dividing the peak area of the hydrocarbons produced during co-pyrolysis by the sum of the peak areas of the corresponding hydrocarbons when biomass model compounds and PE were pyrolyzed independently. The ratio of pyrolysis char was determined by the char weight. The ratios of oxygenates and aliphatic hydrocarbons are shown in Fig. 1a-1g. In these graphs, a ratio higher than 1 indicates that co-pyrolysis promotes the formation of the product, whereas a value lowers than 1 indicates that co-pyrolysis suppresses the formation of the product. As shown in Fig. 1a, the ratio of levoglucosan was about 1 when cellulose was co-pyrolyzed with PE, which suggests that the cleavage of glycosidic bonds was not affected by PE. However, the ratios of dehydrated oxygenates such as furans and 1,4:3,6-Dianhydro-α-d-glucopyranose all exceeded 1, reached up to 1.45 (corresponding to a 45% increase). When it was co-pyrolyzed with PE, xylan produced increased amounts of light oxygenates including acetic acid, furfural and furanone (Fig. 1b). However, the increase in furans was less significant than it was when observed with cellulose. There was a 45% increase in the yield of acetic acid, which was greater than that of other products. Co-pyrolysis with PE also promoted the depolymerization of lignin. As shown in Fig. 1c, up to 43% more phenolic monomers with varied side chains were produced when PE was co-pyrolyzed. Co-pyrolysis

with biomass compounds, on the other hand, facilitated depolymerization of PE. As shown in Fig. 1d-1g, the amounts of aliphatics, including light hydrocarbon gases, increased dramatically during co-pyrolysis. Fast pyrolysis of PE does not produce solid residue. However, the chain length of olefins and alkanes produced from depolymerization of PE can be as high as over C_{40+} during fast pyrolysis due to the short reaction time [24]. The fraction of long-chain aliphatics with low volatility is likely reduced during co-pyrolysis; thus, the amount of GC/MS detectable, shorter-chain aliphatics increased. It is probable that abstraction of hydrogen by biomass derived oxygenated compounds and reactive free radicals facilitated the cleavage of PE polymer chain and its derivatives [25, 26]. Lignin is the main source of reactive free radicals in biomass upon pyrolysis [27, 28]. Thus, it strongly affected depolymerization of PE when co-pyrolyzed. The formation of CO, CO_2 and pyrolysis char from biomass compounds was suppressed when biomass compounds were co-pyrolyzed with PE. Hydrogen transfer from PE to biomass compounds likely reduces polymerization and cross-linking reactions that forming char and also suppresses decarboxylation and decarbonylation reactions of biomass compounds.

Catalytic co-pyrolysis of PE and biomass model compounds

The pyrolysis vapor derived from thermal decomposition of biomass compounds and PE was converted downstream using HZSM-5 catalyst. HZSM-5 is a zeolite catalyst commonly used to deoxygenate biomass due to its unique pore structure and well-balanced acidity [27-29]. Most active sites of HZSM-5 are located inside of its micropores, at which the biomass is deoxygenated to form aromatics and olefins through reactions such as cracking, dehydration, decarboxylation, decarbonylation, oligomerization, isomerization and

aromatization. PE-derived olefins and alkanes are also further cracked through carbocationic intermediates activated by Lewis and Brönsted sites. The light olefins could further subject to oligomerization, cyclization and aromatization reactions to form aromatics.

Table 2 lists the product distribution of catalytic co-pyrolysis of biomass compounds and PE. Theoretical yields of the products are calculated using the yields of the products when biomass compounds and PE were independently pyrolyzed, assuming that there is no interaction between biomass and PE. The measured yields of pyrolysis char, catalytic coke, as well as carbon oxides were lower than their corresponding theoretical yields at all the cases. These changes resulted in the measured yields of hydrocarbons to be higher than the theoretical yields. The total carbon yield of aromatic hydrocarbons increased from 19.7 to 25.0% when cellulose and PE were co-pyrolyzed. The deoxygenation of cellulose-derived vapors mostly occurs at catalyst pores. For example, furans and double anhydrosugar could undergo decarbonylation followed by olefin dimerization to form aromatics. Levoglucosan has a relatively large molecular size and thus may be difficult to enter the zeolite pores. However, it could dehydrate to form furans and other light oxygenates [30] on the catalytic surface and then enter zeolite pores. There was no apparent change in total yield of olefins and alkanes upon co-pyrolysis. However, the selectivity of ethylene and propylene decreased significantly. These olefins that were mostly derived from PE could combine with furan and furfurals to form benzene, toluene and xylene through Diels-Alder reactions followed by dehydration at Brönsted acid sites [31]. The selectivity of xylene was much higher than benzene and toluene, suggesting that the Diels-Alder reaction between furfurals (for example 5-HMF) and olefins was predominant. The selectivity of alkanes decreased upon co-pyrolysis, which implies that oxygenated compounds abstract hydrogen atoms from alkanes

during catalytic deoxygenation. Decarboxylation and decarbonylation of oxygenated products at catalytic sites usually increase the yields of CO and CO_2. Synergy decreased the yields of CO and CO_2 during catalytic co-conversion despite the increasing yield of hydrocarbons, suggesting that hydrodeoxygenation competes with decarboxylation and decarbonylation at catalytic sites. The increase in C_{6+} aliphatic hydrocarbons could be related to the oligomerization of smaller olefins [32]. Due to the thermal interaction of co-pyrolysis described in section 3.1, the concentration of furans, double anhydrosugar, and PE-derived olefins and alkanes with shorter chains in the pyrolysis vapor increased. This allowed an increased amount of pyrolysis products to enter the zeolite pores and be converted. As a result, Diels-Alder reaction between furans and PE-derived light olefins was promoted, which contributed to the increase of the yield of aromatic hydrocarbons. Previously, Mullen et al. [12] traced the origin of carbon in the products during co-pyrolysis of cellulose and plastics. The authors suggested that interaction through the hydrocarbon pool mechanism could exist in addition to Diels-Alder reaction. This is highly likely to occur; for example, some non-furanic compounds from cellulose and PE-derived products could enter the same hydrocarbon pool in the catalytic site and be converted to both aromatics and olefins. Since the total yield of aliphatic hydrocarbons was not increased, we hypothesize Diels-Alder reaction to be the dominant reaction pathway during co-pyrolysis of cellulose and PE compared to the hydrocarbon pool mechanism.

The yields of aromatic and aliphatic hydrocarbons both increased when xylan was co-pyrolyzed with PE. Diel-Alder reaction involving xylan-derived furans and PE-derived olefins could enhance the yields of aromatic hydrocarbons, similarly to that which occurs during co-pyrolysis of cellulose and PE. However, the selectivity of propylene increased

when xylan and PE were co-pyrolyzed, despite that propylene is supposed to be consumed during the Diels-Alder reaction. Acetic acid and other non-furanic light oxygenates do not participate in Diels-Alder reaction. Instead, these compounds are deoxygenated at catalyst sites through hydrocarbon

Table 2. Product distribution during co-pyrolysis of PE and biomass model compounds (pyrolysis temperature: 700 °C; catalytic temperature: 500 °C; zeolite: HZSM-5; catalyst to feedstock ratio=20:1)

Feedstock	Cellulose		Xylan		Lignin	
	Measured	Theoretical	Measured	Theoretical	Measured	Theoretical
Overall yield (C%)						
Pyrolysis char	1.17 ± 0.02	1.73 ± 0.35	8.31 ± 0.27	8.49 ± 0.34	12.85 ± 0.06	13.30 ± 0.79
Catalytic coke	20.63 ± 0.32	24.61 ± 1.02	19.62 ± 0.37	23.12 ± 0.52	21.20 ± 0.42	23.28 ± 1.18
CO	6.84 ± 0.02	8.17 ± 0.47	3.26 ± 0.03	4.87 ± 0.03	3.62 ± 0.18	4.72 ± 0.09
CO_2	2.79 ± 0.03	3.60 ± 0.58	4.44 ± 0.06	5.63 ± 0.06	2.17 ± 0.00	2.02 ± 0.14
Aliphatic hydrocarbon[a]	34.82 ± 2.22	33.51 ± 0.39	38.69 ± 3.94	31.3 ± 0.50	36.63 ± 2.39	30.85 ± 0.93
Aromatic hydrocarbon	25.00 ± 1.03	19.70 ± 0.86	17.95 ± 0.67	13.64 ± 2.25	15.19 ± 0.60	10.16 ± 0.72
Total carbon	91.25 ± 3.65	91.32 ± 3.67	92.26 ± 5.33	87.04 ± 3.81	91.66 ± 3.66	84.32 ± 3.86
Aromatic selectivity (%)						
Benzene	13.75 ± 0.34	15.75 ± 0.91	15.80 ± 0.58	14.55 ± 7.77	13.98 ± 0.87	14.47 ± 1.66
Toluene	35.72 ± 0.62	38.38 ± 1.61	39.75 ± 1.25	37.50 ± 1.48	36.13 ± 0.61	36.76 ± 2.18
Xylene	32.36 ± 1.24	28.11 ± 1.00	30.01 ± 0.93	29.14 ± 5.68	28.82 ± 0.76	27.11 ± 1.84
Alkylated benzene[b]	8.95 ± 0.31	7.18 ± 0.33	6.13 ± 0.21	7.64 ± 0.35	6.68 ± 0.41	7.54 ± 0.74
Naphthalene	2.31 ± 0.25	2.88 ± 0.18	2.25 ± 0.22	3.27 ± 0.72	4.81 ± 0.14	5.30 ± 0.39
PAH[c]	6.92 ± 1.35	7.69 ± 0.37	6.07 ± 0.56	7.89 ± 0.54	9.57 ± 1.17	8.82 ± 0.28
Aliphatic selectivity (%)						
Methane	21.49 ± 1.56	17.60 ± 0.49	17.23 ± 0.70	16.59 ± 0.35	15.01 ± 0.86	16.26 ± 0.42
Ethylene	28.73 ± 0.59	36.90 ± 0.65	33.40 ± 0.63	39.18 ± 0.97	36.88 ± 1.26	38.00 ± 0.58
Propylene	8.99 ± 0.15	11.91 ± 0.11	16.45 ± 1.24	12.62 ± 0.53	22.98 ± 0.56	12.39 ± 0.11
Butene	7.57 ± 0.60	5.37 ± 0.71	6.10 ± 0.46	2.46 ± 0.74	6.44 ± 0.66	3.11 ± 0.07
Pentene	3.77 ± 0.03	2.94 ± 0.23	0.67 ± 0.01	2.03 ± 0.15	0.10 ± 0.02	1.23 ± 0.19
C_2-C_5 alkanes	4.35 ± 0.03	6.69 ± 0.47	6.04 ± 0.02	7.25 ± 0.31	0.49 ± 0.09	8.81 ± 0.42
$\geq C_6$	25.10 ± 0.11	18.59 ± 0.63	20.11 ± 0.85	19.91 ± 0.63	23.09 ± 1.24	20.19 ± 0.63

[a] Aliphatic hydrocarbons do not include cyclic alkanes
[b] Alkylated benzenes include indanes, indenes and alkylbenzene
[c] PAH includes naphthalenes and other larger polyaromatics

pool mechanism to form both aromatics and olefins, though preferentially to the latter [17]. As previously described, thermal interaction between xylan and PE increases the amount of non-furanic compounds, especially acetic acid, thus producing more olefins. The amount of olefins that originated from either xylan or PE is more than the amount that was consumed by the Diels-Alder reaction during co-pyrolysis. It could be that Diels-Alder reaction and hydrocarbon pool mechanism are equally important when xylan and PE are co-pyrolyzed.

The yield of aromatics increased by 50% compared to its theoretical yield (10.16 to 15.19%) when lignin and PE were co-pyrolyzed. Among light hydrocarbons, alkanes became nearly absent (8.81 to 0.49%), which suggests that lignin-derived phenolic compounds act as strong hydrogen acceptors at catalyst sites when they deoxygenate. Lignin usually yields lower amounts of aromatic hydrocarbons compared to cellulose and xylan due to the low reactivity of phenols for catalytic conversion. The lignin-derived phenols are highly unstable and could easily polymerize in the vapor phase during pyrolysis [33, 34]. Most phenolic compounds are too large to enter the micropores of the zeolite. Thus these compounds adsorbed onto the catalyst surface could further polymerize and eventually dehydrate to form coke. Coke on the catalyst surface could block the entrance of zeolite pores and reduce catalyst activity. During co-pyrolysis with PE, these phenolic compounds could abstract hydrogen atoms from PE-derived alkane or accept hydrogen atoms that are released when olefins aromatize. The hydrogen atoms transferred from PE may have stabilized the phenolic compounds and thus the polymerization reaction is inhibited and coke is reduced. Hydrogen transfer could also promote the cracking of the phenolic compounds on the catalyst surface. The resulting side chain fragments could then enter the zeolite pores and be deoxygenated through the hydrocarbon pool mechanism [35]. It is also possible that the stabilized phenolic

compounds are directly deoxygenated on the limited active sites on the catalyst surface through demethoxylation followed by dehydroxylation to form simpler aromatic hydrocarbons. The single-ring aromatic, such as benzene, could then enter the pores to form alkylated aromatics or naphthalene through a series of reactions with light oxygenates and short aliphatics. However, this hypothesis requires further evaluation.

The above observation suggests that the synergistic increase in hydrocarbon yields and the decrease in solid residue during the catalytic co-pyrolysis of biomass and PE is the combined result of thermal and catalytic interaction. Thermal interaction among biomass and PE improved the composition of the pyrolysis vapor by increasing the concentration of the compounds that can more easily access the catalyst pores and get converted. Thus, the catalytic interaction among the resulting pyrolysis products at the catalytic site through Diels-Alder reaction, hydrocarbon pool mechanism, and hydrogen transfer is favored. The reaction mechanisms between biomass model compounds and PE at catalyst sites are illustrated in Fig. 2.

Catalytic pyrolysis of red oak and PE

Effect of pyrolysis temperature

Red oak and PE were also co-pyrolyzed and the effect of pyrolysis temperature was evaluated by changing the pyrolysis temperature of the first reactor from 500 to 700 ºC while fixing the catalyst temperature of the second reactor at 500 ºC. The distribution of the co--pyrolysis products is shown in Table 3. The product distribution of red oak and PE when they were independently pyrolyzed can be found in Table S2.

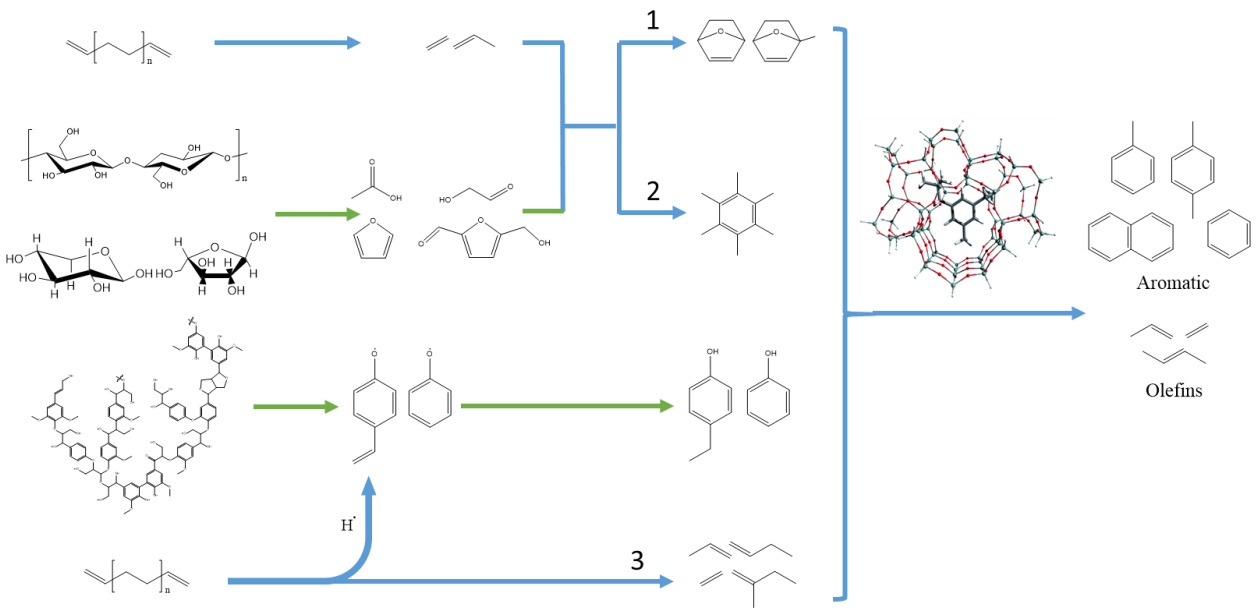

Figure 2. Reaction pathways of catalytic co-pyrolysis of biomass model compounds and PE: 1. Hydrocarbon pool mechanism; 2. Diels-Alder reaction; 3. Hydrogen transfer between PE and lignin.

When the pyrolysis temperature was increased during co-pyrolysis, the yields of pyrolysis char and catalytic coke decreased. Fast pyrolyzing PE at a low pyrolysis temperature produces a larger amount of the long-chained aliphatic hydrocarbons. These products with heavy molecular weights are strongly adsorbed onto the catalyst surface, becoming a yellow, waxy coke that covers the catalyst surface (see Table S2). In biomass, phenolic oligomers and other large molecular weight products are also adsorbed onto the catalyst surface and subject to polymerization followed by dehydration to form coke. Higher pyrolysis temperature favors thermal cracking, which results in co-pyrolysis vapor that contains lighter compounds that are more easily accessible to the catalyst pores and converted to hydrocarbon products. The yield of aromatic hydrocarbons rapidly increased monotonically as the pyrolysis temperature increased, reaching 18.72% at 700 °C. Aliphatic hydrocarbons, on the

Table 3. Product distribution during co-pyrolysis of red oak and PE using various pyrolysis temperatures (catalytic temperature: 500 °C; zeolite: HZSM-5; catalyst to feedstock ratio=20:1)

	Pyrolysis temperature (°C)		
Compound	500	600	700
Overall yield (C%)			
Pyrolysis char	10.09 ± 0.94	8.65 ± 0.13	7.06 ± 0.79
Catalytic coke	27.58 ± 0.33	21.52 ± 0.74	16.67 ± 0.91
CO	3.71 ± 0.09	4.31 ± 0.06	6.05 ± 0.00
CO_2	2.50 ± 0.18	2.72 ± 0.07	2.9 ± 0.03
Aliphatic hydrocarbon[a]	44.12 ± 3.20	47.48 ± 2.05	46.54 ± 1.52
Aromatic hydrocarbon	9.84 ± 0.47	12.82 ± 0.40	18.72 ± 0.17
Total carbon	97.84 ± 5.21	97.49 ± 3.46	97.94 ± 3.43
Aromatic selectivity (%)			
Benzene	14.71 ± 0.42	13.08 ± 0.10	13.78 ± 0.05
Toluene	35.62 ± 1.27	37.59 ± 0.90	36.81 ± 0.00
Xylene	17.52 ± 0.90	22.77 ± 0.92	28.29 ± 0.19
Alkylated benzene[b]	8.74 ± 0.50	10.92 ± 0.10	11.54 ± 0.11
Naphthalene	8.71 ± 1.43	5.33 ± 0.10	3.31 ± 0.16
PAH[c]	14.71 ± 0.24	10.32 ± 1.02	6.28 ± 0.40
Aliphatic selectivity (%)			
Methane	6.32 ± 0.23	10.71 ± 0.24	16.34 ± 0.14
Ethylene	27.24 ± 0.78	33.65 ± 0.69	38.96 ± 0.41
Propylene	11.38 ± 0.81	16.27 ± 0.48	20.90 ± 1.86
Butene	4.61 ± 0.16	4.06 ± 0.03	2.92 ± 0.49
Pentene	3.63 ± 0.37	3.43 ± 0.01	2.14 ± 0.49
C_2-C_5 alkanes	4.09 ± 0.59	4.95 ± 0.04	9.29 ± 0.32
$\geq C_6$	42.73 ± 2.67	26.92 ± 0.56	9.45 ± 0.13

[a] Aliphatic hydrocarbons do not include cyclic alkanes
[b] Alkylated benzenes include indanes, indenes and alkylbenzene
[c] PAH including naphthalenes and higher polyaromatics

other hand, reached the maximum at 600 °C (47.48%) and then leveled off. These trends suggest that aliphatic hydrocarbons were converted to aromatics at the higher pyrolysis temperature. The higher pyrolysis temperature also significantly improved the selectivity of single-ring aromatics and light hydrocarbon gases. The selectivity of single-ring aromatics within the total amount of aromatic hydrocarbons was 90.41% at 700 ºC. Methane, ethylene

and propylene accounted for 75% of the total aliphatic hydrocarbons at this temperature. The selectivity to naphthalene and other polyaromatic hydrocarbons (PAHs) was found to decrease when the pyrolysis temperature increased. Naphthalene and PAHs are catalytic coke precursors [36, 37] and the decrease of the yields of these products is in agreement with the reduction of catalytic coke at higher pyrolysis temperatures.

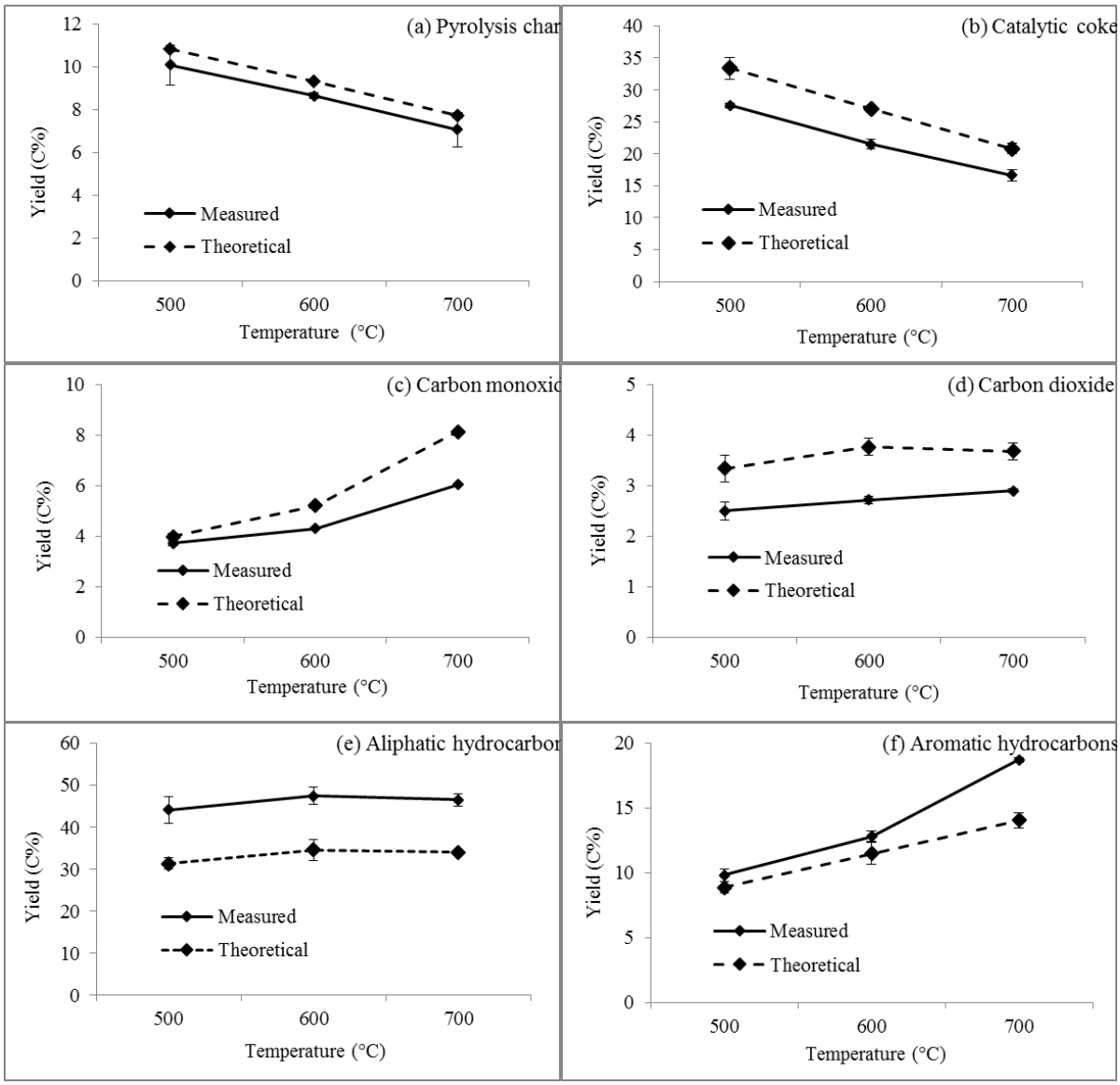

Figure 3. Synergistic effects between PE and red oak during catalytic co-pyrolysis using different pyrolysis temperatures (catalytic temperature: 500 °C; zeolite: HZSM-5; catalyst to feedstock ratio=20:1).

The synergistic effect between red oak and PE at different pyrolysis temperatures is evaluated in Fig. 3. The yields of pyrolysis char and catalyst coke were reduced by about 10% and 20% respectively, upon co-pyrolysis, regardless of the changing pyrolysis temperature (Fig. 3a and 3b). The synergic decrease of CO_2 yield was consistent in the tested range and not affected by the pyrolysis temperature (Fig. 3c). In comparison, CO formation was suppressed more at higher pyrolysis temperatures. At 700 °C, its theoretical yield was 8%, whereas the measured yield was only 5%. The yields of aliphatic and aromatic hydrocarbons were higher than the corresponding theoretical yields for all of the pyrolysis temperatures tested. While the synergy for increasing the yield of aliphatic hydrocarbons was consistent throughout the entire pyrolysis temperature range, the extent of the synergistic increase in the yield of aromatic hydrocarbons was strongly affected by the choice of pyrolysis temperature. At 500 ºC, the measured yield was 10% above the theoretical yield, whereas it was 33% higher at 700 ºC. The interaction between red oak and PE through Diels-Alder cycloaddition and the hydrocarbon pool mechanisms is likely more significant for the pyrolysis vapors produced at higher temperatures.

Effect of catalytic temperature

As shown in Table 3 and Fig. 4, the total hydrocarbon yield was the highest and the synergistic effect most prominent, when the pyrolysis temperature was 700 °C. Thus, the pyrolysis temperature was set at 700 °C and the effect of the catalyst temperature was further evaluated by changing the catalyst bed temperature from 400 to 700 °C. The product distribution for the catalytic co-pyrolysis of red oak and PE at the above conditions is given

in Table 4. The product distribution of the independently pyrolyzed red oak or PE at the corresponding temperatures is reported in Table S2.

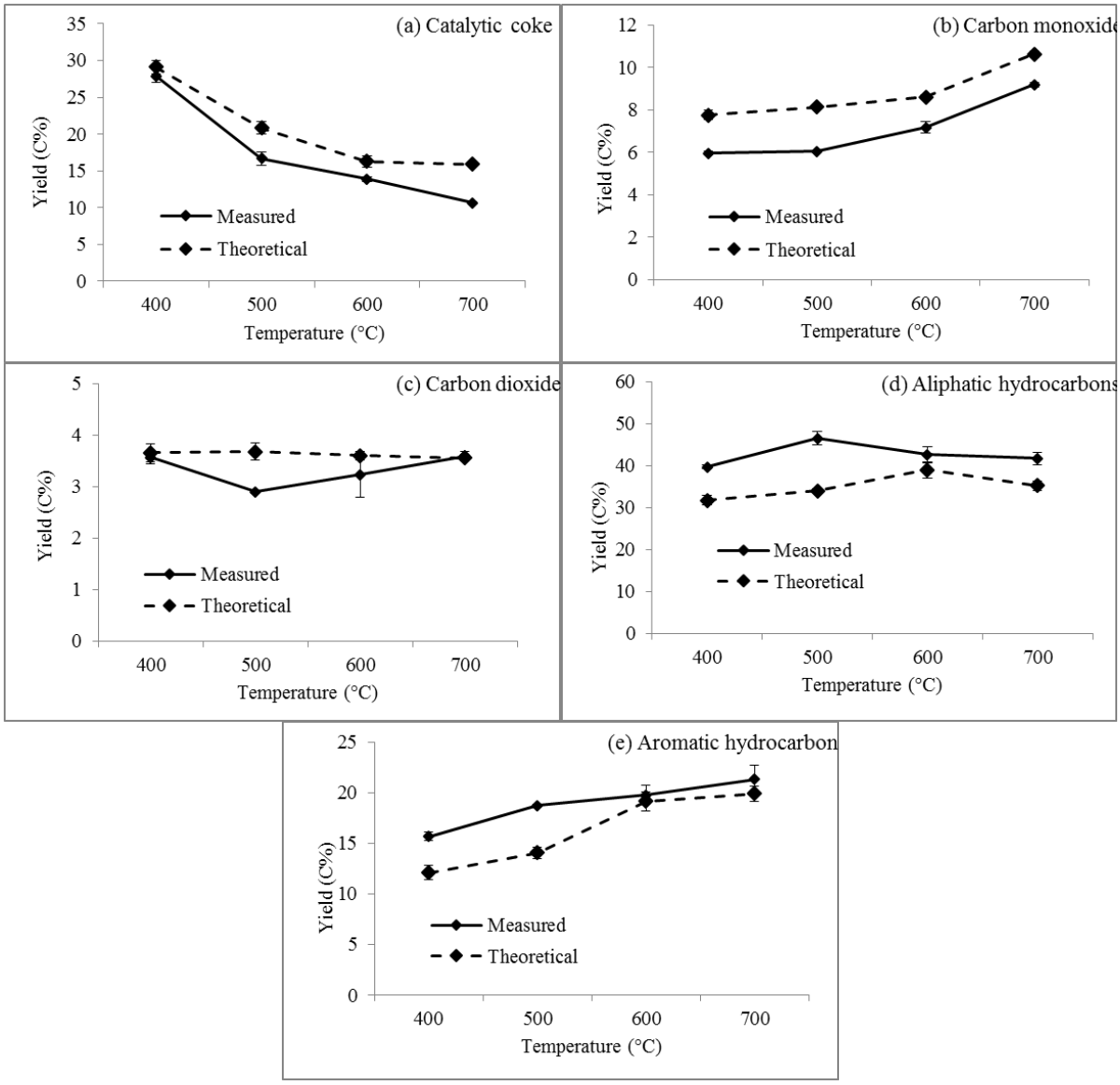

Figure 4. Synergistic effects between PE and red oak during catalytic co-pyrolysis using different catalytic temperatures (catalytic temperature: 500 °C; zeolite: HZSM-5; catalyst to feedstock ratio=20:1)

As expected, the pyrolysis char did not change since the catalyst bed is located downstream from the pyrolysis reactor. Increasing the catalyst temperature reduced the amount of catalyst coke from 27.91% at 400 ºC to 10.63% at 700 ºC due to cracking of the

vapors on the catalytic sites and desorption of heavy compounds. Aliphatic hydrocarbons first increased and reached the maximum of 46.54% at the catalyst temperature of 500 ºC before leveling off. In comparison, aromatics monotonically increased to 21.35% at 700 ºC.

Table 4. Product distribution during co-pyrolysis of red oak and PE using various catalyst temperatures (pyrolysis temperature: 700 °C; zeolite: HZSM-5; catalyst to feedstock ratio=20:1)

	Catalyst temperature (°C)			
Compound	400	500	600	700
Overall yield (C%)				
Pyrolysis char	7.06 ± 0.79	7.06 ± 0.79	7.06 ± 0.79	7.06 ± 0.79
Catalytic coke	27.91 ± 0.84	16.67 ± 0.91	13.89 ± 0.31	10.63 ± 0.13
CO	5.96 ± 0.09	6.05 ± 0.00	7.18 ± 0.27	9.19 ± 0.10
CO_2	3.57 ± 0.13	2.90 ± 0.03	3.94 ± 0.44	3.60 ± 0.08
Aliphatic hydrocarbon[a]	39.74 ± 0.38	46.54 ± 1.51	42.61 ± 1.99	41.73 ± 1.53
Aromatic hydrocarbon	15.68 ± 0.43	18.72 ± 0.16	19.79 ± 0.95	21.35 ± 1.39
Total carbon	99.92 ± 2.66	97.94 ± 3.41	94.47 ± 4.76	93.55 ± 4.03
Aromatic selectivity (%)				
Benzene	9.12 ± 0.21	13.78 ± 0.05	25.74 ± 1.29	48.08 ± 2.54
Toluene	30.31 ± 1.29	36.81 ± 0.00	41.20 ± 1.55	31.82 ± 1.97
Xylene	30.16 ± 0.47	28.29 ± 0.19	15.93 ± 0.56	7.26 ± 0.54
Alkylated benzene[b]	20.79 ± 0.50	11.56 ± 0.06	10.31 ± 0.35	4.54 ± 0.06
Naphthalene	1.68 ± 0.17	3.31 ± 0.16	2.68 ± 0.14	3.29 ± 0.45
PAH[c]	7.95 ± 0.08	6.28 ± 0.40	4.14 ± 0.90	5.00 ± 0.97
Aliphatic selectivity (%)				
Methane	11.54 ± 0.36	16.34 ± 0.16	24.77 ± 0.46	32.67 ± 0.36
Ethylene	29.28 ± 1.03	38.96 ± 0.79	40.02 ± 0.17	46.76 ± 0.18
Propylene	15.76 ± 0.91	16.6 ± 0.33	7.61 ± 0.01	3.15 ± 0.29
Butene	2.47 ± 0.12	2.92 ± 0.01	6.00 ± 0.74	8.57 ± 0.47
Pentene	1.64 ± 0.09	1.52 ± 0.01	1.12 ± 0.45	0.87 ± 0.26
C_2-C_5 alkanes	11.57 ± 0.05	14.21 ± 0.02	13.09 ± 0.26	1.89 ± 0.63
$\geq C_6$	27.73 ± 0.56	9.45 ± 0.47	7.39 ± 0.18	6.09 ± 0.11

[a] Aliphatic hydrocarbons do not include cyclic alkanes
[b] Alkylated benzenes include indanes, indenes and alkylbenzene
[c] PAH including naphthalenes and other polyaromatics

These observed trends were similar to that of when pyrolysis temperature alone was increased. The higher catalyst temperature also favored the formation of aliphatics and

aromatic hydrocarbons with smaller molecular sizes. The selectivity of benzene and toluene accounts for 79.9% of total aromatics, and the sum of the selectivity of methane and ethylene was 79.9% of the total aliphatic hydrocarbons at 700 ºC.

The measured and theoretical yields of the final products are also compared in Fig. 4. The synergetic decrease in catalytic coke was minimal at 400 ºC (Fig. 2a). It is highly probably that heavy aliphatics and oxygenates condense on the catalyst surface when the catalyst temperature low. As the catalyst temperature increased, the synergy for suppression of the coke formation became noticeable. Although the reduction in the yield CO was observed at all of the temperatures, it decreased slightly at temperatures above 500 °C. On the other hand, CO_2 was only reduced at the intermediate catalyst temperature and no noticeable synergy was observed at higher temperatures. It was previously reported that decarbonylation is much favored over decarboxylation when biomass is deoxygenated by zeolite catalyst [17]. It is likely that catalytic co-pyrolysis of biomass and PE changes the mode of oxygen is removed from biomass by substituting decarbonylation reaction with hydrodeoxygenation. The synergistic increase of aromatics and aliphatic hydrocarbons was significant at catalyst temperatures up to 500 °C. It is surprising that the yields of hydrocarbons increased at 400 °C, although no reduction in catalytic coke was found at this temperature. Further increasing catalytic temperatures above 600 °C has weakened the synergic increase of both aromatic and aliphatic hydrocarbons. This trend of synergy for hydrocarbon production agrees the synergic changes observed in CO and CO_2 formation at different catalyst temperatures. Higher catalyst temperatures promote thermal and catalytic cracking of the pyrolysis vapor on the catalytic surface. As a result, hydrogen transfer from PE-derived aliphatics to biomass-derived oxygenates is promoted and more light olefins

participate in Diels-Alder reaction or directly aromatize. However, an excessively high temperature of the catalyst can introduce reverse Diels-Alder reactions to form light olefins instead of aromatics [11, 38, 39]. These light olefins then lose their identity to form a hydrocarbon pool in zeolite pores, thus reducing the synergetic interaction. The dealkylation reaction of aromatics was also enhanced at higher catalyst temperatures, causing increased amounts of benzene, toluene, methane and ethylene.

Conclusion

During fast pyrolysis, strong synergy among biomass and PE was found regardless the presence of catalyst. Co-pyrolysis with PE increased carbohydrate-derived light oxygenates such as furans, acetic acid and double anhydrosugar and enhanced depolymerization of lignin to phenolic monomers. Biomass also promoted the chain scission of PE to form the products with shorter carbon chains. Among biomass model compounds, lignin had stronger interaction with PE compared to cellulose and xylan. When co-pyrolysis vapor of carbohydrates and PE was converted by zeolite catalyst, the Diels-Alder reaction between furans and PE-derived olefins contributed synergistic increase of hydrocarbon yields. Also more hydrocarbons were produced from deoxygenation of the increased amounts of light oxygenates (e.g., acetic acid, double anhydrosugars) through the hydrocarbon pool mechanism. The yield of aromatic hydrocarbons was increased by 50% during catalytic co-pyrolysis of lignin and PE. Strong hydrogen transfer from PE-derived aliphatics to lignin-originated phenolic compounds at catalyst site occurred, which is evidenced by the disappearance of light alkanes among the final products. The study suggests that synergetic effect observed during catalytic co-pyrolysis of biomass and PE is the combination of

thermal interaction in the course of pyrolytic decomposition of raw materials and catalytic interaction of the resulting pyrolysis vapors at catalytic sites. In this study, the effect of pyrolysis temperature and catalytic temperature was also studied by co-pyrolyzing red oak and PE. While higher pyrolysis or catalyst temperatures promoted the yield of aromatic hydrocarbons monotonically, the maximum aliphatic yield was obtained at intermediate pyrolysis or catalyst temperature. A consistently high synergistic effect was observed regardless of the pyrolysis temperature. However, the synergistic increase of hydrocarbons became insignificant at higher catalytic temperature.

Acknowledgement

This research was supported by Iowa Energy center. The authors would like to thank Kwang Ho Kim for preparing the milled wood lignin from red oak.

References

[1] A.V. Bridgwater, G.V.C. Peacocke, Fast pyrolysis processes for biomass, Renewable and Sustainable Energy Reviews, 4 (2000) 1-73.

[2] D. Mohan, C.U. Pittman, P.H. Steele, Pyrolysis of Wood/Biomass for Bio-oil: A Critical Review, Energy & Fuels, 20 (2006) 848-889.

[3] A.V. Bridgwater, Review of fast pyrolysis of biomass and product upgrading, Biomass and Bioenergy, 38 (2012) 68-94.

[4] S. Thangalazhy-Gopakumar, S. Adhikari, R.B. Gupta, M. Tu, S. Taylor, Production of hydrocarbon fuels from biomass using catalytic pyrolysis under helium and hydrogen environments, Bioresource Technology, 102 (2011) 6742-6749.

[5] T.P. Vispute, H. Zhang, A. Sanna, R. Xiao, G.W. Huber, Renewable chemical commodity feedstocks from integrated catalytic processing of pyrolysis oils, Science (New York, N.Y.), 330 (2010) 1222.

[6] F. Melligan, M.H.B. Hayes, W. Kwapinski, J.J. Leahy, Hydro-Pyrolysis of Biomass and Online Catalytic Vapor Upgrading with Ni-ZSM-5 and Ni-MCM-41, Energy & Fuels, 26 (2012) 6080-6090.

[7] N. Miskolczi, L. Bartha, G. Deák, B. Jóver, Thermal degradation of municipal plastic waste for production of fuel-like hydrocarbons, Polymer Degradation and Stability, 86 (2004) 357-366.

[8] F. Abnisa, W.M.A. Wan Daud, A review on co-pyrolysis of biomass: An optional technique to obtain a high-grade pyrolysis oil, Energy Conversion and Management, 87 (2014) 71-85.

[9] C. Dorado, C.A. Mullen, A.A. Boateng, H-ZSM5 Catalyzed Co-Pyrolysis of Biomass and Plastics, ACS Sustainable Chemistry & Engineering, 2 (2013) 301-311.

[10] C. Dorado, C.A. Mullen, A.A. Boateng, Origin of carbon in aromatic and olefin products derived from HZSM-5 catalyzed co- pyrolysis of cellulose and plastics via isotopic labeling, Applied Catalysis B: Environmental, 162 (2015) 338-345.

[11] X. Li, J. Li, G. Zhou, Y. Feng, Y. Wang, G. Yu, S. Deng, J. Huang, B. Wang, Enhancing the production of renewable petrochemicals by co-feeding of biomass with plastics in catalytic fast pyrolysis with ZSM-5 zeolites, Applied Catalysis A, General, 481 (2014) 173-182.

[12] X. Li, H. Zhang, J. Li, L. Su, J. Zuo, S. Komarneni, Y. Wang, Improving the aromatic production in catalytic fast pyrolysis of cellulose by co-feeding low-density polyethylene, Applied Catalysis A: General, 455 (2013) 114-121.

[13] B. Zhang, Z. Zhong, K. Ding, Z. Song, Production of aromatic hydrocarbons from catalytic co-pyrolysis of biomass and high density polyethylene: Analytical Py–GC/MS study, Fuel, 139 (2015) 622-628.

[14] P. Bhattacharya, P.H. Steele, E.B.M. Hassan, B. Mitchell, L. Ingram, C.U. Pittman, Wood/ plastic copyrolysis in an auger reactor: Chemical and physical analysis of the products, Fuel, 88 (2009) 1251-1260.

[15] Y. Xue, S. Zhou, R.C. Brown, A. Kelkar, X. Bai, Fast pyrolysis of biomass and waste plastic in a fluidized bed reactor, Fuel, 156 (2015) 40-46.

[16] A. Björkman, Studies on finely divided wood. Part 1. Extraction of lignin with neutral solvents, Svensk papperstidning, 59 (1956) 477-485.

[17] K. Wang, J. Zhang, B. H. Shanks, R.C. Brown, Catalytic conversion of carbohydrate-derived oxygenates over HZSM-5 in a tandem micro-reactor system, Green Chem., 17 (2014) 557-564.

[18] T. Ikeda, K. Holtman, J.F. Kadla, H.-m. Chang, H. Jameel, Studies on the Effect of Ball Milling on Lignin Structure Using a Modified DFRC Method, Journal of Agricultural and Food Chemistry, 50 (2002) 129-135.

[19] K.H. Kim, X. Bai, M. Rover, R.C. Brown, The effect of low- concentration oxygen in sweep gas during pyrolysis of red oak using a fluidized bed reactor, Fuel, 124 (2014) 49-56.

[20] M. Predel, W. Kaminsky, Pyrolysis of mixed polyolefins in a fluidised-bed reactor and on a pyro-GC/MS to yield aliphatic waxes, Polymer Degradation and Stability, 70 (2000) 373-385.

[21] P.R. Patwardhan, J.A. Satrio, R.C. Brown, B.H. Shanks, Product distribution from fast pyrolysis of glucose-based carbohydrates, Journal of Analytical and Applied Pyrolysis, 86 (2009) 323-330.

[22] P.R. Patwardhan, R.C. Brown, B.H. Shanks, Product Distribution from the Fast Pyrolysis of Hemicellulose, ChemSusChem, 4 (2011) 636-643.

[23] P.R. Patwardhan, R.C. Brown, B.H. Shanks, Understanding the Fast Pyrolysis of Lignin, ChemSusChem, 4 (2011) 1629-1636.

[24] P.T. Williams, E.A. Williams, Fluidised bed pyrolysis of low density polyethylene to produce petrochemical feedstock, Journal of Analytical and Applied Pyrolysis, 51 (1999) 107-126.

[25] Y. Matsuzawa, M. Ayabe, J. Nishino, Acceleration of cellulose co-pyrolysis with polymer, Polymer Degradation and Stability, 71 (2001) 435-444.

[26] V.I. Sharypov, N.G. Beregovtsova, B.N. Kuznetsov, L. Membrado, V.L. Cebolla, N. Marin, J.V. Weber, Co-pyrolysis of wood biomass and synthetic polymers mixtures. Part III: Characterisation of heavy products, Journal of Analytical and Applied Pyrolysis, 67 (2003) 325-340.

[27] M. Brebu, I. Spiridon, Co-pyrolysis of LignoBoost® lignin with synthetic polymers, Polymer Degradation and Stability, 97 (2012) 2104-2109.

[28] P.F. Britt, A.C. Buchanan Iii, K.B. Thomas, S.-K. Lee, Pyrolysis mechanisms of lignin: surface-immobilized model compound investigation of acid-catalyzed and free-radical reaction pathways, Journal of Analytical and Applied Pyrolysis, 33 (1995) 1-19.

[29] J. Jae, G.A. Tompsett, A.J. Foster, K.D. Hammond, S.M. Auerbach, R.F. Lobo, G.W. Huber, Investigation into the shape selectivity of zeolite catalysts for biomass conversion, Journal of Catalysis, 279 (2011) 257-268.

[30] X. Bai, P. Johnston, S. Sadula, R.C. Brown, Role of levoglucosan physiochemistry in cellulose pyrolysis, Journal of Analytical and Applied Pyrolysis, 99 (2013) 58-65.

[31] C.L. Williams, C.-C. Chang, P. Do, N. Nikbin, S. Caratzoulas, D.G. Vlachos, R.F. Lobo, W. Fan, P.J. Dauenhauer, Cycloaddition of Biomass-Derived Furans for Catalytic Production of Renewable p-Xylene, ACS Catalysis, 2 (2012) 935-939.

[32] L. Lin, C. Qiu, Z. Zhuo, D. Zhang, S. Zhao, H. Wu, Y. Liu, M. He, Acid strength controlled reaction pathways for the catalytic cracking of 1-butene to propene over ZSM-5, Journal of Catalysis, 309 (2014) 136-145.

[33] Z. Ma, E. Troussard, J.A. van Bokhoven, Controlling the selectivity to chemicals from lignin via catalytic fast pyrolysis, Applied Catalysis A, General, 423-424 (2012) 130-136.

[34] X. Bai, K.H. Kim, R.C. Brown, E. Dalluge, C. Hutchinson, Y.J. Lee, D. Dalluge, Formation of phenolic oligomers during fast pyrolysis of lignin, Fuel, 128 (2014) 170-179.

[35] C.A. Mullen, A.A. Boateng, Catalytic pyrolysis-GC/MS of lignin from several sources, Fuel Processing Technology, 91 (2010) 1446-1458.

[36] X. Guo, Y. Zheng, B. Zhang, J. Chen, Analysis of coke precursor on catalyst and study on regeneration of catalyst in upgrading of bio-oil, Biomass and Bioenergy, 33 (2009) 1469-1473.

[37] M. Guisnet, L. Costa, F.R. Ribeiro, Prevention of zeolite deactivation by coking, Journal of Molecular Catalysis A: Chemical, 305 (2009) 69-83.

[38] W.G. Dauben, H.O. Krabbenhoft, Organic reactions at high pressure. Cycloadditions with furans, Journal of the American Chemical Society, 98 (1976) 1992-1993.

[39] Y.-t. Cheng, G.W. Huber, Production of targeted aromatics by using Diels–Alder classes of reactions with furans and olefins over ZSM-5, Green Chemistry, 14 (2012) 3114.

SUPPLEMENTAL INFORMATION FOR CHAPTER 3

Table S1. Product distribution during catalytic pyrolysis of red oak and PE when they were pyrolyzed alone using different pyrolysis temperatures (catalytic temperature: 500 °C; zeolite: HZSM-5; catalyst to feedstock ratio=20:1)

	Red oak			PE		
	Pyrolysis temperature (°C)			Pyrolysis temperature (°C)		
Compound	500	600	700	500	600	700
Overall yield/C%						
Pyrolysis char	21.65 ± 0.24	18.61 ± 0.15	15.45 ± 0.23	0.00 ± 0.00	0.00 ± 0.00	0.00 ± 0.00
Catalytic coke	30.6 ± 2.13	23.30 ± 0.64	20.83 ± 0.89	36.16 ± 1.22	30.62 ± 0.53	20.87 ± 0.78
CO	7.98 ± 0.21	10.43 ± 0.15	16.28 ± 0.10	0.00 ± 0.00	0.00 ± 0.00	0.00 ± 0.00
CO_2	6.68 ± 0.52	7.53 ± 0.34	7.37 ± 0.35	0.00 ± 0.00	0.00 ± 0.00	0.00 ± 0.00
Aliphatic hydrocarbon[a]	8.88 ± 0.13	11.04 ± 0.64	13.75 ± 0.20	53.86 ± 2.44	58.13 ± 4.41	54.29 ± 0.71
Aromatic hydrocarbon	13.58 ± 0.30	17.07 ± 0.80	18.01 ± 0.79	4.17 ± 0.56	5.94 ± 0.84	10.10 ± 0.42
Total carbon	89.37 ± 3.53	87.99 ± 2.71	91.69 ± 2.55	94.19 ± 4.21	94.69 ± 5.78	85.27 ± 1.90
Aromatic selectivity/%						
Benzene	12.71 ± 0.57	9.63 ± 0.24	13.44 ± 0.36	21.90 ± 2.25	21.45 ± 3.78	17.58 ± 0.94
Toluene	34.95 ± 0.27	28.23 ± 1.13	33.61 ± 1.08	34.53 ± 1.96	45.03 ± 5.93	43.95 ± 1.67
Xylene	21.26 ± 0.63	17.79 ± 1.23	23.56 ± 1.04	21.98 ± 3.87	26.39 ± 3.14	30.52 ± 1.16
Alkylated benzene[b]	14.51 ± 0.37	33.03 ± 0.70	13.05 ± 0.50	4.56 ± 1.44	4.88 ± 0.51	6.53 ± 0.10
Naphthalene	6.16 ± 0.14	3.96 ± 0.35	5.72 ± 0.41	7.83 ± 2.08	1.01 ± 0.48	0.73 ± 0.02
PAH[c]	10.41 ± 0.24	7.36 ± 1.03	10.62 ± 0.99	9.19 ± 1.75	1.24 ± 0.32	0.69 ± 0.08
Aliphatic selectivity/%						
Methane	18.48 ± 0.23	22.72 ± 0.69	21.55 ± 0.71	5.46 ± 0.21	10.25 ± 0.64	14.42 ± 0.14
Ethylene	28.65 ± 0.05	33.34 ± 0.14	33.47 ± 0.55	32.47 ± 0.33	38.47 ± 0.11	37.56 ± 0.94
Propylene	16.52 ± 0.21	14.02 ± 0.26	13.36 ± 0.34	13.40 ± 1.55	13.30 ± 0.19	12.94 ± 0.07
Butene	4.74 ± 0.01	5.48 ± 0.11	4.96 ± 0.11	2.51 ± 0.12	1.96 ± 0.04	2.05 ± 0.03
Pentene	2.53 ± 0.08	2.09 ± 0.04	2.07 ± 0.19	2.03 ± 0.03	1.72 ± 0.07	1.53 ± 0.26
C_2-C_5 alkanes	29.07 ± 0.14	22.34 ± 0.19	24.59 ± 0.84	2.74 ± 0.51	4.7 ± 0.23	8.55 ± 0.30
$\geq C_6$	0.00 ± 0.00	0.00 ± 0.00	0.00 ± 0.00	41.39 ± 0.15	29.59 ± 1.33	22.95 ± 1.26

Table S2. Product distribution during catalytic pyrolysis of red oak and PE when they were pyrolyzed alone using different catalyst temperatures (pyrolysis temperature: 700 °C; zeolite: HZSM-5; catalyst to feedstock ratio=20:1)

	Red oak				PE			
	Catalytic temperature (°C)				Catalytic temperature/°C			
Compound	400	500	600	700	400	500	600	700
Overall yield/C%								
Pyrolysis char	15.45 ± 0.23	15.45 ± 0.23	15.45 ± 0.23	15.45 ± 0.23	0.00 ± 0.00	0.00 ± 0.00	0.00 ± 0.00	0.00 ± 0.00
Catalytic coke	26.96 ± 0.49	20.83 ± 0.89	16.26 ± 0.94	12.87 ± 0.01	31.26 ± 1.25	20.87 ± 0.78	16.27 ± 0.63	18.97 ± 0.54
CO	15.50 ± 0.46	16.28 ± 0.10	17.23 ± 0.20	21.27 ± 0.32	0.00 ± 0.00	0.00 ± 0.00	0.00 ± 0.00	0.00 ± 0.00
CO_2	7.32 ± 0.36	7.37 ± 0.35	7.21 ± 0.16	7.13 ± .11	0.00 ± 0.00	0.00 ± 0.00	0.00 ± 0.00	0.00 ± 0.00
Aliphatic hydrocarbon[a]	8.87 ± 0.23	13.75 ± 0.20	16.85 ± 0.46	17.59 ± 0.29	54.60 ± 2.09	54.29 ± 0.71	61.11 ± 3.36	52.95 ± 1.96
Aromatic hydrocarbon	14.27 ± 0.80	18.01 ± 0.71	21.61 ± 0.58	19.90 ± 0.60	9.91 ± 0.58	10.10 ± 0.42	16.70 ± 1.30	19.89 ± 0.88
Total carbon	88.37 ± 2.56	91.69 ± 2.47	94.61 ± 2.56	94.21 ± 1.56	95.77 ± 3.92	85.27 ± 1.90	94.08 ± 5.29	91.81 ± 3.37
Aromatic selectivity/%								
Benzene	9.04 ± 0.85	13.44 ± .36	21.72 ± 0.49	40.35 ± 1.10	13.99 ± 0.48	17.58 ± 0.94	36.79 ± 3.46	52.39 ± 1.96
Toluene	23.52 ± 0.60	33.61 ± 1.08	37.81 ± 0.77	30.03 ± 0.65	44.53 ± 2.17	43.95 ± 1.67	42.97 ± 3.03	33.22 ± 1.37
Xylene	25.06 ± 0.73	23.56 ± 1.04	14.78 ± 0.38	6.41 ± 0.13	34.07 ± 1.53	30.52 ± 1.16	16.87 ± 1.11	8.51 ± 1.29
Alkylated benzene[b]	18.57 ± 0.20	13.05 ± 0.07	12.59 ± 0.14	11.00 ± 0.06	3.83 ± 0.62	6.53 ± 0.10	1.26 ± 0.09	2.82 ± 0.12
Naphthalene	3.97 ± 0.20	5.72 ± 0.41	5.48 ± 0.36	7.10 ± 0.39	1.08 ± 0.05	0.73 ± 0.02	0.56 ± 0.03	1.46 ± 0.23
PAH[c]	19.83 ± 3.01	10.62 ± 0.99	7.62 ± 0.53	5.11 ± 0.65	2.49 ± 0.12	0.69 ± 0.08	1.56 ± 0.05	1.61 ± 0.43
Aliphatic selectivity/%								
Methane	20.64 ± 0.21	21.55 ± 0.71	23.64 ± 0.36	30.28 ± 1.43	8.45 ± 0.36	14.42 ± 0.14	20.67 ± 0.68	25.42 ± 0.14
Ethylene	31.17 ± .84	33.47 ± 0.55	33.60 ± 1.15	39.28 ± 0.44	28.27 ± 1.21	37.56 ± 0.94	43.26 ± 0.19	46.35 ± 1.43
Propylene	11.23 ± 0.43	13.36 ± 0.34	9.28 ± 0.84	10.48 ± 0.23	17.57 ± 0.72	12.94 ± 0.07	6.82 ± 0.37	3.36 ± 0.16
Butene	9.66 ± 0.07	4.96 ± 0.11	3.92 ± 0.03	1.72 ± 0.07	1.44 ± 0.11	2.05 ± 0.03	3.97 ± 0.13	4.74 ± 0.22
Pentene	4.14 ± 0.09	2.07 ± 0.19	2.72 ± 0.05	2.44 ± 0.06	2.98 ± 0.21	1.53 ± 0.26	1.59 ± 0.07	0.77 ± 0.08
C_2-C_5 alkanes	23.15 ± 0.37	24.59 ± 0.84	26.84 ± 0.83	15.79 ± 0.77	8.65 ± 0.09	8.55 ± 0.30	8.78 ± 0.06	8.57 ± 0.34
$\geq C_6$	0.00 ± 0.00	0.00 ± 0.00	0.00 ± 0.00	0.00 ± 0.00	32.63 ± 1.25	22.95 ± 1.26	14.91 ± 0.61	10.78 ± 0.63

CHAPTER 4

CO-PYROLYSIS OF ACID TREATED BIOMASS AND WASTE PLASTIC FOR IMPROVED PRODUCTION OF VALUE-ADDED PRODUCTS

Yuan Xue[4], Xiangwei Niu[1],Xianglan Bai[1*]

Abstract

In the present study, co-pyrolysis of corn stovers (CS) and polyethylene (PE) was conducted in a tandem micro-pyrolyzer. Raw CS, acid pretreated CS were co-pyrolyzed with PE through non-catalytic and catalytic co-pyrolysis processes to investigate the effects of biomass pretreatment to co-pyrolysis. As for non-catalytic co-pyrolysis, the interaction between acid infused CS and PE was stronger than that between raw CS/acid leached CS and PE. The yields of phenolic monomers and total sugars from acid infused CS increased from 3.12 and 12.82% to 3.52 and 16.91% when acid infused CS was co-pyrolyzed with PE. Lignin component in CS promoted the cracking of PE, resulting in the decrease of carbon content of pyrolysis char and increase of phenolic monomers. The radicals from lignin decomposition abstracted hydrogen from PE rather than levoglucosan, thus increasing the production of levoglucosan. The neutralized potassium sulfate was able to catalyze the cleavage of polyethylene chain. Alkane, alkene and diene with shorter chain length from PE increased by 15, 17, 38% when co-pyrolyzed with acid infused CS, which indicated an enhanced cracking as well as interactions between CS and PE. Furans from the dehydration reaction of levoglucosan reacted with PE derived olefins into aromatic hydrocarbons through the Diels-Alder reaction pathway. Compared to that from ex-situ pyrolysis, the synergistic

[4] Department of Mechanical Engineering, Iowa State University, Ames, Iowa 5001
* Corresponding author. Postal address: Iowa State University, 2070 Black Engineering Building, Ames, IA 50011; Tel: +1 515 294 6886; Fax: +1 515 294 3261; E-mail address: bxl9801@iastate.edu (X. Bai)

effects between CS and PE during in-situ pyrolysis were found more prominent since PE donated more hydrogen atoms to CS. The amount of 4 wt% sulfuric acid infused into CS was the optimized for catalytic co-pyrolysis of acid infused CS and PE in terms of highest aromatic hydrocarbons and lowest catalytic coke formation. Excessive acid infusion into corn stover may result in CS char formation and catalyst poison.

Keyword: Corn stover, polyethylene, catalytic pyrolysis, acid pretreatment, hydrocarbons

Introduction

Biomass is a complex biopolymer consisting of cellulose, hemicellulose and lignin, and other inorganic elements. As a clean and zero GHG emission energy source, it is a potential alternative for petroleum products. Fast pyrolysis is the rapid thermochemical decomposition of biomass into char, light gas and oil accounting for 50-70% of the original biomass. Through different separation and upgrading techniques, the oil can be either converted into value-added platform chemicals, such as levoglucosan, furfural, acetic acid etc., or drop-in hydrocarbon fuels. However, oxygen-induced problems of pyrolysis oil, including acidity, high viscosity, moisture as well as instability during storage, stand in the way for further large-scale and cost-effective application of biomass pyrolysis technique. To solve the problem, Catalytic Fast Pyrolysis (CFP) stands out as one feasible way to lower/remove the oxygen in pyrolysis oil through decarboxylation, decarbonylation and dehydration pathways. Up till now, HZSM-5 zeolite is the most-studied catalyst due to its

strong deoxygenation ability, thermal stability and low coke formation due to its well-balanced acidity and physical structure [1].

On the other hand, previous studies showed that co-pyrolysis of biomass and hydrogen rich plastic could improve both the quantity and quality of pyrolysis oil. Polyethylene, the most common plastic, can be recovered from waste stream at low cost. The cross-reaction between biomass and plastic derived products during co-pyrolysis are able to improve the oil properties by increasing heating value, and lowering oxygen and moisture contents [2, 3]. In the presence of zeolite catalysts, biomass carbon can be more efficiently converted into hydrocarbons since the formation of carbon oxides and catalytic coke was reduced due to hydrogen transfer from plastic to biomass [4-7].

It should be noted that the indigenous alkali and alkaline earth metals (AAEMs) are also one of the most impediments for improving the oil yield in addition to the presence of oxygen atoms and hydrogen deficiency in biomass. While ash content depends on biomass species, it is particularly high in herbaceous biomass. The AAEMs mainly comprise of potassium, calcium, magnesium and sodium. Whether AAEMs are organically bonded to biomass compounds or present as metal oxides or salts in the cells and channels are unclear [8, 9]. Regardless of their forms, it is widely known that even small amount of AAEMs in biomass has significant deleterious effects on biomass pyrolysis by increasing char, water and light gases yields at the expense of reduced yield of organic oil [10-12]. It has shown that AAEMs can catalyze the homolytic glucose ring opening reaction and dehydration to form light oxygenates and char from carbohydrates [13]. Since the depolymerization through glycosidic bond cleavage is strongly inhibited, AAEMs containing biomass usually produces minimal amounts of cellulosic sugars. In terms of catalytic pyrolysis, AAEMs in biomass

also reduce the hydrocarbon yield, and increase char and carbon oxides yield. The detrimental effect of AAEMs can be mitigated by pretreating biomass prior to pyrolysis. Acid leaching of biomass removes AAEM using acidic solution followed by water rinsing and drying. Acid infusion of biomass is the addition of an appropriate amount of acid to biomass followed by direct drying. Both the methods have been found to be effective in increasing bio-oil yield, especially sugar yield [11, 12, 14]. It has been reported that the infused acid converts AAEMs into thermally stable and chemically less reactive salts, thus passivating the catalytic effect of AAEMs [15]. However, it also has been reported that pyrolysis of acid pretreated biomass could easily cause char agglomeration for an unknown reason, which may lead to reactor clogging during scaled pyrolysis.

In the present study, acid pretreated (leached or infused) corn stover(CS) and polyethylene (PE) were non-catalytically and catalytically co-pyrolyzed in order to evaluate if it is possible to further enhance the benefits of both acid treatment and the plastic addition in biomass pyrolysis for quality products. To our best knowledge, this is the first time that acid pretreated biomass and plastic are co-pyrolyzed to obtain an improved conversion.

Material and Method

Material

Corn stover was obtained from BioCentury Research Farm (BCRF). The size of corn stover was reduced to less than 70 μm by ball milling. Some characterization information of the as-received CS are summarized in Table 1. A 98% sulfuric acid was purchase from Sigma Aldrich, US.

Table 1. Characterization of as-received raw CS

Raw CS	**AAEMs (ppm)**	**K**	**Na**	**Ca**	**Mg**	
		15500.24	0	2734.65	1261.68	
	Others (ppm)	**Al**	**Cu**	**Fe**	**Mn**	**Zn**
		18.35	0	359.63	30.01	0.43
Proximate analysis	**wt%**	**Moisture**	**Volatile**	**FC**	**Ash**	
Raw CS		3.18	73.83	18.56	4.44	
Ultimate analysis	**wt%**	**N**	**C**	**H**	**S**	**O***
Raw CS		0.61	44.15	5.13	0.08	50.03

*Determined by difference

Acid leached or acid infused CS was prepared by pretreating the as-received corn stover with sulfuric acid. For acid leaching process, five grams of biomass was first mixed with 100 mL 0.1 M sulfuric acid solution. The slurry was then stirred at room temperature for 4 hours. After the solution being filtered, the solids was further washed with deionized water until the rinsed water become neutral before it was dried in a muffle furnace at 50 °C for 24 hrs. For acid infusion, calculated amounts of sulfuric acid were diluted in 15 g of deionized water. The solutions were then mixed with 5 grams of corn stover. After being stirred at room temperature for 2 hours, the slurry was dried in the oven overnight. Upon drying, the amounts of acid infusion equivalence to 3, 4, 5, 6 wt% of corn stover by weight. The three types of corn stover feedstocks are denoted as raw CS, acid infused CS and acid leached CS in the following texts.

PE with particle sizes between 53 and 75 μm was purchased from Sigma Aldrich, USA. NH_4ZSM-5 (CBV 2314, SiO_2/Al_2O_3=23:1) was purchased from Zeolyst International. The as-received catalyst was activated at 550 °C for 5 hours to obtain proton form HZSM-5 zeolite, and then pelletized and screened to 50-70 mesh sizes. Authentic chemicals of aromatic hydrocarbons, sugars, light oxygenated compounds and phenolic compounds, were

purchased from Sigma Aldrich, Acros Organics and Fisher Scientific, respectively. A gas mixture (helium, CO, CO_2, CH_4, C_2H_4, C_2H_6, C_3H_8, C_3H_4, C_4H_8, C_5H_{10}) was custom-ordered from Praxair, USA.

Pyrolysis

Fast pyrolysis was conducted in a Tandem micro-pyrolyzer system (Rx-3050 TR, Frontier Laboratory, Japan). The micro-pyrolyzer consists of a pyrolysis reactor and a subsequent catalyst bed connected by a needle. Temperatures of two reactors can be controlled independently from room temperature to a maximum at 900 °C. The schematic setup of the reactor can be found from literature [16]. A quartz tube was inserted inside the catalyst bed to hold catalyst. Helium was used as the carrier gas in the reactor.

For non-catalytic pyrolysis, an empty quartz tube was placed in the catalytic bed. Each time, 500 ± 10 μg of CS, PE or the mixture of CS and PE was placed in a deactivated stainless steel cup, which was then dropped into the pyrolysis reactor. The temperatures at both the sections were preset at 600 °C. In case of *in-situ* catalytic pyrolysis, a 250 μg of biomass/PE sample was premixed with 5 mg of catalyst. For *ex-situ* catalytic pyrolysis, the quartz tube was filled with 10mg of catalyst. The pyrolysis vapor evolving from the pyrolysis reactor on the top was sent to the catalytic bed for further conversion. The mixture was then pyrolyzed at 600 °C with an empty catalyst bed.

Both the volatile compounds and non-condensable gases from the pyrolysis were characterized by an online Agilent 7890B Gas Chromatograph (GC) equipped with mass spectrometer (MS), flame ion detector (FID) and thermal conductivity detector (TCD). Helium was also the purge gas for the GC, and its flow rate at the front inlet was 156 mL/min

with a split ratio of 50:1. The temperature of the GC oven stayed at 40 °C for the initial 3 min, then increased to 280 °C at a heating rate of 6 °C/min. Finally it was held at 280 °C for 3 minutes. The columns used in both the MS and FID were Phenomenex ZB 1701 (60 m × 0.250 mm × 0.250 μm thickness) and it was Porous Layer Open Tubular (PLOT) (60 m × 0.320 mm) for the TCD. The products were identified by the MS, and quantified by the FID. The FID was calibrated with authentic chemicals. Non-condensable gases were measured by TCD that was pre-calibrated with the standard gas mixture. All calibration curves were made with five different concentrations of each compound having the regression coefficient above 0.99. The char left in the sample cup was quantified by weighing the cup before and after the experiment. The catalytic coke was quantified with analyzing the used catalyst using a CHNS elemental analyzer (Vario Micro Cube). The product yields from non-catalytic pyrolysis were reported as weight-based yields and reported as carbon-based yields for catalytic pyrolysis. The carbon yield was calculated based on following equation:

$$Carbon\ yield\ of\ a\ product\ (C\%) = \frac{Mole\ of\ carbon\ in\ product}{Total\ mole\ of\ carbon\ in\ feedstock} \times 100\% \qquad (1)$$

Carbon selectivity of individual aromatic hydrocarbons among the total aromatic hydrocarbon group was calculated based on Equation (2):

$$Product\ carbon\ selectivity\ (\%) = \frac{Mole\ of\ carbon\ in\ an\ aromatic\ hydrocarbon\ compound}{Total\ mole\ of\ carbon\ in\ aromatic\ hydrocarbon\ group} \times 100\% \qquad (2)$$

Carbon selectivity of individual aliphatic hydrocarbons among the total aliphatic hydrocarbon group was calculated based on Equation (3):

$$Product\ carbon\ selectivity\ (\%)$$

$$= \frac{Mole\ of\ carbon\ in\ an\ aliphatic\ hydrocarbon\ compound}{Total\ mole\ of\ carbon\ in\ aliphatic\ hydrocarbon\ group} \times 100\% \quad (3)$$

The three different types of corn stovers were also pyrolyzed using a thermal gravimetric analyzer with and without PE. Each time, 20 mg of CS or a mixture of 10 mg corn stover and 10 mg PE was placed in a 150 μL crucible. The samples were later heated to 500 °C with 25 °C/min in nitrogen environment. The resulting chars were cooled down with nitrogen flow to ambient temperature and subjected to other tests.

Results and Discussions

Non-catalytic co-pyrolysis of acid treated biomass and PE

The pyrolysis products from corn stover are mostly oxygenated compounds, including carbon oxides, phenols, sugars, furans and acids. In comparison, pyrolysis products from PE are hydrocarbons including linear alkane, alkenes and dienes. Table 2 summarizes the corn stover-derived oxygenated product distribution from non-catalytic co-pyrolysis of PE and three kinds of corn stovers. The quantified products are grouped as char, carbon oxides, light oxygenates, sugars and phenols. When raw CS was co-pyrolyzed with PE, pyrolysis char was about 25% (per CS weight in the CS/PE mixture). CO_2 yield was significantly higher than CO yield, indicating decarboxylation is a dominant reaction. Acetic acid was the major light oxygenates, mainly produced from hemicellulose decomposition. Due to the high AAEMs content, sugar was nearly not formed except 0.5% (of CS weight) of levoglucosan (LG). Compared to pyrolysis of raw CS alone, small decreases in CO and CO_2 yields were found with co-pyrolysis with PE. The total yield of light oxygenates increased from 11.29 to 12.20% due to the presence of PE, which is mostly attributed to the increases

in acetic acid and acetol yields. The yields of sugars and phenolics were not affected by co-pyrolysis. Overall, the interactions between raw CS and PE were not significant compared to that for red oak and PE co-pyrolysis as reported in our previous study [5].

As also shown in Table 2, compared to co-pyrolysis of raw CS and PE, the yield of pyrolysis char decreased to about 11% (per CS weight) when acid leached CS was co-pyrolyzed with PE, in addition to significant decreases in CO and CO_2 yields. The total yield of light oxygenates also decreased from 12.20% with the raw CS/PE pyrolysis to 7.24%. Interestingly, the yields of 5-hydroxylmethylfuran, levoglucosenone and DAXP (dianhydro xylose) among light oxygenates, increased with the acid leached CS/PE compared to the raw CS/PE mixture. As expected, LG yield increased to 15.24% during pyrolysis of acid leached CS/PE mixture due to the removal of AAEMs. Total quantified phenolic monomer yield only slightly decreased compared to raw CS/PE. Compared to pyrolysis of the acid leached CS alone, the presence of PE was beneficial in reducing pyrolysis char as the char yield was 15.65% without PE. A slight increase in CO yield was found. However, no obvious difference in the rest of the product yields was observed by co-pyrolysis. While the decrease in char yield by co-pyrolysis has to be compensated by increase in other products, it was not observed with the GC detectable products. Thus, the GC non-detectable products, for example sugar oligomers, hemicellulose derived sugars or phenolic oligomers, must be increased.

Table 2. Product distribution from non-catalytic co-pyrolysis of corn stover and PE

	Raw CS		Acid leached CS		Acid infused CS	
Yield based on corn stover (wt%)	W/O PE	W/ PE	W/O PE	W/ PE	W/O PE	W/ PE
Pyrolysis char	24.54 ± 1.14	25.12 ± 0.41	15.65 ± 0.31	11.15 ± 0.26	20.74 ± 0.83	18.50 ± 0.13
CO	5.16 ± 0.27	4.93 ± 0.05	2.30 ± 0.07	2.66 ± 0.11	2.22 ± 0.03	2.65 ± 0.03
CO_2	15.33 ± 0.22	14.70 ± 0.29	8.45 ± 0.17	7.95 ± 0.49	9.12 ± 0.06	9.11 ± 0.14
Light Oxygenates						
2,3-Butanedione	0.45 ± 0.03	0.50 ± 0.01	0.15 ± 0.02	0.17 ± 0.01	0.14 ± 0.01	0.20 ± 0.02
3-Pentanone	0.47 ± 0.03	0.99 ± 0.08	0.05 ± 0.02	0.09 ± 0.01	0.05 ± 0.00	0.03 ± 0.01
Glycolaldehyde	1.14 ± 0.01	1.03 ± 0.02	0.52 ± 0.02	0.76 ± 0.04	0.29 ± 0.01	0.25 ± 0.01
Acetic Acid	3.28 ± 0.12	3.49 ± 0.16	2.08 ± 1.02	1.91 ± 0.12	1.53 ± 0.07	1.49 ± 0.04
Acetol	1.91 ± 0.03	2.39 ± 0.03	0.13 ± 0.02	0.11 ± 0.01	0.08 ± 0.01	0.05 ± 0.01
Succindialdehyde	2.29 ± 0.03	2.20 ± 0.02	0.14 ± 0.02	0.23 ± 0.01	0.11 ± 0.00	0.16 ± 0.00
Furfural	0.59 ± 0.02	0.56 ± 0.01	1.08 ± 0.02	0.98 ± 0.05	1.89 ± 0.01	1.86 ± 0.04
2-Hydroxycyclopent-2-en-1-one	0.60 ± 0.01	0.55 ± 0.01	0.26 ± 0.02	0.23 ± 0.01	0.19 ± 0.00	0.19 ± 0.00
2-Hydroxy-1-methylcyclopenten-3-one	0.56 ± 0.02	0.49 ± 0.00	0.13 ± 0.02	0.12 ± 0.01	0.10 ± 0.01	0.11 ± 0.01
5-Hydroxymethylfurfural	0.00 ± 0.00	0.00 ± 0.00	0.28 ± 0.02	0.29 ± 0.05	0.39 ± 0.01	0.44 ± 0.02
Levoglucosenone	0.00 ± 0.00	0.00 ± 0.00	0.17 ± 0.02	0.17 ± 0.02	0.28 ± 0.06	0.31 ± 0.01
DAXP	0.00 ± 0.00	0.00 ± 0.00	2.08 ± 0.02	2.18 ± 0.06	1.92 ± 0.13	2.01 ± 0.09
Sum	**11.29 ± 0.30**	**12.20 ± 0.34**	**7.07 ± 0.41**	**7.24 ± 0.39**	**6.98 ± 0.33**	**7.11 ± 0.27**
Sugars						
1,4:3,6-Dianhydro-α-d-glucopyranose	0.00 ± 0.00	0.00 ± 0.00	0.10 ± 0.01	0.05 ± 0.00	0.64 ± 0.04	0.65 ± 0.03
Dianhydromannitol	0.00 ± 0.00	0.00 ± 0.00	0.40 ± 0.01	0.33 ± 0.01	0.41 ± 0.04	0.43 ± 0.00
d-Mannose	0.00 ± 0.00	0.00 ± 0.00	0.24 ± 0.01	0.23 ± 0.01	0.16 ± 0.00	0.19 ± 0.01
Levoglucosan	0.44 ± 0.02	0.50 ± 0.07	15.93 ± 0.27	15.24 ± 0.37	11.19 ± 0.48	15.03 ± 0.43
1,6-Anhydro-α-d-galactofuranose	0.00 ± 0.00	0.00 ± 0.00	0.44 ± 0.02	0.61 ± 0.06	0.42 ± 0.07	0.61 ± 0.01
Sum	**0.44 ± 0.02**	**0.50 ± 0.07**	**17.12 ± 0.32**	**16.47 ± 0.46**	**12.82 ± 0.65**	**16.91 ± 0.48**
Phenols						
Phenol	0.18 ± 0.01	0.20 ± 0.00	0.08 ± 0.00	0.07 ± 0.00	0.12 ± 0.00	0.14 ± 0.00
Guaiacol	0.29 ± 0.03	0.27 ± 0.01	0.17 ± 0.01	0.16 ± 0.02	0.21 ± 0.00	0.18 ± 0.00
Cresol	0.08 ± 0.01	0.08 ± 0.00	0.14 ± 0.01	0.13 ± 0.01	0.13 ± 0.01	0.12 ± 0.00
4-vinyl Phenol	2.03 ± 0.06	1.99 ± 0.06	1.54 ± 0.06	1.60 ± 0.08	1.39 ± 0.03	1.56 ± 0.04
4-vinyl Guaiacol	0.55 ± 0.02	0.52 ± 0.02	0.69 ± 0.02	0.65 ± 0.05	0.61 ± 0.01	0.66 ± 0.03
Syringol	0.23 ± 0.01	0.20 ± 0.01	0.08 ± 0.00	0.07 ± 0.00	0.10 ± 0.00	0.08 ± 0.00
Isoeugenol	0.07 ± 0.00	0.10 ± 0.01	0.46 ± 0.02	0.41 ± 0.06	0.27 ± 0.06	0.43 ± 0.05
1,2,4-Trimethoxybenzene	0.00 ± 0.00	0.00 ± 0.00	0.13 ± 0.01	0.16 ± 0.02	0.11 ± 0.01	0.10 ± 0.01
4-Methoxy-3-(methoxymethyl)phenol	0.03 ± 0.00	0.03 ± 0.00	0.00 ± 0.00	0.00 ± 0.00	0.00 ± 0.00	0.00 ± 0.00
Vanillin	0.07 ± 0.00	0.07 ± 0.00	0.05 ± 0.00	0.06 ± 0.00	0.03 ± 0.00	0.04 ± 0.00
3',5'-Dimethoxyacetophenone	0.13 ± 0.00	0.12 ± 0.00	0.07 ± 0.00	0.08 ± 0.00	0.05 ± 0.00	0.06 ± 0.00
2,6-Dimethoxy-4-allylphenol	0.08 ± 0.00	0.09 ± 0.00	0.16 ± 0.01	0.16 ± 0.01	0.09 ± 0.01	0.11 ± 0.00
Syringolaldehyde	0.02 ± 0.00	0.02 ± 0.00	0.02 ± 0.00	0.03 ± 0.00	0.02 ± 0.00	0.02 ± 0.00
Sum	**3.77 ± 0.14**	**3.69 ± 0.11**	**3.61 ± 0.15**	**3.58 ± 0.26**	**3.12 ± 0.13**	**3.52 ± 0.14**

Our previous pyrolysis experiments of CS with 3, 4, 5, 6 wt% acid infusion has shown that 4 wt% acid infused CS produced the highest yield of levoglucosan (Table S1), thus 4 wt% acid infused CS was studied in the following section. Compared to pyrolysis of acid leached CS/PE mixture, pyrolysis char was higher from pyrolysis of 4% acid infused CS/PE mixture at 18.5% (per the CS weight). A slight increase in CO_2 yield was also found. While the total yield of light oxygenates was similar between acid infused CS/PE and acid leached CS/PE, glycolaldehyde and acetic acid yields both decreased whereas furfural and levoglucosenone yields increased. On the other hand, both the sugar and phenolic monomer yields were similar for pyrolysis of 4% acid infused CS/PE mixture and the acid leached CS/PE mixture. In terms of synergetic effect with PE, the presence of PE inhibited the pyrolysis char formation from the acid infused CS, otherwise it was 20.74%. The presence of PE also slightly increased CO yield from the acid infused CS, similar to it was observed with the acid leached CS. Co-pyrolysis with PE also strongly benefited sugar production from acid infused CS. The total sugar yield increased from 12.82 to 16.91% by PE, which is largely due to the increase of LG yield from 11.19 to 15.03%. Co-pyrolysis with PE also increased total phenolic monomers to 3.52% from 3.12% without PE. The formation of phenol, 4-vinyl phenol, 4-vinyl guaiacol and isoeugenol from acid infused CS was promoted with the addition of PE.

Table 3. Yield change of products from PE

	PE	Raw CS PE	Acid leached CS PE	Acid infused CS PE	Acid infused PE	K_2SO_4 infused PE
Alkane	1.00	1.07	1.14	1.15	0.98	1.05
Alkene	1.00	1.12	1.16	1.17	0.97	1.08
Diene	1.00	1.27	1.25	1.38	1.08	1.14

PE-derived pyrolysis products include alkanes, alkenes and dienes. In the present study, a total of 48 aliphatic hydrocarbons with carbon number ranging from C_7 to C_{26} were quantified. To evaluate the effect of co-pyrolysis on the yields of the PE-derived hydrocarbons, a changing factor was defined as dividing a hydrocarbon product yield when PE was co-pyrolyzed with the corn stovers by the yield from pyrolysis of PE alone. For a specific product, a factor greater than 1 indicates that the product formation is promoted by co-pyrolysis. On the opposite site, the product formation is inhibited with the factor lower than 1. The results are given in Table 3 for co-pyrolysis of PE with raw CS, acid leached CS or acid infused CS. As can be seen, the changing factors were greater than 1 for all quantified aliphatic hydrocarbons when PE was co-pyrolyzed with all three types of corn stover. The results indicate that PE cracking was enhanced by co-pyrolyzing with corn stover. The increased extents were varied depending on the pretreatment method, which increased in the order of raw CS <<acid leached CS < acid infused CS. Additionally, the changing factor of diene was 1.38 for acid infused CS, which is significantly higher than the corresponding values for PE co-pyrolysis with raw CS or acid infused CS, implying the strong hydrogen abstraction reaction from PE by the acid infused CS. The changing factor was highest for co-pyrolysis of PE with the acid-infused CS, which was 1.38. The synergistic effects between biomass compounds and PE were described in our previous study [2, 5]. Since lignin decomposition occurs at lower temperatures than PE depolymerization, the phenolic radicals of lignin could facilitate PE depolymerization via radical-initiate mechanism. The phenolic free radicals, otherwise polymerize to form char precursor, could abstract hydrogen from PE pyrolysis products. Without PE, the phenolic radicals could also abstract hydrogen from cellulose derivatives, such as LG. As a result, the LG free radicals could convert to light

oxygenates and char [17, 18]. During co-pyrolysis with PE, PE becomes the hydrogen source to suppress both the pathways, recovering more LG and phenolic monomers and reducing char formation. Recall that both LG and phenolic monomer yields increased whereas char yield decreased from pyrolysis of acid infused CS and PE. In comparison, only char yield decreased significantly during co-pyrolysis of PE and acid leached CS; and the synergistic effect was even less obvious with co-pyrolysis of raw CS and PE. It is noteworthy that phenolic oligomers are not detected by the GC. Thus, the presence of PE may affect the formation of phenolic oligomers. Since lignin is the main source of pyrolysis char formation, the elemental compositions of pyrolysis char recovered from the three CS feedstocks and corresponding co-pyrolysis with PE are compared in Table 4. As shown, acid pretreatment increased the carbon content in the pyrolysis char and the effect was more dramatic with acid leached CS. Since acid pretreatments are expected to reduce carbohydrate-derived char, the aromatic carbon condensed char derived from lignin is dominant in pyrolysis chars of acid pretreated CS feedstocks. In comparison, the carbon contents of char produced from co-pyrolysis of the three CS and PE were lower than the carbon contents of pyrolysis char produced from corresponding CS feedstocks without PE, suggesting co-pyrolysis derived char has a less carbon condense structure. This is an indication that the presence of PE inhibits lignin-derived char formation, probably also increasing phenolic oligomer content since the oligomers are not converted to char. The synergistic effect with PE was strongest with the acid infused CS due to significant hydrogen transfer. Since the acid infusion to raw CS forms sulfate AAEMs salts, there is a possibility that the sulfate salts influence PE depolymerization. Recall that raw CS contained a high amount of potassium (15500 ppm), the acid infusion pretreatment could convert the potassium into the corresponding sulfate

salt. Thus, PE infused with 5 wt% K_2SO_4 was pyrolyzed. Interestingly, the cracking of PE was enhanced in the presence of K_2SO_4 since all the changing factors of the hydrocarbons were greater than 1. However, the increased extent for K_2SO_4 added PE was not as much as those for co-pyrolysis of acid infused CS and PE, suggesting that both corn stover and K_2SO_4 are responsible for the enhanced cracking of PE. For co-pyrolysis of acid leached CS and PE, the PE cracking is only enhanced only by CS. Although raw CS also contains potassium, previous studies showed that that only neutral potassium salts can enhance the cracking of PE polymer chain while potassium in basic or basic salts form are not effective or even has some negative catalytic effects [19, 20]. The above differences may explain why the synergistic effects were highest with the acid infused CS and PE.

Table 4. Elemental analysis of char

	Raw CS		Acid leached CS		Acid infused CS	
wt%	W/O PE	W/PE	W/O PE	W/PE	W/O PE	W/PE
N	0.88 ± 0.02	0.80 ± 0.01	1.84 ± 0.03	1.79 ± 0.01	1.12 ± 0.02	1.09 ± 0.01
C	68.18 ± 0.25	65.97 ± 0.15	75.62 ± 0.22	72.78 ± 0.29	70.11 ± 0.46	67.14 ± 0.27
H	2.35 ± 0.06	2.31 ± 0.08	2.40 ± 0.09	2.32 ± 0.09	2.16 ± 0.08	2.06 ± 0.08
S	0.04 ± 0.00	0.06 ± 0.01	0.04 ± 0.00	0.06 ± 0.01	2.35 ± 0.06	2.12 ± 0.15

The physical appearance of the chars produced from pyrolysis of CS alone or the mixtures of CS and PE (by TGA) are shown in Fig. 1. As can be seen, the chars produced when raw CS was pyrolyzed alone agglomerated. Agglomeration of char was frequently found during pyrolysis of ash rich herbaceous biomass in reactors. This is because some AAEMs in the biomass could melt during pyrolysis at relatively low temperatures and serve as adhesive. The char agglomeration was also observed during pyrolysis of the acid leached CS or acid infused CS. Char agglomeration resulting from pyrolysis of acid-pretreated biomass is also reported in literature as this causes reactor clogging and defluidization of

sand in fluidized bed reactors [21, 22]. Although it requires further confirmation, the removal of AAEMs from raw CS may have caused lignin melting and agglomeration during pyrolysis. Agglomeration was also observed for the acid infused CS, probably both lignin and carbohydrates decomposed at lower temperatures due to acid infusion. As a result, the sugars and phenols reacted in the liquid state to form agglomerate. In the case, a part of sugars were also converted to char. Thus, the carbon content in the pyrolysis char of acid infused CS is lower than that in the pyrolysis char of acid leached char, which is mainly lignin-derived char. Although the addition of PE to the acid leached CS reduced the char yield, it could not prevent the char agglomeration. The agglomerated char blocks were also found with co-pyrolysis of raw CS and PE. Interestingly, the agglomeration was suppressed when the acid infused CS was co-pyrolyzed with PE. It is likely that PE acted as an effective hydrogen donor during co-pyrolysis to prevent hydrogen abstraction from the sugars by the phenols. As a result, the sugars evaporated instead of reacting with the phenolics to form char. Also, the sulfate salts formed by the acid infusion prevented lignin melting and agglomeration. Although the cause for reduced agglomeration requires further confirmation, the present study provides a potentially effective approach to increase the quality of pyrolysis product while solving the char agglomeration problem during the reactor operation.

Catalytic co-pyrolysis of acid treated CS and PE

The products from catalytic conversion of CS and PE include pyrolysis char, catalytic coke, aromatic hydrocarbons, carbon oxides and aliphatic hydrocarbons. For *in-situ* catalytic pyrolysis, the sum of pyrolysis char and catalytic coke was denoted as solid residue. To evaluate the synergistic effects between PE and CS during catalytic co-pyrolysis, CS or PE

was independently converted by the catalyst and the product yields from PE and CS were mathematically added to obtain "calculated" product yields and compared with "experimental" product yields of the same products during catalytic co-pyrolysis of CS and PE.

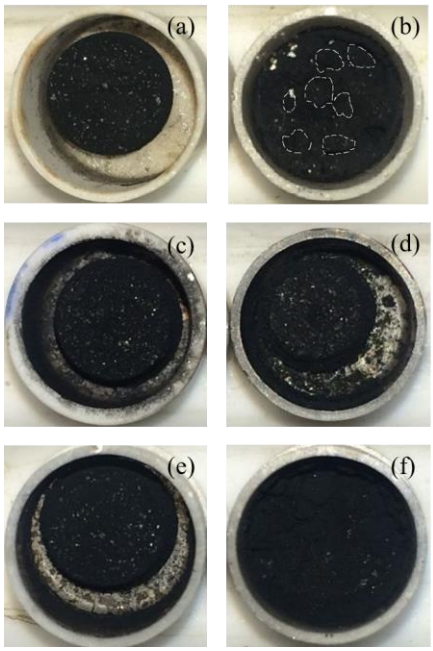

Figure 1. Chars from corn stover pyrolysis and corn stover-polyethylene co-pyrolysis a). Raw CS char; b) Raw CS PE char; c) Acid leached CS char; d) Acid leached CS PE char; e) Acid infused CS char; f) Acid infused CS PE char

Effects of different acid pretreatment methods to *ex-situ* catalytic co-pyrolysis

The product distributions from *ex-situ* catalytic co-pyrolysis of CS and PE are listed in Table 5. The acid pretreatments of CS had a pronounced effect on the product distribution during co-pyrolysis. The pyrolysis char yields are same as they were obtained for non-catalytic co-pyrolysis shown in Table 2, but given as carbon based yields per the total weights of CS and PE. Co-converting PE with acid leached CS produced maximum yield of

aromatic hydrocarbon, which was 17.58 C%. Converting the mixture of PE and the acid leached CS also produced highest yields of catalytic coke and CO, but lowest yield of CO_2. The aromatic hydrocarbons from co-pyrolysis of acid leached CS and PE more selectively produced benzene, while those of raw CS and the acid infused CS selectively produced xylene, ethyl benzene and polyaromatics hydrocarbons (PAHs). The product distribution from co-pyrolysis of the acid infused CS and PE produced slight less aromatic hydrocarbons than that from the mixture of the acid leached CS and PE, but higher than the yield from co-conversion of PE and raw CS. The mixture of PE and the acid infused CS produced higher yield of alkanes and lower yield of alkenes compared to other feedstock mixtures, although the variations between different feedstocks were not significant. Clearly, reducing deleterious effects of AAEMs by acid pretreating biomass increased the amount of cellulose-derived vapors during the ex-situ pyrolysis, thus increasing the yields of aromatic hydrocarbons produced by zeolite catalyst [23]. Catalytic coke increased when the mixtures containing the acid pretreated CS were converted, because of increased pyrolysis vapors reaching the zeolite catalyst bed.

Comparing the experimental and calculated product yields, it was found that the synergistic effects between PE and CS were significantly affected by the CS pretreatment methods. For raw CS, co-conversion with PE reduced the yield of catalytic coke, and promoted the yield of alkene from 55.62 to 57.26 C%. A slight decrease in CO yield from 3.31 to 3.09 C% was also observed. For co-pyrolysis of the acid leached CS and PE, the aromatic hydrocarbons increased from 12.78 to 17.58 C%, and alkenes from 55.06 to 56.17 C% due to the synergistic effects. The decreases in CO and alkane were also observed.

Table 5. Product distribution from *ex-situ* catalytic co-pyrolysis of corn stover and polyethylene

Catalyst bed temperature: 600 °C

	Raw CS PE		Acid Leached CS PE		Acid Infused CS PE	
Yield (C%)	Experimental	Calculated	Experimental	Calculated	Experimental	Calculated
Pyrolysis char	12.56 ± 0.21	12.27	5.58 ± 0.13	7.82	9.25 ± 0.57	10.37
Catalytic coke	7.19 ± 0.00	8.14	8.94 ± 0.00	9.36	8.11 ± 0.00	8.21
Aromatic	11.49 ± 0.28	11.32	17.58 ± 0.26	12.78	15.45 ± 0.06	11.32
CO	4.57 ± 0.05	4.56	6.67 ± 0.19	6.96	5.40 ± 0.17	5.64
CO2	3.09 ± 0.08	3.31	2.24 ± 0.10	2.11	2.56 ± 0.25	2.41
Alkane(C≤5)	3.68 ± 0.06	5.32	3.73 ± 0.42	5.34	3.95 ± 0.21	5.65
Alkene(C≤5)	57.26 ± 0.75	55.62	56.17 ± 0.52	55.06	54.42 ± 0.36	55.40
Aromatic Selectivity (%)						
Benzene	17.78		23.24		15.16	
Toluene	36.46		37.27		38.50	
C_8	22.84		18.64		24.27	
C_9	4.98		4.63		4.80	
C_{10}	7.65		7.29		7.05	
C_{10+}	10.29		8.93		10.22	
Aliphatic selectivity (%)						
CH_4	2.75		3.67		3.00	
C_2H_6	0.82		0.97		1.37	
C_3H_8	1.86		1.28		2.22	
C_4H_{10}	1.46		1.17		1.75	
C_2H_4	19.48		21.67		19.34	
C_3H_6	50.90		50.53		49.93	
C_4H_8	22.13		20.26		21.77	
C_5H_{10}	0.60		0.45		0.63	

The differences between the experimental and the calculated product yields for co-conversion of the acid infused CS and PE resembled to that for the mixture of the acid leached CS and PE, suggesting the synergistic effects may be caused through similar reaction pathways. As shown in Table 2, the pyrolysis of raw CS mostly produced light oxygenates, consisting of predominantly acetic acid, acetol, glycoaldehyde and succindialdehyde, while the main products from the acid leached CS and the acid infused CS were sugars. The light oxygenates produced from the acid leached CS and the acid infused CS were mainly acetic

acid, furfural, and dianhydro xylose (DAXP). During catalytic conversion, the light oxygenate compounds derived from the decomposition of cellulose and hemicellulose first undergo deoxygenation reaction through dehydration, decarbonylation, decarboxylation to form hydrocarbon intermediates including light alkanes and olefins. These intermediates either leave the catalyst zone as final products or oligomerize to aromatic hydrocarbons catalyzed by acid sites located both on the surface and inside the pore of the catalyst [24]. LG is the major product from the acid leached or acid infused CS. The dehydration of LG produces furans as the important intermediates during catalytic conversion with zeolite [25]. For PE, its catalytic conversion of starts with the cracking of the polymer chain into smaller hydrocarbon molecules, followed by reforming, isomerization and aromatization [26]. When the acid infused CS or the acid leached CS was co-converted with PE, increased amounts of furans produced from both primary decomposition of the CS carbohydrates and secondary dehydration reaction of LG by zeolite could react with PE-derived olefins through Diels-Alder reaction to increase aromatic hydrocarbon yields [5]. The deoxygenation pathway of furans is, thus, changed from decarbonylation to dehydration [27]. Although raw CS produced abundant light oxygenates including acetic acid, glycoaldehyde etc., the synergistic effects between raw CS and PE were much limited. Mullen et al. [28] previously reported that in addition to Diels-Alder reaction, a hydrocarbon pool based interaction is also possible when biomass and PE are co-converted. Although both CS and PE-derived hydrocarbons can co-enter the hydrocarbon pool to be converted into aromatics and olefins, this reaction pathway is less likely to contribute the synergistic effects since the way of oxygen removal was not altered.

Comparison of *in-situ* and *ex-situ* catalytic co-pyrolysis

Previous studies have shown that the product distribution during catalytic pyrolysis of biomass or plastics is significantly affected by the contact mode of the feedstock and catalyst (*in-situ* vs. *ex-situ*)[16, 29]. Different from *ex-situ* pyrolysis that only the pyrolysis vapor enters the catalytic bed, the solid feedstock and catalyst are co-mixed during *in-situ* pyrolysis. The solid or liquid interactions during *in-situ* pyrolysis could alter the conversion mechanisms and therefore the synergy between PE and the CS feedstocks. The results obtained from *in-situ* catalytic co-pyrolysis of PE and the CS feedstocks with different pretreatments are shown in Table 6.

Table 6. Product distribution from *in-situ* catalytic co-pyrolysis of corn stover and polyethylene Temperature: 600 °C

	Acid leached CS PE			Acid infused CS PE		
Yield (C%)	Experimental	Calculated	Percent change	Experimental	Calculated	Percent change
Solid residue	9.22 ± 0.39	12.10	-23.80	6.53 ± 0.22	10.21	-36.04
Aromatic	33.49 ± 0.58	25.88	29.40	36.30 ± 1.82	26.65	36.21
CO	5.98 ± 0.16	6.75	-11.41	6.05 ± 0.15	7.55	-19.87
CO_2	3.25 ± 0.26	2.29	41.92	1.25 ± 0.69	2.78	-55.04
Alkane(C≤5)	21.88 ± 1.18	23.73	-7.80	19.11 ± 0.80	23.79	-19.67
Alkene(C≤5)	25.60 ± 0.95	20.61	24.21	23.80 ± 0.72	20.72	14.86
Aromatic Selectivity						
Benzene	16.02			16.02		
Toluene	36.98			36.08		
C_8	30.87			29.56		
C_9	5.33			5.23		
C_{10}	3.94			4.67		
C_{10+}	6.86			8.44		
Alkane and Alkene selectivity						
CH_4	4.15			4.96		
C_2H_6	2.55			3.09		
C_3H_8	26.42			26.85		
C_4H_{10}	17.15			14.37		
C_2H_4	13.86			14.63		
C_3H_6	20.33			20.41		
C_4H_8	12.09			12.64		
C_5H_{10}	3.45			3.05		

Since synergistic effects were found be prominent between PE and acid leached CS/acid infused CS, thus only acid leached CS and acid infused CS were *in-situ* co-pyrolyzed with PE. Comparing the results given in Table 5 for *ex-situ* catalytic pyrolysis and Table 6 for *in-situ* catalytic pyrolysis, it was found that aromatic yield changed from 17.58 and 15.45 C% to 33.49 and 36.30 C% for the mixtures of PE with the acid leached CS, and PE and the acid infused CS, respectively. Alkanes also underwent significant increase during *in-situ* catalytic pyrolysis at the expense of decreased alkene yields from over 50 C% to about 25 C%. Different from that of *ex-situ* catalytic pyrolysis, the aromatic hydrocarbons produced from *in-situ* catalytic pyrolysis were more selective to C_8 and C_9 that are alkylated aromatic, indane and indene, which are the cases for both the acid leached CS and the acid infused CS in the mixtures. During *in-situ* catalytic pyrolysis, the synergistic effects between CS and PE in terms of reducing the yields of solid residues and CO, and increasing aromatic hydrocarbon yields were more prominent than they were observed during *ex-situ* catalytic pyrolysis. Our previous study has revealed that aromatization reaction of light olefins is favored during *in-situ* catalytic pyrolysis of PE [16]. The increased amount of free hydrogen atoms released can be more easily abstracted by the CS derived products during *in-situ* catalytic pyrolysis.

Some variations in the product distributions between the conversion of the acid leached CS and PE and the conversion of the acid infused CS and PE were also observed. The solid residues produced from co-pyrolysis of the acid leached CS and PE were 9.22 C%, much higher than 6.53 C% produced from co-conversion of the acid infused CS and PE. The co-pyrolysis of the acid infused CS and PE produced higher amount of total aromatics but a fewer amount of total aliphatic hydrocarbons in comparison to co-pyrolysis of the acid

leached CS and PE. By comparing the experimental and calculated yields, it can be seen that the extent of decrease in total alkane hydrocarbons was more prominent with the acid infused CS than the acid leached CS when they were both converted with PE. Compared to their corresponding calculated yields, the yields of aromatic hydrocarbons increased by 29.40% for co-pyrolysis of the acid leached CS and PE, and 36.21% for co-conversion of the acid infused CS and PE due to the synergistic effects. Additionally, CO yield decreased by 19.87% for the acid infused CS and PE mixture, in comparison to a 11.41% decrease for the mixture of the acid leached CS and PE. This result indicates that oxygen removal in acid infused CS was removed through dehydration rather than decarbonylation. As discussed above, the primary products were quite similar for the acid leached CS and the acid infused CS when they were both co-pyrolyzed with PE. However, the synergistic effects were stronger with the acid infused CS than acid leached CS when co-pyrolyzed with PE. During *in-situ* catalytic pyrolysis, the sulfate salts formed by the acid infusion to CS may promoted PE cracking to provide more aliphatic hydrocarbons as the source of hydrogen donors and Dies-alder reaction to promote the synergistic effects between CS and PE.

Effects of acid infusion concentration in CS on catalytic co-pyrolysis with PE

As described above, the synergistic effects between the acid infused CS and PE were stronger than the co-conversion of PE with raw CS or the acid leached CS. The CS feedstocks infused with different amounts of acid (3, 4, 5 and 6 wt%) were catalytically *in-situ* co-pyrolyzed with PE. The results are shown in Fig. 2. The yield of solid residue was the highest in the case of the CS with 3 wt% acid, which is 12.79 C%. In comparison, the yield dramatically decreased to 6.53 wt% when the acid concentration increased to 4 wt% in the CS. However, further increase in the acid concentration to 5 and 6 wt% increased the solid

residue yields to 9.27 and 10.03 C%, respectively. The maximum aromatic hydrocarbon yield was obtained during co-conversion of PE and the CS with 4 wt% acid infusion. CO and CO_2 yields were also highest under the same condition. The aromatic yields from co-conversion with 3, 5 and 6 wt% acid infused CS were similar, all about 30 C%. On the other hand, the yields of alkanes and alkenes both showed increase as the amount of acid concentration increased. During catalytic co-conversion, the infused acid acts as Brönsted acid in addition to it is provided by the zeolite. The increased acidity could enhance depolymerization, dehydration and carbonization reactions. When the acid content is low, it may react with the AAEMs in CS to form salts, thus, cannot act as an acid catalyst. Thus, the Diels-Alder reaction between furans and olefins was less favored due to the lacking in furans. One the other hand, excessive amount of acid presented in biomass could promote less desired reactions, such as dehydration and carbonization to form char. The acid could also catalyze repolymerization of primary products, thus reducing the chances of the decomposition products from entering the catalytic pores for deoxygenation. For example, the presence of acid could increase the formation of phenolic oligomers whereas phenolic oligomers have strong tendency for adsorption on zeolite surface for coking [30], which eventually deactivates the catalyst [31]. In another hand, the excessive sulfuric acid could decompose into SO_2 during pyrolysis whereas the sulfur compound can be chemisorbed on the catalyst surface. Sulfur is a strong catalyst poison reagent for zeolite-involved process including hydrogenation, hydrocracking, oxidation and dehydrogenation [32]. As a result, hydrodeoxygenation reactions of CS-derived compounds that utilize hydrogen abstracted from PE were probably hindered due to the deactivation of zeolite.

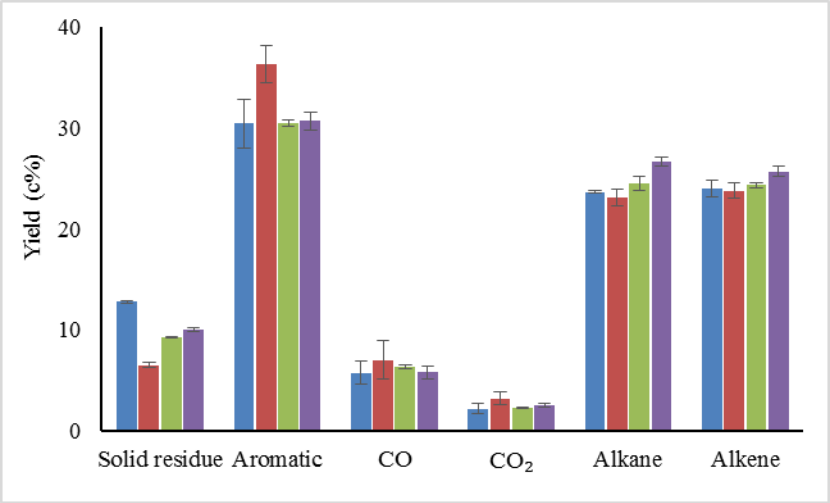

Figure 2. Product distribution from *in-situ* pyrolysis of PE and corn stover with different acid infusion amount, 3 wt% (blue), 4 wt% (red), 5 wt% (green), 6 wt% (purple)

Conclusion

The results presented in this study demonstrated the synergistic effects between CS and PE during fast pyrolysis. Pretreatments of CS by acid leaching and acid infusion were found to enhance the cross reactions between CS and PE. For non-catalytic co-pyrolysis, strong interactions were observed between the acid infused CS and PE. It is likely that the cracking of PE was enhanced by AAEM sulfate salts formed by the acid infusion in CS, thus promoting hydrogen abstraction from PE by the CS-derived compounds. Co-pyrolysis of the acid infused CS and PE also inhibited char agglomeration during pyrolysis, probably because the hydrogen donor effect of PE promoted sugar evaporation and the newly formed AAEM salts prevented lignin agglomeration. For *ex-situ* catalytic co-pyrolysis, strong synergistic effects were observed with the mixtures of PE and the acid leached CS as well as PE and the acid infused CS due to the enhanced Diels-Alder reactions between the CS-derived furans and the PE-derived olefins. The synergistic effects were further improved by *in-situ* catalytic

co-pyrolysis of the acid infused CS and PE. Co-pyrolysis of PE with 4% acid infusion CS produced optimum results. Excessive amount of acid infusion not only promoted coke formation, but could also poison the zeolite catalyst.

Acknowledgement

The authors would like to thank Dr. Robert Brown, Dr. Patrick Johnston and Dr. Marjorie Rover at Bioeconomy Institute of Iowa State University for technical support. This research did not receive any specific grant from funding agency.

Reference

[1] J. Jae, G.A. Tompsett, A.J. Foster, K.D. Hammond, S.M. Auerbach, R.F. Lobo, G.W. Huber, Investigation into the shape selectivity of zeolite catalysts for biomass conversion, Journal of Catalysis, 279 (2011) 257-268.

[2] Y. Xue, S. Zhou, R.C. Brown, A. Kelkar, X. Bai, Fast pyrolysis of biomass and waste plastic in a fluidized bed reactor, Fuel, 156 (2015) 40-46.

[3] I. Boumanchar, Y. Chhiti, F.E.M.h. Alaoui, A. El Ouinani, A. Sahibed-Dine, F. Bentiss, C. Jama, M. Bensitel, Effect of materials mixture on the higher heating value: Case of biomass, biochar and municipal solid waste, Waste Management, (2016).

[4] X. Zhang, H. Lei, S. Chen, J. Wu, Catalytic co-pyrolysis of lignocellulosic biomass with polymers: a critical review, Green Chemistry, (2016).

[5] Y. Xue, A. Kelkar, X. Bai, Catalytic co-pyrolysis of biomass and polyethylene in a tandem micropyrolyzer, Fuel, 166 (2016) 227-236.

[6] X. Li, J. Li, G. Zhou, Y. Feng, Y. Wang, G. Yu, S. Deng, J. Huang, B. Wang, Enhancing the production of renewable petrochemicals by co-feeding of biomass with plastics in catalytic fast pyrolysis with ZSM-5 zeolites, Applied Catalysis A: General, 481 (2014) 173-182.

[7] C. Dorado, C.A. Mullen, A.A. Boateng, H-ZSM5 Catalyzed Co-Pyrolysis of Biomass and Plastics, ACS Sustainable Chemistry & Engineering, 2 (2014) 301-311.

[8] A.V. Barker, D.J. Pilbeam, Handbook of plant nutrition, CRC press, 2015.

[9] Q. Liu, S.C. Chmely, N. Abdoulmoumine, Biomass treatment strategies for thermochemical conversion, Energy & Fuels, 31 (2017) 3525-3536.

[10] S. Oudenhoven, R.J.M. Westerhof, N. Aldenkamp, D.W.F. Brilman, S.R. Kersten, Demineralization of wood using wood-derived acid: Towards a selective pyrolysis process for fuel and chemicals production, Journal of analytical and applied pyrolysis, 103 (2013) 112-118.

[11] S. Oudenhoven, R.J.M. Westerhof, S.R. Kersten, Fast pyrolysis of organic acid leached wood, straw, hay and bagasse: Improved oil and sugar yields, Journal of analytical and applied pyrolysis, 116 (2015) 253-262.

[12] S. Oudenhoven, C. Lievens, R.J.M. Westerhof, S.R. Kersten, Effect of temperature on the fast pyrolysis of organic-acid leached pinewood; the potential of low temperature pyrolysis, Biomass and Bioenergy, 89 (2016) 78-90.

[13] P.R. Patwardhan, J.A. Satrio, R.C. Brown, B.H. Shanks, Influence of inorganic salts on the primary pyrolysis products of cellulose, Bioresource technology, 101 (2010) 4646-4655.

[14] G.F. David, V.H. Perez, O.R. Justo, M. Garcia-Perez, Effect of acid additives on sugarcane bagasse pyrolysis: Production of high yields of sugars, Bioresource technology, 223 (2017) 74-83.

[15] N. Kuzhiyil, D. Dalluge, X. Bai, K.H. Kim, R.C. Brown, Pyrolytic sugars from cellulosic biomass, ChemSusChem, 5 (2012) 2228-2236.

[16] Y. Xue, P. Johnston, X. Bai, Effect of catalyst contact mode and gas atmosphere during catalytic pyrolysis of waste plastics, Energy Conversion and Management, 142 (2017) 441-451.

[17] S. Kumagai, K. Fujita, T. Kameda, T. Yoshioka, Interactions of beech wood–polyethylene mixtures during co-pyrolysis, Journal of Analytical and Applied Pyrolysis, 122 (2016) 531-540.

[18] T. Hosoya, H. Kawamoto, S. Saka, Solid/liquid-and vapor-phase interactions between cellulose-and lignin-derived pyrolysis products, Journal of Analytical and Applied Pyrolysis, 85 (2009) 237-246.

[19] P. Rutkowski, Chemical composition of bio-oil produced by co-pyrolysis of biopolymer/polypropylene mixtures with K2CO3 and ZnCl2 addition, Journal of Analytical and Applied Pyrolysis, 95 (2012) 38-47.

[20] J.-L. Shie, J.-P. Lin, C.-Y. Chang, D.-J. Lee, C.-H. Wu, Pyrolysis of oil sludge with additives of sodium and potassium compounds, Resources, Conservation and Recycling, 39 (2003) 51-64.

[21] D.L. Dalluge, T. Daugaard, P. Johnston, N. Kuzhiyil, M.M. Wright, R.C. Brown, Continuous production of sugars from pyrolysis of acid-infused lignocellulosic biomass, Green Chemistry, 16 (2014) 4144-4155.

[22] K.H. Kim, R.C. Brown, X. Bai, Partial oxidative pyrolysis of acid infused red oak using a fluidized bed reactor to produce sugar rich bio-oil, Fuel, 130 (2014) 135-141.

[23] K. Wang, J. Zhang, B.H. Shanks, R.C. Brown, The deleterious effect of inorganic salts on hydrocarbon yields from catalytic pyrolysis of lignocellulosic biomass and its mitigation, Applied Energy, 148 (2015) 115-120.

[24] T.R. Carlson, J. Jae, G.W. Huber, Mechanistic Insights from Isotopic Studies of Glucose Conversion to Aromatics Over ZSM‐5, ChemCatChem, 1 (2009) 107-110.

[25] T.R. Carlson, T.P. Vispute, G.W. Huber, Green gasoline by catalytic fast pyrolysis of solid biomass derived compounds, ChemSusChem, 1 (2008) 397-400.

[26] W. Vermeiren, J.-P. Gilson, Impact of zeolites on the petroleum and petrochemical industry, Topics in Catalysis, 52 (2009) 1131-1161.

[27] Y.-T. Cheng, G.W. Huber, Production of targeted aromatics by using Diels–Alder classes of reactions with furans and olefins over ZSM-5, Green Chemistry, 14 (2012) 3114-3125.

[28] C. Dorado, C.A. Mullen, A.A. Boateng, Origin of carbon in aromatic and olefin products derived from HZSM-5 catalyzed co-pyrolysis of cellulose and plastics via isotopic labeling, Applied Catalysis B: Environmental, 162 (2015) 338-345.

[29] K. Wang, P.A. Johnston, R.C. Brown, Comparison of in-situ and ex-situ catalytic pyrolysis in a micro-reactor system, Bioresource Technology, 173 (2014) 124-131.

[30] P.R. Patwardhan, R.C. Brown, B.H. Shanks, Understanding the fast pyrolysis of lignin, ChemSusChem, 4 (2011) 1629-1636.

[31] C.A. Mullen, A.A. Boateng, Catalytic pyrolysis-GC/MS of lignin from several sources, Fuel Processing Technology, 91 (2010) 1446-1458.

[32] S. Bhatia, J. Beltramini, D. Do, Deactivation of zeolite catalysts, Catalysis Reviews—Science and Engineering, 31 (1989) 431-480.

SUPPLEMENTAL INFORMATION FOR CHAPTER 4

Table S1. Levoglucosan yield from pyrolysis of acid infused CS

Acid infusion amount (wt%)	3	4	5	6
Levoglucosan yield (wt%)	7.50 ± 0.23	11.19 ± 0.48	7.86 ± 0.70	1.82 ± 0.25

CHAPTER 5

EFFECT OF CATALYST CONTACT MODE AND GAS ATMOSPHERE DURING CATALYTIC PYROLYSIS OF WASTE PLASTICS

A paper published to the journal *Energy Conversion and Management*

Yuan Xue[1], Patrick Johnston[2], Xianglan Bai[1*]

Abstract

In the present study, polyethylene (PE), polypropylene (PP), polystyrene (PS) and polyethylene terephthalate (PET) were pyrolyzed using HZSM-5 zeolite in a tandem micro-pyrolyzer to investigate the effects of plastic type, catalyst and feedstock contact mode, as well as the type of carrier gas on product distribution. Among the four plastics, PS produced highest aromatic yields up to 85% whereas PE and PP mainly produced aliphatic hydrocarbons. In comparison to *ex-situ* pyrolysis, *in-situ* pyrolysis of the plastics produced more solid residue but also promoted the formation of aromatic hydrocarbons, except PS. For PS, *ex-situ* pyrolysis produced a higher yield of aromatics than *in-situ* pyrolysis, mostly contributed by high styrene yield. During *in-situ* pyrolysis, the catalyst reduced the decomposition temperatures of the plastics in the order of PE, PP, PS and PET from high to low. Hydrogen carrier gas reduced solid residue and also increased the selectivity of single ring aromatics in comparison to inert pyrolysis. Hydrogen atmosphere was more beneficial to PS and PET than PE and PP in terms of reducing coke yield and increasing hydrocarbon yield. The present study also showed that catalytically co-pyrolyzing PS and PE, or PET and PE increases the yield of aromatics and reduces the yield of solid residue due to hydrogen transfer from PE to PS or PET and alkylation reactions among the plastic-derivatives.

[1] Department of Mechanical Engineering, Iowa State University, Ames, Iowa 5001
[2] Bioeconomy Institute, Iowa State University, Ames, Iowa USA, 50011
* Corresponding author. Postal address: Iowa State University, 2070 Black Engineering Building, Ames, IA 50011; Tel: +1 515 294 6886; Fax: +1 515 294 3261; E-mail address: bxl9801@iastate.edu (X. Bai)

Key words: Waste plastics; hydropyrolysis; zeolite catalyst; *in-situ* & *ex-situ*; hydrocarbons

Introduction

As one of the most important petroleum-based materials, plastics have significantly contributed to our modern society. Plastic production has been increasing 3~4% annually since 1990s [1]. It is projected the plastic consumption to increase dramatically in the developing countries due to the economic expansion [2, 3]. On the other hand, the disposal of end-life plastics has become significant environmental and economic issue. Not only transporting bulky and large quantity of waste plastics to remoted landfills are costly, non-biodegradable plastics continue to invade the valuable land resource [4, 5]. Waste-to-energy technologies enable converting waste plastics into heat, hydrocarbon fuels and chemicals, therefore reducing the amount of plastics to be landfilled [6]. The common waste plastics include polyethylene (PE, both low density and high density PEs), polypropylene (PP), polystyrene (PS), and polyethylene terephthalate (PET). Pyrolysis products of plastics include pyrolysis oil, char and light gases. Among them, pyrolysis oil is the main product and usually reaches optimum when pyrolysis temperatures is 500-600 °C [7]. Often, pyrolysis products of plastics need downstream separation and upgrading due to the wide range of carbon numbers among the products. Typically, the carbon chain length of the liquid products produced from pyrolysis of PE or PP ranging from C_5 to C_{30}. The products with longer chain lengths are waxy materials upon condensation. The wax has low volatility and octane number, thus requiring additional cracking step in order to be used as liquid fuels. Moreover, the formation of waxy materials may also result in clogging and defluidization in pyrolysis reactors [8]. Catalytic pyrolysis of plastics is a method for upgrading the pyrolysis

products before the vapor condenses by introducing catalyst during pyrolysis. Upon catalytic pyrolysis, the final products could have a narrower carbon-number distribution and better product selectivity [9, 10].

In general, polyolefins (e.g., PE, PP and PS) are more easily cracked with acid catalyst [11]. Zeolite catalyst (e.g., HZSM-5, HY, Hβ) or zeolite based catalysts (FCC) are frequently chosen to crack polyolefins because these catalysts contain abundant Brønsted and Lewis acid sites [12]. For polyester (e. g., PET) depolymerization, base catalysts, such as calcium oxide and sodium carbonate, are also used [13-15].

The results of catalytic pyrolysis are affected by a number of factors [9, 16-19]. For example, Wong et al. [19] pyrolyzed LDPE in a fixed bed reactor and found that the yield of pyrolysis oil and its composition depend on the catalyst amount, feeding rate of plastics, carrier gas flow rate and pyrolysis temperature. Lopez et al. [9, 18] converted HDPE in a conical spouted reactor by mixing the plastic with HZSM-5 catalysts with different acidities and reported that zeolite acidity and pore structure affect the product selectivity and coke formation. In addition to the well-studied parameters, the contact mode of the feedstock and catalyst could also affect the product distribution during catalytic pyrolysis. During *in-situ* catalytic pyrolysis, catalyst and feedstock material are physically mixed during pyrolysis. The examples include pyrolyzing the premixed plastics and catalyst using batch reactors, or feeding plastics into a fluidized reactor or conical spouted bed reactor and allowing the solid plastics to mix with the catalyst and sand inside the reactor [9, 20, 21]. Alternatively, plastics are thermally pyrolyzed first and the evolving pyrolysis vapors are sent to downstream catalytic bed before the vapor exists the system, which is referred as *ex-situ* catalytic pyrolysis [22, 23]. *Ex-situ* catalytic pyrolysis is also denoted as a stage pyrolysis consisting

of pyrolysis step and catalysis step. Although the products with improved quality are obtained upon the completion of pyrolysis, advantages and disadvantages of *in-situ* and *ex-situ* pyrolysis are noted. *In-situ* catalytic pyrolysis is simple and no mechanical modification of existing reactors is required. It also potentially reduces the energy required for pyrolysis by lowering decomposition temperatures. However, recovering used catalyst from its mixture with solid residue is difficult during *in-situ* pyrolysis. The solid residue could also facilitate deactivation of catalyst, especially if the feedstock is high in ash content or metal impurities. Compared to *in-situ* catalytic pyrolysis, *ex-situ* catalytic pyrolysis requires external catalytic bed. The temperatures in the pyrolysis unit have to be moderately high to ensure pyrolysis vapor to be upgraded at the catalyst bed. On the other hand, catalyst regeneration is much simpler with *ex-situ* catalytic pyrolysis. *Ex-situ* catalytic pyrolysis is also particularly attractive in converting high ash content feedstock or the feedstock forming char [24, 25]. In addition, the overall product distribution and selectivity of products could be varied between *in-situ* catalytic pyrolysis and *ex-situ* catalytic pyrolysis because of the different contact modes between catalyst and feedstock during pyrolysis. However, few studied *in-situ* and *ex-situ* catalytic pyrolysis of common waste plastics [26].

The type of carrier gas during catalytic pyrolysis could also affect the conversion of the plastics. Although catalytic pyrolysis of plastics was mostly conducted under inert environment, using reactive carrier gas could potentially improve the yields of desired products. It has been reported that catalytic hydropyrolysis of biomass (i.e., H_2 as the carrier gas) reduces coke yield and promotes hydrodeoxygenation of biomass [27]. Hydrogen could quench reactive radicals to inhibit polymerization reactions. Hydrocracking also reduces the formation of high molecular weight products [28]. Sun et al. previously reported that the

yields of styrene monomer increases when PS was converted in a fixed bed reactor in the presence of H_2 using Pt-Ce/α-Al_2O_3 and Rh-Ce/α-Al_2O_3 as the catalysts [29]. However, catalytic hydropyrolysis of plastics was seldom investigated with other plastics.

In the present study, *in-situ* and *ex-situ* catalytic pyrolysis of major waste plastics were investigated. The plastics, including PS, PET, PE and PP, were converted in a tandem micro-pyrolyzer using HZSM-5 zeolite as the catalyst and the product distribution was analyzed. HZSM-5 zeolite was selected because it has an excellent cracking and deoxygenation abilities. HZSM-5 is also known for its low deactivation rate and efficient regeneration, in comparison to other types of zeolite catalysts [30]. The *in-situ* and *ex-situ* catalytic pyrolysis of the plastics were also performed using H_2 as the carrier gas. In addition, PE was also catalytically co-pyrolyzed with PS or PET to investigate possible synergy between the hydrogen rich plastic and the hydrogen deficient plastics.

Experimental

Material

PE was purchased from Sigma-Aldrich. PP, PS and PET were purchased from Yangli Tech Company, China. The purity of all plastics is above 99%. The range of particle size of the PE with ultra-high molecular weight is between 53-75μm. The particle sizes of other plastics are also less than 75μm. Characterization of the plastics is listed in Table 1. The elemental compositions were calculated based on the molecular formulas of the plastics because of the high purity of the samples.

The standard chemicals of aromatic hydrocarbons were purchased from Sigma Aldrich. The gas standards for calibration, which include CO, CO_2, CH_4, C_2H_6, C_3H_8, C_4H_{10}, C_2H_4, C_3H_6 and C_5H_{10}, were purchased from Praxair, USA.

HZSM-5 zeolite (CBV 2314, SiO_2/Al_2O_3=23:1) was purchased from Zeolyst International. The ammonium form zeolite was calcinated inside a muffle furnace at 550 °C for 5 hours with sufficient air flow. The activated catalyst powders were pelletized using a hydraulic pressure pelletizer. The pellets were then crushed and screened to 50-70 mesh size.

Table 1. Characterization of plastics used in this study

Plastic	Formula	Volatile	Fixed carbon	Ash
PE	$(C_2H_4)_n$	100	0	-
PP	$(C_3H_6)_n$	99.40	0.60	-
PET	$(C_{10}H_8O_4)_n$	81.80	18.20	-
PS	$(C_8H_8)_n$	99.47	0.53	-

Pyrolysis and analysis

The pyrolysis experiment was carried out in a Tandem micro-pyrolyzer (Frontier Lab, Japan). The reactor system consists of two sequential furnaces and the temperature of each furnace can be adjusted from room temperature to 900 °C. The top furnace is a pyrolysis reactor. A removable quartz tube packed with catalyst is placed inside the bottom furnace. The two furnaces are 5 cm apart and connected by a needle with heat insulation. In the reactor system, sample was loaded to a deactivated stainless cup and then dropped into the preheated top furnace. The heating rate of the sample in the reactor is estimated to be about 250 °C/s [31]. The pyrolysis vapor of the sample was converted in downstream catalyst-bed and the final products exiting the bottom furnace is directly analyzed by an online Agilent GC/MS-FID-TCD system (Agilent 6890) for chemical composition. During pyrolysis, He or H_2 was used as the carrier gas in both the micro-pyrolyzer and GC/MS. The flow rate of the carrier gas in the micro-pyrolyzer was 156 mL/min. Thus, the residence time of pyrolysis vapor in the reactor is less than a second. The GC oven temperature was initially kept at 40

°C for 3 min, increased to 280 °C with a heating rate of 6 °C/min, and then held at 280 °C for another 3 min. The front-injector temperature was set at 280 °C to prevent product condensation. Two Phenomenex ZB-1701 (60 m × 250 µm × 0.25 µm) capillary columns were separately connected to a mass spectrometer (MS 5975 C, Agilent, USA) and flame ionization detector (FID). A Porous Layer Open Tubular (PLOT) column (60 m × 0.320 mm) (GS-GasPro, Agilent, USA) was connected to a thermal conductivity detector (TCD). The products were first identified by the MS and then quantified by FID. For quantification, five different concentrations of each compound were injected into the GC/MS-FID-TCD to generate a calibration curve with regression coefficient >99%. Non-condensable-gases (NCGs), which includes carbon oxides and light hydrocarbons were quantified by the TCD using the standard gas mixture.

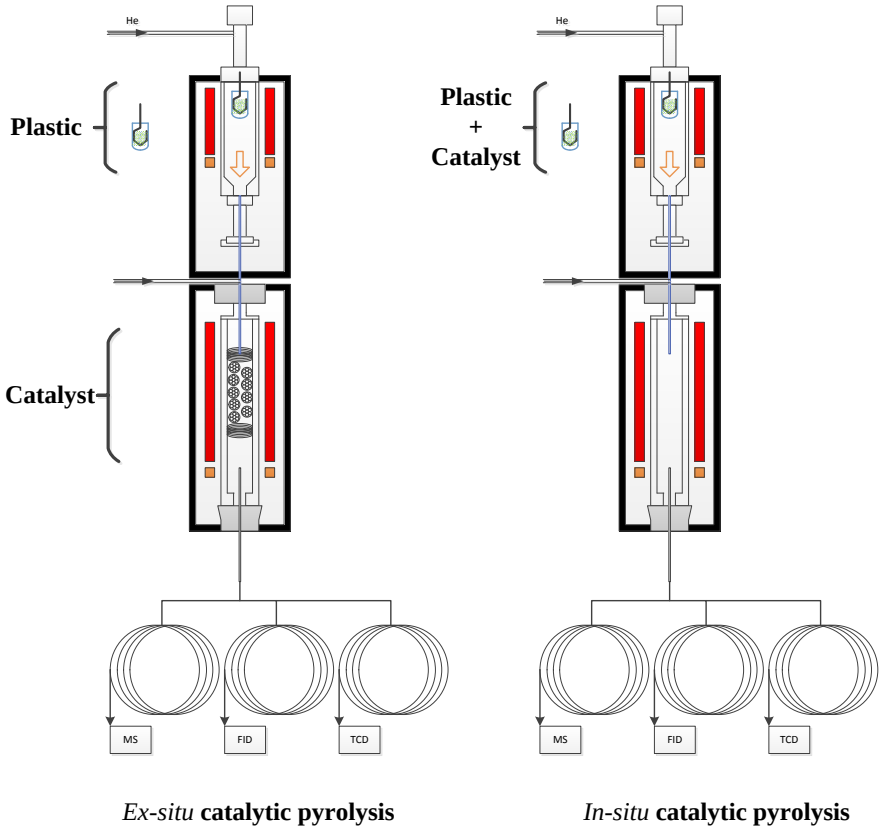

Figure 1. The configuration of *in-situ* and *ex-situ* pyrolysis in Tandem micro-pyrolyzer

During pyrolysis, the temperatures of both furnaces were set at 600 °C to ensure the plastics to decompose within the short pyrolysis time. For *ex-situ* catalytic pyrolysis, a 500 μg of a plastic sample was pyrolyzed in the first furnace. For catalytic co-pyrolysis, 250 μg of PE was premixed with 250 μg of PET or PS. Inside the second furnace, the quartz tube was loaded with 10mg of loosely packed catalyst particles, which is equivalence to 20 times of plastics. The relatively high catalyst to plastic ratio was used in this study because the retention time of the pyrolysis vapor in the catalyst bed is very short due to the high flow rate of the carrier gas and short length of the catalyst bed. The length of the catalyst bed occupied by 10 mg of catalyst was only 4mm. Thus, the residence time of the pyrolysis vapor in the catalytic bed is about 0.01s. For *in-situ* catalytic pyrolysis, the same ratio of plastic powders and catalyst were premixed. During pyrolysis, approximate 5 mg of the plastic/catalyst mixture was pyrolyzed inside the first furnace and the vapor was sent to the second furnace with the catalyst bed removed. The configuration of tandem reactor and the layout of catalyst and plastic materials during *ex-situ* and *in-situ* pyrolysis are illustrated Fig. 1.

Each test condition was triplicated to ensure the reproducibility of the results. For *ex-situ* pyrolysis, the residues remaining inside the cup and carbons deposited on the catalyst are denoted as char and coke, respectively. The carbon contents of char and coke were further analyzed by an elemental analyzer (vario MICRO cube, Elementar, USA). Because the catalyst and plastic were mixed during *in-situ* pyrolysis, the separation of char and catalytic coke after pyrolysis was impossible. In the case, the carbon content in the total solid carbon residue left inside the cup was measured and reported in the present study.

In this work, the yields of products were reported on carbon basis, calculated using Equation (1):

$$Carbon\ yield\ of\ a\ product\ (C\%) = \frac{Mole\ of\ carbon\ in\ product}{Total\ mole\ of\ carbon\ in\ plastic} \times 100\% \quad (1)$$

Carbon selectivity of individual aromatic hydrocarbons among the total aromatic hydrocarbon group was calculated based on Equation (2):

$$Product\ carbon\ selectivity\ (\%) = \frac{Mole\ of\ carbon\ in\ an\ aromatic\ hydrocarbon\ compound}{Total\ mole\ of\ carbon\ in\ aromatic\ hydrocarbon\ group} \times 100\% \quad (2)$$

Carbon selectivity of individual aliphatic hydrocarbons among the total aliphatic hydrocarbon group was calculated based on Equation (3):

$$Product\ carbon\ selectivity\ (\%) = \frac{Mole\ of\ carbon\ in\ an\ aliphatic\ hydrocarbon\ compound}{Total\ mole\ of\ carbon\ in\ aliphatic\ hydrocarbon\ group} \times 100\% \quad (3)$$

To determine the cross reactions and synergetic effects between PE and PET, or PE and PS, the experimental yields of the products were compared with their additive yields. The additive yields are the mathematic sum of the product yields if different plastics are independently converted. Thus, additive yields are the yields of the products under an assumption that there is no cross reaction between different plastics. The additive yield was calculated based on Equation (4):

$$Additive\ yield\ (C\%) = \frac{C_1 P_1 + C_2 P_2}{C_1 + C_2} \times 100\% \quad (4)$$

C_i: Carbon content of different plastics; (i=1 or 2);

P_i: The carbon yield of a product when plastics are pyrolyzed individually.

Thermogravimetric Analysis (TGA)

Thermogravimetric analysis of pyrolysis of different plastics with or without catalyst was performed in a Mettler Toledo TGA/DSC system (TGA/DSC 1 STARe system, Mettler

Toledo). A total 20 mg of the mixture of plastic and catalyst with mass ratio of 1:1 was placed in a crucible. The mixture was heated from room temperature up to 105 °C at 10 °C/min and kept at the temperature for 40 min to remove the moisture trapped inside the catalyst pores. The sample was then continued to be heated to 900 °C using the same heating rate. Nitrogen with a flow rate of 100 ml/min was used as the sweep gas to quickly remove the pyrolysis vapor from the sample cup.

Results and discussions

Catalytic pyrolysis of PS

The product distributions of PS during *in-situ* and *ex-situ* catalytic pyrolysis with different carrier gases are compared in Fig. 2. The detailed product yields and product selectivity for the corresponding tests are given in Table S1. When PS was *ex-situ* pyrolyzed with the catalyst using He gas, no pyrolysis char was found in the sample cup because the ash content in the sample was negligible. When the vaporized products were upgraded by zeolite in the catalytic bed, 4.44 C% of coke was collected from the used catalyst bed. On the other hand, the solid carbon residue accounted for 15.86 C% during *in-situ* catalytic pyrolysis of PS, which is more than three times of the total solid residue produced from *ex-situ* catalytic pyrolysis of PS (i.e., the sum of pyrolysis char and catalytic coke). Aromatic hydrocarbons were the major products from catalytic pyrolysis of PS and the yield was nearly 80 C% during *ex-situ* catalytic pyrolysis. The total yield of aromatic is comparable with that was reported by Williams et al. [32]. They obtained 86.2wt% of liquid product by catalytically pyrolyzing PS in a fixed bed reactor. Styrene was the most abundant hydrocarbon followed by benzene. The yield of aromatic was 67.36 C% during *in-situ* catalytic pyrolysis, lower that

it obtained from *ex-situ* pyrolysis. However, benzene yield was 39.6 C%, much higher than it was obtained from *ex-situ* pyrolysis of PS (i.e., 23.59 C%). It was also noted that the selectivity of benzene and naphthalenes among the aromatic hydrocarbons both increased during *in-situ* catalytic pyrolysis, which suggests that de-alkylation and aromatization were promoted simultaneously. The yields of aliphatic hydrocarbons (the sum of alkane and alkene) were very low during both *in-situ* and *ex-situ* catalytic pyrolysis. Although the yields of alkane were lower than alkene all the time, *in-situ* pyrolysis produced slightly more alkane than *ex-situ* pyrolysis.

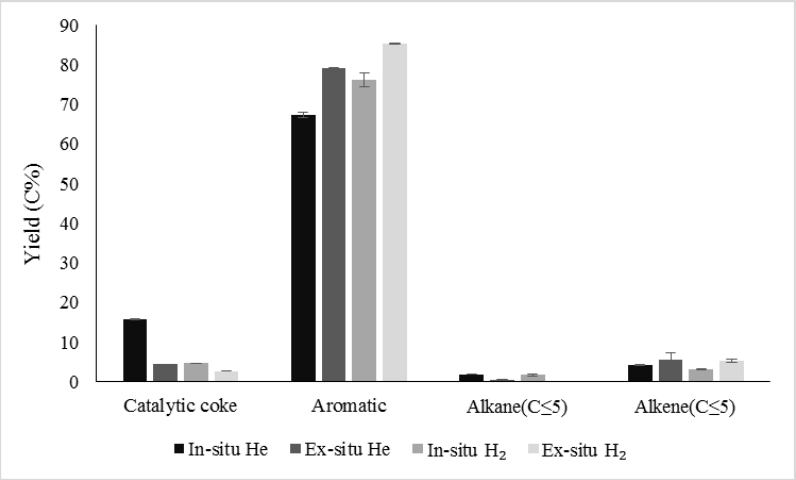

Figure 2. Product distributions during catalytic pyrolysis of PS

The proposed mechanisms during catalytic pyrolysis of PS are illustrated in Fig. 3. During *ex-situ* catalytic pyrolysis, PS first underwent thermal decomposition in the pyrolysis reactor prior to the vapor entering the catalytic bed. According to previous studies [29, 33-35], free radical mechanism dominates the thermal decomposition of PS. At elevated pyrolysis temperatures, the initiation step starts with phenyl group detachment or hydrogen abstraction from the polymer chain which produce phenyl radicals and polystyrene fragment radicals. The propagation step includes the self-scission of polystyrene fragment radicals and

the attacking of the polymer chain by phenyl radical, causing mid-chain and end-chain β-scissions [36]. The chain lengths of the pyrolysis products are highly dependent on the reaction time and scission position [34]. When PS was pyrolyzed in the absence of catalyst, thermal cracking of PS induces β-scission from the chain end free radical to produce styrene. Styrene dimers are also one of the major products from the thermal decomposition of PS. After a tertiary carbon was attacked by a free radical, β-scission immediately occurred to produce styrene dimers or even trimers [33]. In the present study, no aliphatic hydrocarbons were produced when PS was pyrolyzed in absence of catalyst. The results indicate that de-alkylation of styrene does not occur during the thermal cracking of PS under the pyrolysis condition. Therefore, the aliphatic hydrocarbons observed during *ex-situ* catalytic pyrolysis must be due to catalytic cracking. Styrene monomers could be de-alkylated in the catalyst bed to produce benzene and ethylene. On the other hand, a significant amount of styrene was found among the final products during *ex-situ* pyrolysis. The styrene vapor is highly volatile (i.e., the boiling point of styrene is 145 °C) and the flow rate of the carrier gas passing through the catalytic bed was also high during the *ex-situ* catalytic pyrolysis. Thus, the residence time of the styrene vapor in the catalytic bed may be not sufficient to completely de-alkylate styrene.

According to Marczewski et al. [35], the acid-catalyzed cracking of styrene dimers could start from either the aliphatic chain or the aromatic ring of the dimers, attacked by Brønsted acid sites on the catalyst. Compared to the double bond in the aromatic ring, the double bond located on the aliphatic chain is far more easily to be attacked by Brønsted acid sites. This is because the aromatic double bond is more stable and sterically hindered, thus requiring higher dissociation energy and sufficient feedstock-catalyst contact. During *ex-situ*

catalytic pyrolysis of PS, the aromatic double bonds are less likely being attacked due to the limited contact between the catalyst and the vapor products. After the aliphatic chain in styrene dimers being attacked by protons from the acid sites, the protonated styrene dimers further underwent chain scission to styrene monomer or cyclization to methyl-phenyl-indane. Methyl-indene and benzene could be produced from further cracking of methyl-phenyl-indane.

Compared to *ex-situ* catalytic pyrolysis, there was significant change in the product selectivity when PS was *in-situ* pyrolyzed with the catalysis. Styrene nearly disappeared while benzene yield increased significantly during *in-situ* catalytic pyrolysis of PS. The reactions of plastics over the catalyst include cracking on the catalyst surface and reforming inside the catalyst pores [37]. In the initial stage, the cracking of the polymer chain is carried out on the catalytic surface by the surface Lewis acid sites grabbing hydrides to form carbocationic intermediates. The decomposed short chain products could either directly evaporate or enter the zeolite pores for further reforming. In general, cracking, isomerization, oligomerization, aromatization and alkylation could occur [38]. Both the yields of gasoline range compounds and octane number improved through the reforming reactions. For PS, dealkylation of styrene, as well as the aromatization of the side chain fragments could occur inside the pores. During *in-situ* catalytic pyrolysis, the melted plastics could adhere to the surface of zeolite catalyst to greatly enhance the interaction between the plastic and the catalyst. The cracking of the plastic polymer chain on the catalyst surface could produce higher concentration of smaller molecules that can be further converted inside the catalyst pores. Wang et al. [39] previously investigated *in-situ* and *ex-situ* catalytic pyrolysis of biomass and concluded that the catalyst is exposed to a more concentrated pyrolysis product

stream during *in-situ* catalytic pyrolysis, which resulted in an enhanced opportunity for catalytic conversion. In this study, possible mass transfer limitation inside the sample cup during *in-situ* catalytic pyrolysis may also delay evaporation of the decomposed products of PS, thus in turn promoting the reforming reactions inside the zeolite pores to increase dealkylation of styrene. In addition, aromatic double bonds in styrene dimers could be attacked by the surface active sites during *in-situ* catalytic pyrolysis to produce benzene and alkenyl aromatic cation due to the sufficient contact with the catalyst. With benzene detached from the styrene dimer, the remaining cations could lose one proton at the aliphatic chain and form phenyl butadiene. The phenyl butadiene is the reactive precursors of naphthalenes and coke [35].

As shown in Fig. 2 and Table S1, using hydrogen carrier gas in the catalytic pyrolysis (i.e., catalytic hydropyrolysis) also affected the product distribution during catalytic pyrolysis of PS. For both *in-situ* and *ex-situ* catalytic pyrolysis, H_2 as the carrier gas reduced the yield of solid residue and increased the aromatic yield compared to using He as the carrier gas. For *in-situ* catalytic hydropyrolysis, the yield of solid residue was only 4.66 C%, significantly lower than that from *in-situ* pyrolysis using inert gas. The alkene yield became as low as 0.47 C% and the alkane yield was decreased by H_2 as the carrier gas. On the other hand, the aromatic yield increased to 76.06 C%, mainly contributed by the increased yields of benzene, indane and naphthalenes. Since the reactor was operated under atmospheric pressure with moderate temperature, the homogeneous dissociation of hydrogen molecules into hydrogen radicals is unlikely to occur in this condition. Previous study conducted by Hideshi et al. [40] revealed that H_2 molecule could be converted into a protonic acid site and a hydride in the presence of strong Lewis acid site. After the heterogeneous dissociation, the Lewis acid site

is occupied with the hydride. With the double bond being reduced by H_2 (i.e., the alkenyl aromatic cation is first neutralized by hydride followed by a proton attack at the double bond), the alkenyl aromatic cation, which is the intermediate produced from the attacking of the aromatic double bond in styrene dimer, is converted into butylated aromatic cation. Part of the butylated aromatic cation is possible neutralized by hydride. During *in-situ* catalytic hydropyrolysis, a trace amount of butyl benzene (i. e., the neutralized butylated aromatic cation) was observed in the GC/MS chromatogram of the products, which supports the above argument. In a more favored pathway, the alkenyl aromatic cations further reacted into methyl indane, naphthalenes, or benzene, toluene and ethyl benzene, ether by internal cyclization or side chain cleavage.

For *ex-situ* catalytic hydropyrolysis, H_2 gas reduced the coke yield from 4.44 to 2.73 C% and increased aromatic yield from 79.06 to 85.38 C%. The yield of aliphatic hydrocarbons decreased and only a trace amount of alkane was found. Among the aromatic hydrocarbons, the yields of benzene and ethyl benzene increased significantly, indicating hydrocracking and hydrogenation of styrene were strongly promoted by H_2. The cyclization of protonated styrene dimers and the cracking of methyl-phenyl-indane were also enhanced due to the increased protonic acid sites produced from the heterogeneous dissociation of hydrogen. As a result, the yields of methyl-indene and benzene increased.

Catalytic pyrolysis of PET

The product distributions of catalytic pyrolysis of PET are compared in Fig. 4. The detailed product yields and product selectivity are summarized in Table S2. A 4.03 C% of pyrolysis char was obtained during *ex-situ* catalytic pyrolysis of PET with inert gas,

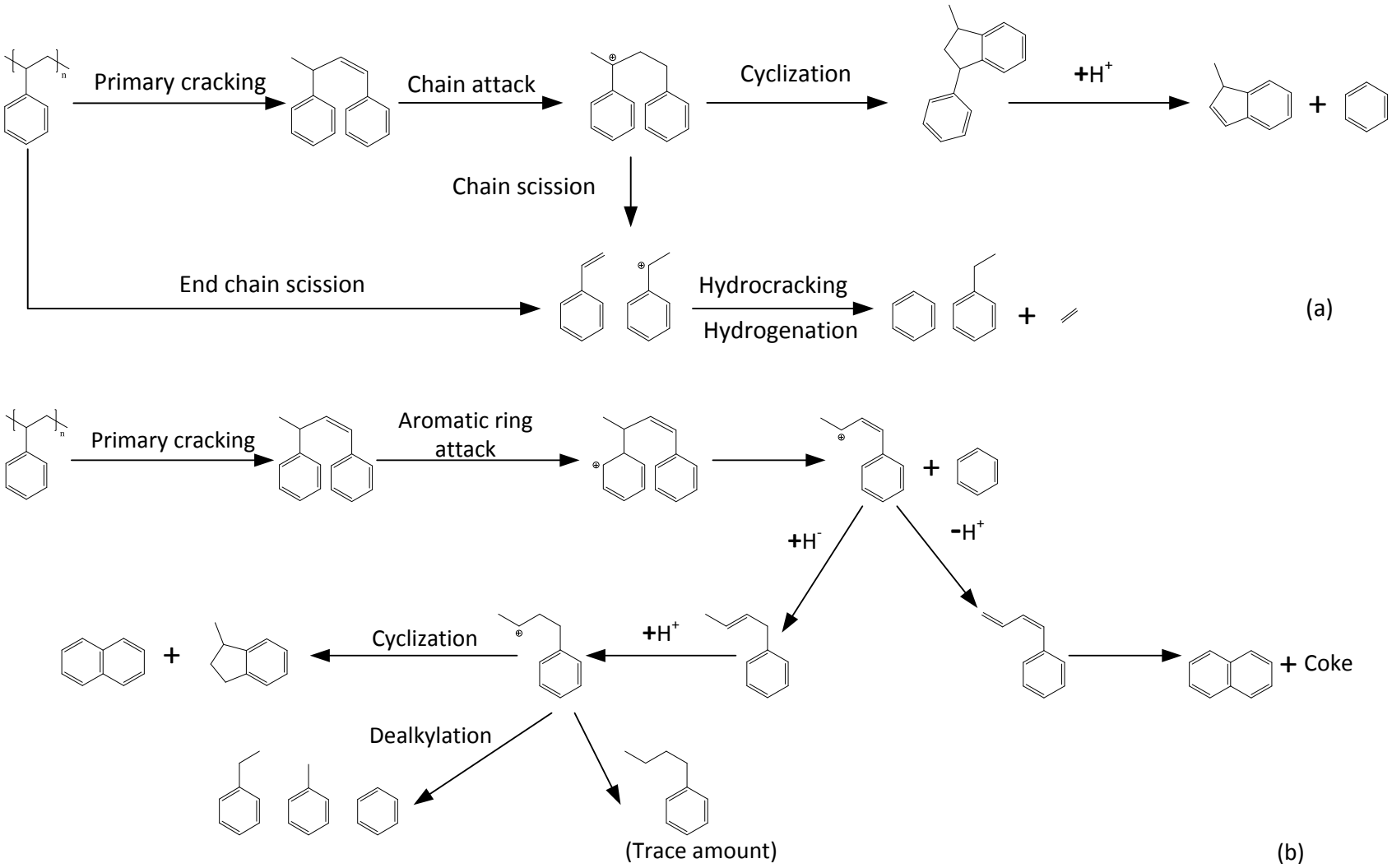

Figure 3. Proposed reaction mechanisms of PS during catalytic pyrolysis: a) *Ex-situ* pyrolysis; b) *In-situ* pyrolysis

indicating PET cannot fully volatilize upon thermal decomposition. In addition to the pyrolysis char, 8.28 C % of coke was also recovered from used catalyst. The yield of solid carbon residue was 16.48 C% during *in-situ* catalytic pyrolysis of PET, which is higher than the sum of pyrolysis char and coke recovered during *ex-situ* catalytic pyrolysis of PET. Conversion of PET produces overall high yields of solid residue because of oxygen atoms presenting in PET. Aromatic hydrocarbons were the major products from catalytic pyrolysis of PET, and *in-situ* catalytic pyrolysis produced a higher yield of total aromatics than *ex-situ* catalytic pyrolysis (52.71 C% Vs. 42.75 C%). Du et al. [13] reported 20 C% of aromatic hydrocarbons by pyrolyzing waste carpet made of PET packed between two HZSM-5 catalyst bed (catalyst:feedstock=20) in a 5200 HP PyGC system. The yield was much lower compared to the result from the present study, probably because of high ash content in their feedstock. On the other hand, the yield of total aliphatic hydrocarbons was higher during *ex-situ* catalytic pyrolysis, mostly due to the higher yield of alkane. Carbon oxides were also produced because PET is deoxygenated during the catalytic pyrolysis. *In-situ* catalytic pyrolysis of PET produced more CO_2 but fewer amount of CO than that with *ex-situ* catalytic pyrolysis, suggesting decarboxylation is preferred over decarbonylation during *in-situ* catalytic pyrolysis.

The proposed reaction pathways of PET during both *in-situ* and *ex-situ* catalytic pyrolysis are illustrated in Fig. 5. Different from the thermal depolymerization of polyolefin, the homolytic fission of the polyolefin to produce the corresponding monomers is unlikely to occur in PET during pyrolysis. According to Grause et al. [14], thermal cracking of polyester which has one β-hydrogen, mostly undergoes a cyclic transition state. The hydrogen in C_β

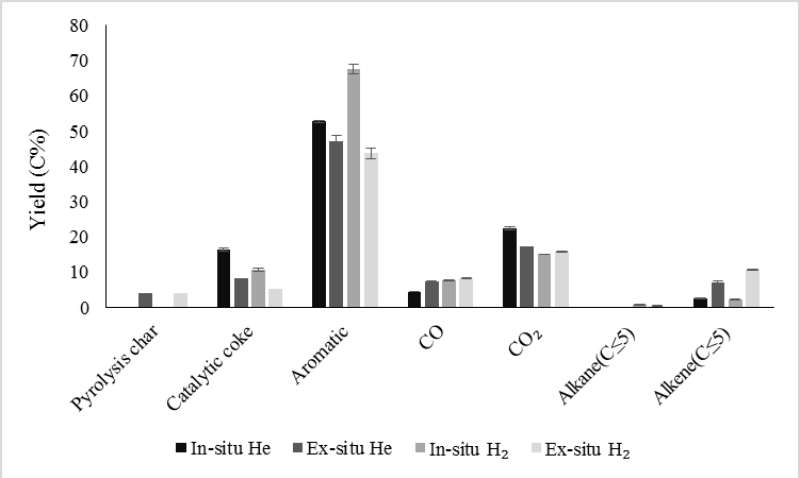

Figure 4. Product distributions during catalytic pyrolysis of PET

moves to the oxygen at ester C=O bond. Subsequently, C_β-H bond and alkoxy C_α-O bond are partially cleaved, and C_α=C_β double bond and O-H bond are formed. The heterolytic breakage of alkoxy C_α-O bond makes the C_α partially positively charged [41]. The major products from the thermal cracking of PET were terephthalic acid and benzoic acid vinyl ester in the present study when the catalyst was absent. Due to the instability of benzoic acid vinyl ester, the ester will further undergo isomerization and de-carbonylation to produce acetophenone. HZSM-5 zeolite has strong de-oxygenation ability for carboxylic and ketone groups [42, 43]. Thus, terephthalic acid and acetophenone derived from thermal depolymerization of PET could easily be converted into aromatic hydrocarbons during *ex-situ* catalytic pyrolysis. The carboxylic and ketone groups in terephthalic acid and acetophenone are removed as carbon oxides during the process.

Due to the strong interaction between PET and the zeolite catalyst during *in-situ* pyrolysis, the C=O bond of PET is attacked not only by the hydrogen at C_β, but also by external protons in Brønsted acid sites. After the oxygen located at C=O being attacked by the proton, the carbon is positively charged, followed by the cracking at phenyl alkyl bond

where the bond energy is lowest [44]. The homolytic scission of phenyl-alkyl bond generated benzene free radicals, as well as ethylene and CO_2, which explains the high yield of CO_2 during *in-situ* catalytic pyrolysis. Thilakaratne et al.[45] have shown that the benzene free radicals could react with olefins (e. g., ethylene and propylene) to produce naphthalenes. With two carbon atoms being activated, the benzene free radicals produced from PET cracking are extremely reactive precursors of catalytic coke.

When the carrier gas was H_2, the coke yield decreased from 8.28 to 5.15 C% during *ex-situ* catalytic pyrolysis. On the other hand, H_2 also reduced the yield of total aromatic hydrocarbons from 47.15 to 43.72 C%, while increasing the alkene yield from 7.17 to 10.70 C% in comparison to He as the carrier gas. Among aromatic hydrocarbons, the yields of benzene and naphthalenes both decreased by switching to H_2. The yield of benzene decreased, possibly due to hydrocracking of benzene into aliphatic hydrocarbons. H_2 also suppressed the formation of polyaromatics hydrocarbons from the PET derived terephathalic acid and acetophenone. Polyaromatics are known as coke precursor, thus the decreased polyaromatic yield corresponds to the decreased yield of coke during the hydropyrolysis.

H_2 atmosphere also strongly affected the product distribution during *in-situ* catalytic pyrolysis of PET. The yield of solid carbon residue decreased from 16.48 to 10.72 C %, accompanied by increasing yield of aromatic hydrocarbon from 52.71 to 67.51 C%. H_2 reduced CO_2 yield from 22.41 to 15.11 C%, whereas increasing CO yield from 4.49 to 7.62 C%. Among the aromatic products, benzene and anthracene increased significantly. As depicted in Fig. 5, PET was activated by Brønsted acid sites and then attacked by a hydride originated from H_2. The cleavage of alkoxy C_α-O bond produced diols and ethylene. The benzene aldehyde, which is derived from dehydration of diol, was converted into benzene by

losing CO. This is correspondent to the decrease in CO_2 yield and increase in CO yield in the presence of H_2. The increases of indane, indene, naphthalenes, and anthracene suggest that some benzene molecules underwent alkylation with ethylene at the active sites. Since benzene is much less reactive than benzene free radicals, the coke formation was suppressed during *in-situ* hydropyrolysis.

Catalytic pyrolysis of PE and PP

The product distributions of PE during catalytic pyrolysis are compared in Fig. 6 (a) and the product selectivity are summarized in Table S3. PE does not form pyrolysis char during *ex-situ* pyrolysis. The coke yield of PE during *ex-situ* catalytic pyrolysis was only 2.45 C%. The yield of solid carbon residue was also low at 4.43 C% during *in-situ* catalytic pyrolysis. Compared to PS and PET, the yields of aromatic hydrocarbons were much lower with catalytic conversion of PE. The aromatic yield was only 26.55 C% during *in-situ* catalytic pyrolysis of PE, and decreased to 10.94 C% when PE was *ex-situ* pyrolyzed with the catalyst. Li et al. [46] previously reported 28.3C% of aromatics and 6.74C% of solid residue by pyrolyzing the mixture of PE and HZSM-5 (catalyst:feedstock=15) in a Pyroprobe microreactor. In this study, benzene, toluene and xylene were the major aromatic hydrocarbons in both *in-situ* and *ex-situ* pyrolysis. During *ex-situ* catalytic pyrolysis, nearly 80 C% of alkenes and 6.81 C% of alkanes were produced. The yields of alkene and alkane were comparable during *in-situ* catalytic pyrolysis, which are 28.41 C% and 34.12 C%, respectively. Propylene, ethylene and butylene more selectively produced from *ex-situ* catalytic pyrolysis, whereas propane, butane and propylene were abundant during *in-situ* catalytic pyrolysis.

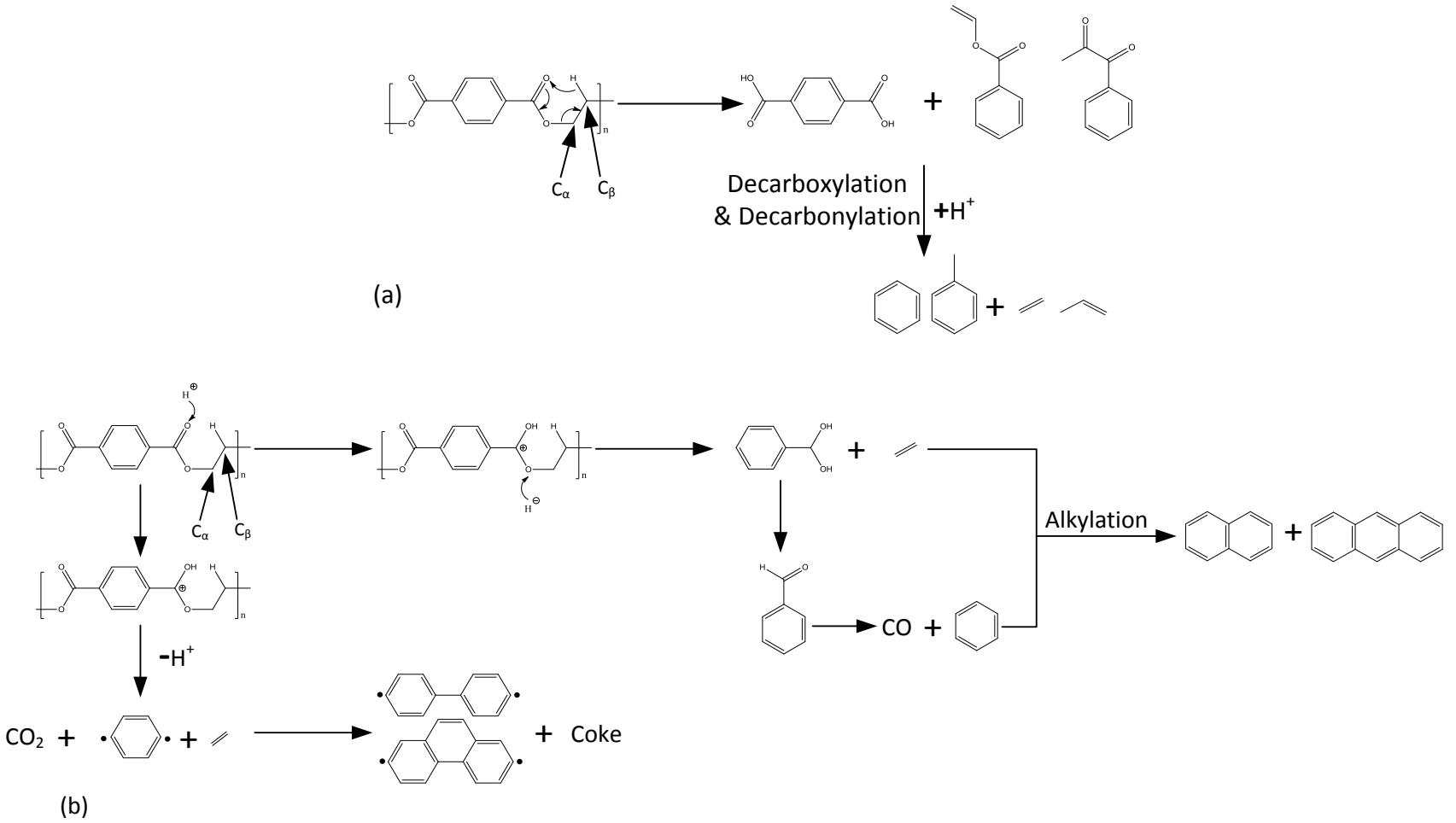

Figure 5. Proposed reaction mechanisms of PET during catalytic pyrolysis: a) *Ex-situ* pyrolysis; b) *In-situ* pyrolysis

During catalytic pyrolysis of PE with HZSM-5, the olefins produced from cracking of PE could be aromatized inside the catalyst pores. On the other hand, the aromatization reactions also release free hydrogen atoms. The hydrogen atoms could promote cracking reaction as well as saturation of alkenes to alkanes. *In-situ* catalytic pyrolysis produced a higher amount of aromatic hydrocarbons due to the enhanced aromatization inside the pores. The alkane yield was higher during *in-situ* catalytic pyrolysis, suggesting more hydrogen atoms were available for the saturation reactions. The alkylation of benzene and toluene into alkylated benzene followed by aromatization into naphthalenes were also likely occurred during *in-situ* pyrolysis. During *ex-situ* catalytic pyrolysis, the olefin vapors produced from thermal decomposition of PE were also converted by the zeolite but the zeolite catalyzed cracking was the main reaction.

Using H_2 reduced the coke to below 1.0 C% during both *in-situ* and *ex-situ* catalytic pyrolysis. The main reactions occurring during hydro-reforming are hydrogenation, hydroisomerization and hydrocracking [47]. Since C_2-C_4 hydrocarbons are the main aliphatic hydrocarbons produced from catalytic pyrolysis of PE polymer, hydroisomerization and hydrocracking of these olefins are unlike to occur due to their short carbon chain lengths. On the other hand, hydrogenation took place during both *in-situ* and *ex-situ* hydropyrolysis, evident by the increased yields of alkanes in comparison to the corresponding yields obtained from the catalytic pyrolysis with inert gas. The formation of aromatic hydrocarbons was suppressed during *ex-situ* catalytic hydropyrolysis, which agrees with the previous results by Abbas-Abadi et al.[48] The mechanisms of catalytic pyrolysis of PE are summarized in Fig. 7.

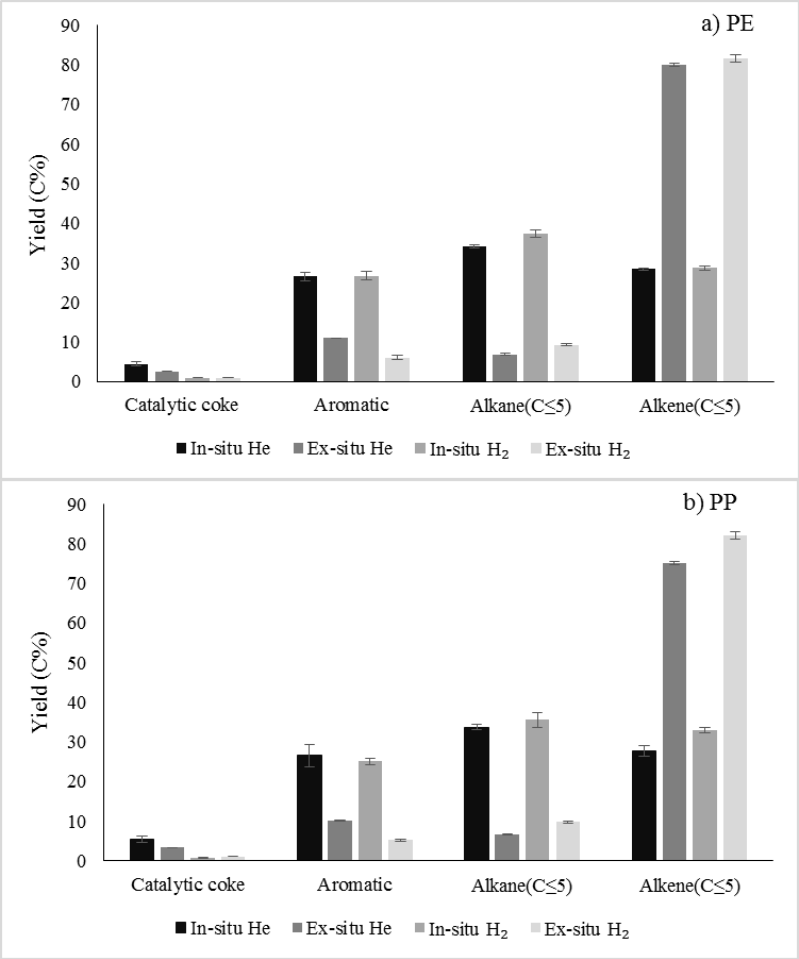

Figure 6. Product distribution during catalytic pyrolysis of a) PE; b) PP

The product distributions and the product selectivity of catalytic pyrolysis of PP are given in Fig. 6 (b) and Table S4, respectively. Overall, the conversion results are similar to that of PE. Although PP is a branched polymer whereas PE is a linear polymer, they share the same chemical formula and both produce olefins by thermal cracking. Thus, catalytic conversion pathway of PP is similar to that of PE as discussed above.

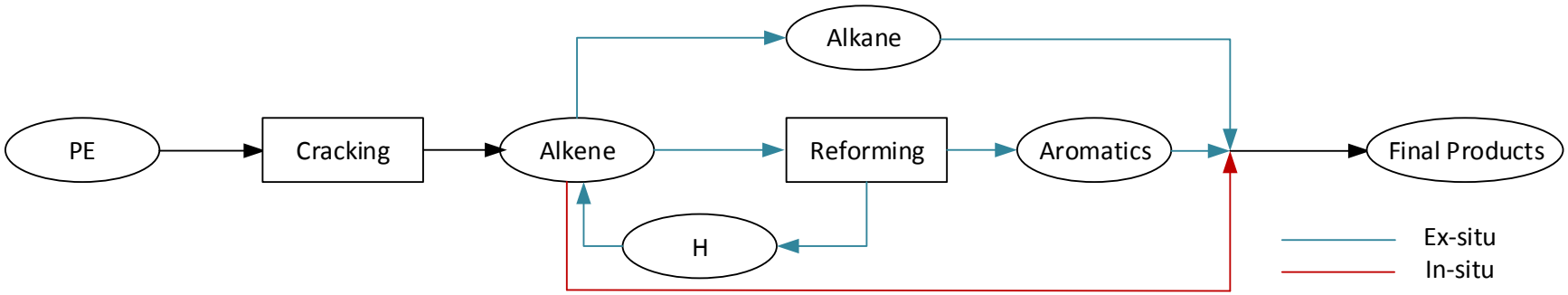

Figure 7. Proposed reaction mechanisms of PE (also PP) during catalytic pyrolysis

Thermogravimetric Analysis *of in-situ* Catalytic Pyrolysis of Plastics

In the present study, the effect of the catalyst in changing the decomposition temperatures of the plastics during *in-situ* catalytic pyrolysis was investigated using a TGA and the results are shown in Fig. 8. As shown, the temperatures at where the maximum decomposition rates occur were 481, 460, 417 and 436 °C, respectively, for pyrolysis of PE, PP, PS and PET in the absence of catalyst. When the plastics were mixed with HZSM-5 and then pyrolyzed, the corresponding temperatures decreased to 278, 315, 372 and 420 °C, respectively. It is noteworthy that the ability of the catalyst in lowering the decomposition temperature depends on the type of plastics. For polyolefins (PE, PP and PS), the mechanisms of the plastic decomposition changes from the free radical initiated chain scission with non-catalytic pyrolysis to carbocationic-intermediate chain scission with catalytic pyrolysis. As the size of the substituent decreases (i.e., $-C_6H_5$ for PS, -H for PE and $-CH_3$ for PP), the effect of HZSM-5 in lowering the decomposition temperatures of the plastics increases in the order of PS < PP < PE. It is possible that the substituents function as the steric hindrance for the catalyst active sites contacting the polymer chain. Among the four plastics investigated in this study, HZSM-5 lowered the decomposition temperature of PET least, only by 16 °C. Similar as PS, the aromatic ring in PET structure can be steric hindrance. In addition, as described above, the initiation step in the decomposition mechanism of PET in the absence and presence of HZSM-5 were quite similar, both are the hydride shift from either neighboring C_β hydrogen or the acid sites to C=O oxygen. Thus, the decomposition of temperature of PET was least affected by the catalyst.

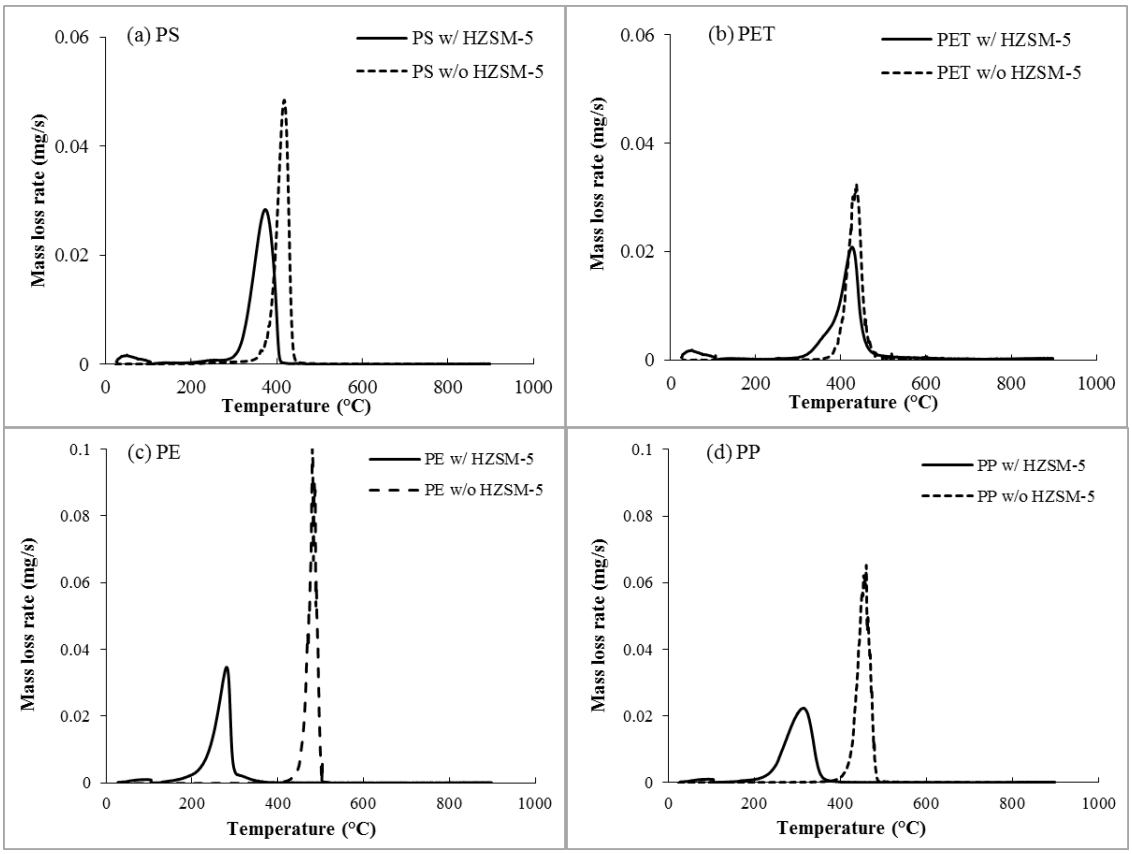

Figure 8. Differential thermogravimetric (DTG) curves of plastics pyrolyzed with and without HZSM-5. (a) PS; (b) PET; (c) PE; (d) PP.

Previous studies show that thermal decompositions of plastics start at relative high temperatures, after the plastics melt [7]. Thus, the temperature of the pyrolysis reactor must be sufficiently high during *ex-situ* catalytic pyrolysis in order for the volatilized vapors to be converted in the catalytic bed downstream. In practice, low temperatures at the pyrolysis reactor could also result in the reactor clogging during the operation, attributed to the agglomeration of the melted plastics and/or waxy products from incomplete cracking of the plastics [49, 50]. To address this problem, the reactor configurations that promote strong mass transfer, such as fluidized bed and conical spouted bed reactor, were chosen for plastic pyrolysis [9, 51, 52]. Comparison to *ex-situ* catalytic pyrolysis of plastics, mixing the plastics and catalyst during *in-situ* catalytic pyrolysis could promote decomposition of the plastics at

lower temperatures, therefore potentially mitigating the above mentioned reactor operating issues and also lower the energy input.

Synergistic Effects between Hydrogen-rich and Hydrogen-deficient Plastics during Catalytic Co-pyrolysis

As shown above, catalytic hydropyrolysis of plastics has some positive effects compared to the catalytic pyrolysis of the plastics with inert gas. For example, the decreased coke yield by hydropyrolysis could contribute to extended catalyst lifetime [53, 54]. From the results described above, it can be seen that the effect of hydropyrolysis is more pronounced with PET and PS than that with PE and PP. The differences in the results could be related to hydrogen abundancy in different plastic polymers. PE and PP are hydrogen rich polymers, whereas PS and PET are hydrogen deficient plastics. Thus, externally provided hydrogen (i.e., H_2) could influence the catalytic conversion of PS and PET more than the conversion of PE or PP. The results also suggest that hydrogen rich plastics could act as the hydrogen source to the hydrogen deficient plastics if they are catalytically co-converted. Previous studies reported that co-pyrolysis of PE with hydrogen-deficient biomass improves the product distributions due to hydrogen transfer between the feedstock materials [38, 49]. Thus, hydrogen rich and hydrogen deficient plastics were catalytically co-pyrolyzed with inert gas and the interactions were investigated. In fact, the real-world plastic wastes are usually a mixture of different types of plastics [55].

Table 2. Product distribution during *in-situ* catalytic co-pyrolysis of PE and PET: comparison of experimental yields and additive yields

PE & PET	Experimental	Additive
Overall yield (C%)		
Solid carbon residue	9.27	9.51
Aromatic	47.14	37.58
CO	1.57	1.89
CO_2	4.86	9.45
Alkane(C≤5)	12.89	19.76
Alkene(C≤5)	15.93	17.54
Sum	**91.64**	**95.74**
Aromatic hydrocarbon yield (C%)		
Benzene	25.36	18.72
Toluene	9.39	7.17
Ethyl-benzene	1.45	0.68
p-Xylene	4.77	3.33
o-Xylene	1.43	1.02
Styrene	0.11	0.18
Benzene, 1-ethyl-3-methyl	0.06	0.63
Benzene, 1,2,3-trimethyl-	1.47	0.42
Indane	0.56	0.19
Indene	0.38	0.34
3-Methyl-1H-Indene	0.99	0
Naphthalene	0.07	1.83
Naphthalene, 2-methyl-	0.17	1.55
1,2-Dimethyl-Napthalene	0.26	1.11
Fluorene	0.21	-
Anthracene	0.24	0.4
2-Methyl Panthracene	0.31	-

The results from *in-situ* catalytic co-pyrolysis of PE and PET, and co-pyrolysis of PE and PS are listed in Table 2 and 3, respectively. The additive yields of the products are also given in the tables to determine synergistic effects among different plastics during catalytic co-pyrolysis. When PE and PET were catalytically co-pyrolyzed, the yields of coke and CO slightly were lower in comparison to their additive yields. On the other hand, the yield of

total aromatics significantly increased by co-pyrolysis, whereas the yields of CO_2, CO and aliphatic hydrocarbons decreased. The yield of total aromatics increased, mainly because more benzene and alkylated benzenes were formed by co-pyrolysis. This result, together with the decrease of the yields of alkane and alkenes by co-pyrolysis, suggests that hydrogen atoms produced from the aromatization of PE-derived olefins are utilized by benzene free radicals produced from PET to increase benzene yield. It is also possible that the alkanes and alkenes reacted with the benzene free radicals to form alkylated benzenes.

Table 3. Product distribution during *in-situ* catalytic co-pyrolysis of PE and PS: comparison of experimental yields and additive yields

PE & PS	Experimental	Additive
Overall yield (C%)		
Solid carbon residue	5.92	10.36
Aromatic	51.28	47.71
Alkane(C≤5)	16.64	17.43
Alkene(C≤5)	15.56	15.86
Sum	**89.39**	**91.36**
Aromatic hydrocarbon yield (C%)		
Benzene	20.15	22.86
Toluene	8.69	7.76
Ethyl-benzene	2.89	1.57
p-Xylene	3.09	2.87
o-Xylene	0.95	0.88
Styrene	0.16	0.2
Benzene, 1-ethyl-3-methyl	0.18	0.52
Benzene, 1,2,3-trimethyl-	1.37	0.44
Indane	4.11	2.63
Indene	0.43	0.92
3-Methyl-1H-Indene	0.18	-
Naphthalene	2.66	2.42
Naphthalene, 2-methyl-	3.89	2.77
1-Ethyl-Napthalene	1.67	-
1,2-Dimethyl-Napthalene	-	1.27
Fluorene	0.15	-
Anthracene	0.22	0.27
2-Methyl Panthracene	0.23	0.33

In comparison to converting PE and PS independently, catalytic co-pyrolysis of PE and PS also reduced the coke and alkane yields, whereas increasing aromatic yield (Table 2). The yields of indane and naphthalenes increased, which were also previously observed during catalytic hydropyrolysis of PS described above. This result suggests that hydrogen atoms transferred from PE to PS are responsible for the synergistic effects observed during co-pyrolysis. The alkylation reactions among the PE and PS derivatives also reduced benzene yield whereas increasing the yield of alkylated benzene. However, the extent of the alkylation between PE and PS was not as strong as it was observed during co-pyrolysis of PE and PET due to the scarcity of benzene free radicals from PS pyrolysis.

Conclusions

Four main waste plastics were catalytically pyrolyzed using a tandem micro-pyrolyzer at atmospheric pressure. The effects of the feedstock-catalyst contact mode as well as the types of carrier gas (He and H_2) on the product distribution were investigated. It was found that *in-situ* catalytic pyrolysis produces higher yields of aromatics than *ex-situ* catalytic pyrolysis for PET, PE and PP. For PS, *ex-situ* catalytic pyrolysis produced more aromatics than *in-situ* catalytic pyrolysis because of a high yield of styrene in the products. On the other hand, styrene was rarely found during *in-situ* catalytic pyrolysis of PS. For PET, *in-situ* catalytic pyrolysis generated more CO_2 and a fewer amount of CO than *ex-situ* catalytic pyrolysis. For PE and PP, the yields of alkenes and alkanes were comparable during *in-situ* catalytic pyrolysis whereas alkene yields were significantly higher than alkane yields during *ex-situ* catalytic pyrolysis. However, *in-situ* catalytic pyrolysis also produced more solid carbon residue and promoted the formation of polyaromatics of the plastics.

The results suggest that *in-situ* and *ex-situ* catalytic pyrolysis of the plastics occur at different reaction mechanisms. For PS, *ex-situ* catalytic pyrolysis favored proton attachments to aliphatic double bond, whereas proton attachment to aromatic double bond was enhanced during *in-situ* catalytic pyrolysis. Because of the affinity to the Brønsted acid site during *in-situ* catalytic pyrolysis, the depolymerization of PET was enhanced by external proton attachments to ester C=O oxygen instead of internal hydrogen transfer from β-carbon. Reforming reactions of PE to produce aromatics and saturation of alkenes were favored for *in-situ* catalytic pyrolysis, while cracking to olefins was preferred during *ex-situ* catalytic pyrolysis. TGA analysis shows that *in-situ* catalytic pyrolysis lowers decomposition temperatures of all plastics. For polyolefins, the decrease in the decomposition temperatures became less significant with increasing size of the plastic substituents because of the increasing steric hindrance. For PET, the steric hindrance, together with similar decomposition mechanisms of the plastic in the presence and absence of catalyst, causing the least decrease in the decomposition temperature of PET. During catalytic hydropyrolysis of the plastics, hydride produced from heterolytic dissociation of hydrogen gas inhibited the coke formation and improved the yield of aromatics. Such effects were most significant with PS and PET due to their hydrogen deficiency. The synergy among hydrogen-rich and hydrogen-deficient plastics during catalytic co-pyrolysis was also investigated. *In-situ* catalytic co-pyrolysis of PE with PET or PS reduced the yield of solid residue whereas increasing the yield of aromatics in comparison to their corresponding additive yields. The synergistic effects were contributed by hydrogen transfer from PE to PET or PS, and aromatic alkylation by the olefins derived from the cracking of PE.

Acknowledgements

This work is supported by Iowa Energy Center (IEC) project. The authors also acknowledge Prof. Robert Brown, Dr. Marjorie Rover, Ryan Smith, and Patrick Hall at Bioeconomy Institute of Iowa State University for useful discussions and technical support.

Reference

[1] G. Gourmelon. Global Plastic Production Rises, Recycling Lags. New Worldwatch Institute analysis explores trends in global plastic consumption and recycling Recuperado de http://www worldwatch org. (2015).

[2] S. Gupta, K. Mohan, R. Prasad, S. Gupta, A. Kansal. Solid waste management in India: options and opportunities. Resources, conservation and recycling. 24 (1998) 137-54.

[3] P. van Beukering, L. Yongjiang, Z. Yumin, Z. Xin. Trends and issues in the plastics cycle in China with special emphasis on trade and recycling1997.

[4] J.R. Jambeck, R. Geyer, C. Wilcox, T.R. Siegler, M. Perryman, A. Andrady, et al. Plastic waste inputs from land into the ocean. Science. 347 (2015) 768-71.

[5] J.G. Derraik. The pollution of the marine environment by plastic debris: a review. Marine pollution bulletin. 44 (2002) 842-52.

[6] S. Al-Salem, P. Lettieri, J. Baeyens. Recycling and recovery routes of plastic solid waste (PSW): A review. Waste management. 29 (2009) 2625-43.

[7] A. Demirbas. Pyrolysis of municipal plastic wastes for recovery of gasoline-range hydrocarbons. Journal of Analytical and Applied Pyrolysis. 72 (2004) 97-102.

[8] G. Lopez, M. Artetxe, M. Amutio, J. Bilbao, M. Olazar. Thermochemical routes for the valorization of waste polyolefinic plastics to produce fuels and chemicals. A review. Renewable and Sustainable Energy Reviews. 73 (2017) 346-68.

[9] G. Elordi, M. Olazar, G. Lopez, P. Castaño, J. Bilbao. Role of pore structure in the deactivation of zeolites (HZSM-5, Hβ and HY) by coke in the pyrolysis of polyethylene in a conical spouted bed reactor. Applied Catalysis B: Environmental. 102 (2011) 224-31.

[10] G. Elordi, M. Olazar, G. Lopez, M. Amutio, M. Artetxe, R. Aguado, et al. Catalytic pyrolysis of HDPE in continuous mode over zeolite catalysts in a conical spouted bed reactor. Journal of Analytical and Applied Pyrolysis. 85 (2009) 345-51.

[11] A. Marcilla, A. Gómez-Siurana, D. Berenguer. Study of the influence of the characteristics of different acid solids in the catalytic pyrolysis of different polymers. Applied Catalysis A: General. 301 (2006) 222-31.

[12] R. Miandad, M. Barakat, A.S. Aburiazaiza, M. Rehan, A. Nizami. Catalytic pyrolysis of plastic waste: A review. Process Safety and Environmental Protection. 102 (2016) 822-38.

[13] S. Du, J.A. Valla, R.S. Parnas, G.M. Bollas. Conversion of Polyethylene Terephthalate Based Waste Carpet to Benzene-Rich Oils through Thermal, Catalytic, and Catalytic Steam Pyrolysis. ACS Sustainable Chemistry & Engineering. 4 (2016) 2852-60.

[14] G. Grause, T. Handa, T. Kameda, T. Mizoguchi, T. Yoshioka. Effect of temperature management on the hydrolytic degradation of PET in a calcium oxide filled tube reactor. Chemical engineering journal. 166 (2011) 523-8.

[15] S. Shukla, K. Kulkarni. Depolymerization of poly (ethylene terephthalate) waste. Journal of applied polymer science. 85 (2002) 1765-70.

[16] A. López, I. De Marco, B. Caballero, M. Laresgoiti, A. Adrados. Influence of time and temperature on pyrolysis of plastic wastes in a semi-batch reactor. Chemical Engineering Journal. 173 (2011) 62-71.

[17] P.T. Williams, E.A. Williams. Fluidised bed pyrolysis of low density polyethylene to produce petrochemical feedstock. Journal of Analytical and Applied Pyrolysis. 51 (1999) 107-26.

[18] M. Artetxe, G. Lopez, M. Amutio, G. Elordi, J. Bilbao, M. Olazar. Cracking of high density polyethylene pyrolysis waxes on HZSM-5 catalysts of different acidity. Industrial & Engineering Chemistry Research. 52 (2013) 10637-45.

[19] S.L. Wong, T.A. Tuan Abdullah, N. Ngadi, A. Ahmad, I.M. Inuwa. Parametric study on catalytic cracking of LDPE to liquid fuel over ZSM-5 zeolite. Energy Conversion and Management. 122 (2016) 428-38.

[20] P. Sharratt, Y.-H. Lin, A. Garforth, J. Dwyer. Investigation of the catalytic pyrolysis of high-density polyethylene over a HZSM-5 catalyst in a laboratory fluidized-bed reactor. Industrial & engineering chemistry research. 36 (1997) 5118-24.

[21] A. Marcilla, M. Beltrán, R. Navarro. Thermal and catalytic pyrolysis of polyethylene over HZSM5 and HUSY zeolites in a batch reactor under dynamic conditions. Applied Catalysis B: Environmental. 86 (2009) 78-86.

[22] D.K. Ratnasari, M.A. Nahil, P.T. Williams. Catalytic pyrolysis of waste plastics using staged catalysis for production of gasoline range hydrocarbon oils. Journal of Analytical and Applied Pyrolysis.

[23] M. Syamsiro, H. Saptoadi, T. Norsujianto, P. Noviasri, S. Cheng, Z. Alimuddin, et al. Fuel oil production from municipal plastic wastes in sequential pyrolysis and catalytic reforming reactors. Energy Procedia. 47 (2014) 180-8.

[24] R. Mahadevan, S. Adhikari, R. Shakya, K. Wang, D. Dayton, M. Lehrich, et al. Effect of Alkali and Alkaline Earth Metals on in-Situ Catalytic Fast Pyrolysis of Lignocellulosic Biomass: A Microreactor Study. Energy & Fuels. 30 (2016) 3045-56.

[25] K. Wang, J. Zhang, B.H. Shanks, R.C. Brown. The deleterious effect of inorganic salts on hydrocarbon yields from catalytic pyrolysis of lignocellulosic biomass and its mitigation. Applied Energy. 148 (2015) 115-20.

[26] Y. Sakata, M.A. Uddin, A. Muto. Degradation of polyethylene and polypropylene into fuel oil by using solid acid and non-acid catalysts. Journal of Analytical and Applied Pyrolysis. 51 (1999) 135-55.

[27] O. Jan, R. Marchand, L.C. Anjos, G.V. Seufitelli, E. Nikolla, F.L. Resende. Hydropyrolysis of Lignin Using Pd/HZSM-5. Energy & Fuels. 29 (2015) 1793-800.

[28] F.L. Resende. Recent advances on fast hydropyrolysis of biomass. Catalysis Today. 269 (2016) 148-55.

[29] H. Sun, C. Rosenthal, L.D. Schmidt. Oxidative Pyrolysis of Polystyrene into Styrene Monomers in an Autothermal Fixed-Bed Catalytic Reactor. ChemSusChem. 5 (2012) 1883-7.

[30] S.D.A. Sharuddin, F. Abnisa, W.M.A.W. Daud, M.K. Aroua. A review on pyrolysis of plastic wastes. Energy Conversion and Management. 115 (2016) 308-26.

[31] J. Proano-Aviles, J.K. Lindstrom, P.A. Johnston, R.C. Brown. Heat and Mass Transfer Effects in a Furnace-Based Micropyrolyzer. Energy Technology. (2016).

[32] P.T. Williams, R. Bagri. Hydrocarbon gases and oils from the recycling of polystyrene waste by catalytic pyrolysis. International Journal of Energy Research. 28 (2004) 31-44.

[33] A. Guyot. Recent developments in the thermal degradation of polystyrene—A review. Polymer degradation and stability. 15 (1986) 219-35.

[34] T.M. Kruse, O.S. Woo, L.J. Broadbelt. Detailed mechanistic modeling of polymer degradation: application to polystyrene. Chemical engineering science. 56 (2001) 971-9.

[35] M. Marczewski, E. Kamińska, H. Marczewska, M. Godek, G. Rokicki, J. Sokołowski. Catalytic decomposition of polystyrene. The role of acid and basic active centers. Applied Catalysis B: Environmental. 129 (2013) 236-46.

[36] T. Maharana, Y. Negi, B. Mohanty. Review article: recycling of polystyrene. Polymer-Plastics Technology and Engineering. 46 (2007) 729-36.

[37] Y. Uemichi, J. Nakamura, T. Itoh, M. Sugioka, A.A. Garforth, J. Dwyer. Conversion of polyethylene into gasoline-range fuels by two-stage catalytic degradation using silica-alumina and HZSM-5 zeolite. Industrial & engineering chemistry research. 38 (1999) 385-90.

[38] Y. Xue, A. Kelkar, X. Bai. Catalytic co-pyrolysis of biomass and polyethylene in a tandem micropyrolyzer. Fuel. 166 (2016) 227-36.

[39] K. Wang, P.A. Johnston, R.C. Brown. Comparison of in-situ and ex-situ catalytic pyrolysis in a micro-reactor system. Bioresource Technology. 173 (2014) 124-31.

[40] H. Hattori, T. Shishido. Molecular hydrogen-originated protonic acid site as active site on solid acid catalyst. Catalysis Surveys from Asia. 1 (1997) 205-13.

[41] L. Buxbaum. The degradation of poly (ethylene terephthalate). Angewandte Chemie International Edition in English. 7 (1968) 182-90.

[42] K. Wang, J. Zhang, B.H. Shanks, R.C. Brown. Catalytic conversion of carbohydrate-derived oxygenates over HZSM-5 in a tandem micro-reactor system. Green Chemistry. 17 (2015) 557-64.

[43] A.J. Foster, J. Jae, Y.-T. Cheng, G.W. Huber, R.F. Lobo. Optimizing the aromatic yield and distribution from catalytic fast pyrolysis of biomass over ZSM-5. Applied Catalysis A: General. 423 (2012) 154-61.

[44] A. Carven. A simple method of estimating exothermicity by average bond energy summation. Hazardous from Pressure: Exothermic Reactions, Unstable Substances, Pressure Relief, and Accidental Discharge, Symposium Series1987. pp. 97-111.

[45] R. Thilakaratne, J.-P. Tessonnier, R.C. Brown. Conversion of methoxy and hydroxyl functionalities of phenolic monomers over zeolites. Green Chemistry. (2016).

[46] X. Li, J. Li, G. Zhou, Y. Feng, Y. Wang, G. Yu, et al. Enhancing the production of renewable petrochemicals by co-feeding of biomass with plastics in catalytic fast pyrolysis with ZSM-5 zeolites. Applied Catalysis A: General. 481 (2014) 173-82.

[47] J. Escola, J. Aguado, D. Serrano, A. García, A. Peral, L. Briones, et al. Catalytic hydroreforming of the polyethylene thermal cracking oil over Ni supported hierarchical zeolites and mesostructured aluminosilicates. Applied Catalysis B: Environmental. 106 (2011) 405-15.

[48] M.S. Abbas-Abadi, M.N. Haghighi, H. Yeganeh, A.G. McDonald. Evaluation of pyrolysis process parameters on polypropylene degradation products. Journal of Analytical and Applied Pyrolysis. 109 (2014) 272-7.

[49] Y. Xue, S. Zhou, R.C. Brown, A. Kelkar, X. Bai. Fast pyrolysis of biomass and waste plastic in a fluidized bed reactor. Fuel. 156 (2015) 40-6.

[50] C. Dorado, C.A. Mullen, A.A. Boateng. Coprocessing of Agricultural Plastic Waste and Switchgrass via Tail Gas Reactive Pyrolysis. Industrial & Engineering Chemistry Research. 54 (2015) 9887-93.

[51] R. Aguado, R. Prieto, M.J. San José, S. Alvarez, M.n. Olazar, J. Bilbao. Defluidization modelling of pyrolysis of plastics in a conical spouted bed reactor. Chemical Engineering and Processing: Process Intensification. 44 (2005) 231-5.

[52] R. Aguado, B. Gaisán, R. Prieto, J. Bilbao. Kinetics of polystyrene pyrolysis in a conical spouted bed reactor. Chemical Engineering Journal. 92 (2003) 91-9.

[53] M. Canel, Z. Mısırlıogˇlu, A. Sınagˇ. Hydropyrolysis of a Turkish lignite (Tunçbilek) and effect of temperature and pressure on product distribution. Energy Conversion and Management. 46 (2005) 2185-97.

[54] S. Thangalazhy-Gopakumar, S. Adhikari, R.B. Gupta. Catalytic pyrolysis of biomass over H+ ZSM-5 under hydrogen pressure. Energy & fuels. 26 (2012) 5300-6.

[55] M.E. Edjabou, M.B. Jensen, R. Götze, K. Pivnenko, C. Petersen, C. Scheutz, et al. Municipal solid waste composition: Sampling methodology, statistical analyses, and case study evaluation. Waste Management. 36 (2015) 12-23.

SUPPLEMENTAL INFORMATION FOR CHAPTER 5

Table S1. Product yields and selectivity during catalytic pyrolysis of PS

PS	*In-situ* **He**	*Ex-situ* **He**	*In-situ* $\mathbf{H_2}$	*Ex-situ* $\mathbf{H_2}$
Aromatic hydrocarbon yield/C% (selectivity/%)				
Benzene	39.60 (58.79)	23.59 (29.84)	43.36 (57.01)	33.09 (38.75)
Toluene	5.39 (8.01)	2.49 (3.15)	4.72 (6.20)	3.15 (3.69)
Ethyl-benzene	2.42 (3.59)	0.38 (0.48)	2.77 (3.64)	4.05 (4.74)
p-Xylene	0.62 (0.92)	0.14 (0.17)	0.56 (0.74)	0.11 (0.13)
o-Xylene	0.19 (0.28)	0.03 (0.04)	0.82 (1.08)	0.02 (0.03)
Styrene	0.38 (0.57)	34.57 (43.72)	-	20.41 (23.90)
Benzene, 1-ethyl-3-methyl	0.11 (0.16)	0.01 (0.01)	-	0.28 (0.33)
Benzene, 1,2,3-trimethyl-	0.33 (0.48)	0.16 (0.20)	-	-
Indane	4.90 (7.28)	0.26 (0.33)	6.33 (8.32)	0.77 (0.90)
Indene	1.68 (2.50)	4.72 (5.97)	1.64 (2.16)	6.04 (7.08)
3-Methyl-1H-Indene	-	5.64 (7.13)	-	11.21 (13.13)
Naphthalene	4.18 (6.20)	4.10 (5.19)	5.87 (7.71)	3.16 (3.70)
Naphthalene, 2-methyl-	4.75 (7.05)	1.94 (2.45)	6.64 (8.72)	2.10 (2.46)
1,2-Dimethyl-Napthalene	1.80 (2.67)	0.53 (0.67)	3.36 (4.42)	0.69 (0.81)
Fluorene	-	-	-	-
Anthracene	0.37 (0.55)	0.15 (0.18)	-	-
2-Methyl panthracene	0.64 (0.96)	0.36 (0.46)	-	0.19 (0.22)
Aliphatic hydrocarbon yield/C% (selectivity/%)				
CH_4	0.15 (2.44)	0.12 (1.94)	0.43 (8.92)	-
C_2H_6	0.33 (5.40)	0.26 (4.29)	-	-
C_3H_8	0.70 (11.37)	0.05 (0.77)	0.54 (11.05)	-

Table S1. Continued

PS	*In-situ* **He**	*Ex-situ* **He**	*In-situ* $\mathbf{H_2}$	*Ex-situ* $\mathbf{H_2}$
Aliphatic hydrocarbon yield/C% (selectivity/%)				
C_4H_{10}	0.76 (12.27)	-	0.74 (15.17)	0.01 (0.20)
C_2H_4	1.84 (29.82)	2.73 (44.44)	1.61 (33.03)	3.62 (69.09)
C_3H_6	1.41(22.88)	2.00 (32.65)	1.55 (31.83)	1.18 (22.47)
C_4H_8	0.80 (12.93)	0.98 (15.91)	-	0.43 (8.25)
C_5H_{10}	0.18 (2.90)	-	-	-

Table S2. Product yields and selectivity during catalytic pyrolysis of PET

PET	*In-situ* **He**	*Ex-situ* **He**	*In-situ* $\mathbf{H_2}$	*Ex-situ* $\mathbf{H_2}$
Aromatic hydrocarbon yield/C% (selectivity/%)				
Benzene	37.78 (71.67)	33.39 (70.82)	42.89 (63.54)	29.92 (68.43)
Toluene	2.85 (5.41)	3.73 (7.91)	4.38 (6.49)	3.25 (7.43)
Ethyl-benzene	0.72 (1.37)	0.06 (0.13)	0.14 (0.20)	0.21(0.48)
p-Xylene	0.65 (1.23)	0.57 (1.22)	0.81 (1.20)	0.51(1.18)
o-Xylene	0.17 (0.32)	0.17 (0.36)	0.80 (1.18)	0.11 (0.25)
Styrene	0.44 (0.83)	1.42 (3.02)	-	1.48 (3.38)
Benzene, 1-ethyl-3-methyl	0.19 (0.35)	0.02 (0.03)	0.90 (1.33)	0.10 (0.23)
Benzene, 1,2,3-trimethyl-	0.22 (0.42)	0.05 (0.12)	0.17 (0.25)	-
Indane	0.22 (0.42)	0.09 (0.18)	1.53 (2.27)	0.11 (0.25)
Indene	0.66 (1.26)	1.22 (2.59)	1.27 (1.88)	1.14 (2.61)
3-Methyl-1H-Indene	-	-	-	1.06 (2.42)
Naphthalene	3.62 (6.88)	2.15 (4.57)	4.73 (7.01)	1.92 (4.38)
Naphthalene, 2-methyl-	2.78 (5.28)	0.87 (1.84)	3.60 (5.33)	1.03 (2.37)
1,2-Dimethyl-Napthalene	1.67 (3.17)	3.05 (6.48)	2.54 (3.76)	2.55 (5.83)
Anthracene	0.73 (1.38)	0.35 (0.74)	3.75 (5.56)	–
2-Methyl Panthracene	–	–	–	0.33 (0.75)
Aliphatic hydrocarbon yield/C% (selectivity/%)				
CH_4	-	-	-	-
C_2H_6	-	-	-	-
C_3H_8	0.08 (2.87)	0.16 (2.17)	0.08 (2.53)	0.14 (1.24)
C_4H_{10}	-	-	0.60 (19.96)	0.72 (6.42)
C_2H_4	1.56 (57.51)	3.81 (51.95)	1.51 (49.92)	5.26 (47.06)
C_3H_6	0.58 (21.56)	2.80 (38.23)	0.84 (27.59)	3.77 (33.74)
C_4H_8	0.33 (12.02)	0.48 (6.57)	-	1.29 (11.54)
C_5H_{10}	0.16 (6.04)	0.08 (1.08)	-	-

Table S3. Product yields and selectivity during catalytic pyrolysis of PE

PE	*In-situ* **He**	*Ex-situ* **He**	*In-situ* $\mathbf{H_2}$	*Ex-situ* $\mathbf{H_2}$
Aromatic hydrocarbon yield/C% (selectivity/%)				
Benzene	4.83 (18.19)	3.34 (30.50)	3.92 (14.71)	1.27 (20.96)
Toluene	10.31 (38.84)	4.80 (43.87)	10.21 (38.29)	2.62 (43.33)
Ethyl-benzene	0.65 (2.45)	0.07 (0.63)	0.71 (2.65)	0.06 (0.96)
p-Xylene	5.29 (19.91)	1.61 (14.68)	6.02 (22.56)	1.16 (19.14)
o-Xylene	1.63 (6.15)	0.44 (3.99)	1.76 (6.62)	0.27 (4.38)
Styrene	–	0.04 (0.32)	-	0.01 (0.12)
Benzene, 1-ethyl-3-methyl	0.96 (3.60)	0.09 (0.80)	0.80 (3.01)	0.11 (1.81)
Benzene, 1,2,3-trimethyl-	0.57 (2.16)	0.10 (0.95)	0.63 (2.37)	-
Indane	0.17 (0.66)	0.06 (0.55)	0.58 (2.16)	0.03 (0.43)
Indene	0.10 (0.39)	0.06 (0.56)	0.26 (0.99)	0.01 (0.23)
1-Methyl-1H-Indene	-	-	-	0.03 (0.58)
Naphthalene	0.53 (1.99)	0.06 (0.56)	0.41 (1.54)	0.02 (0.38)
Naphthalene, 2-methyl-	0.64 (2.43)	0.08 (0.77)	0.79 (2.98)	0.04 (0.73)
1,2-Dimethyl-Napthalene	0.70 (2.63)	0.20 (1.79)	0.57 (2.14)	0.03 (0.49)
Anthracene	0.16 (0.61)	-	-	0.01 (0.13)
2-Methyl Panthracene	–	-	-	0.02 (0.30)
Aliphatic hydrocarbon yield/C% (selectivity/%)				
CH_4	1.27 (2.04)	0.91 (1.05)	2.85 (4.33)	1.42 (1.57)
C_2H_6	2.11 (3.38)	1.07 (1.23)	1.56 (2.37)	0.64 (0.71)
C_3H_8	20.98 (33.56)	2.65 (3.06)	17.40 (26.42)	3.58 (3.94)
C_4H_{10}	13.67 (21.86)	1.47 (1.69)	13.58 (20.61)	2.90 (3.19)
C_2H_4	5.92 (9.47)	25.30 (29.15)	7.45 (11.31)	19.08 (20.98)
C_3H_6	9.39 (15.02)	41.89 (48.26)	12.65 (19.20)	44.94 (49.40)
C_4H_8	5.91 (9.45)	13.14 (15.14)	8.27 (12.56)	18.11 (19.92)
C_5H_{10}	3.27 (5.24)	0.36 (0.42)	2.11 (3.20)	0.28 (0.31)

Table S4. Products yield and selectivity during catalytic pyrolysis of PP

PP	*In-situ* **He**	*Ex-situ* **He**	*In-situ* $\mathbf{H_2}$	*Ex-situ* $\mathbf{H_2}$
Aromatic hydrocarbon C% (selectivity %)				
Benzene	4.81 (18.11)	3.60 (35.30)	4.17 (16.64)	1.18 (22.63)
Toluene	10.17 (38.29)	4.13 (40.52)	9.74 (38.84)	2.47 (47.42)
Ethyl-benzene	0.64 (2.40)	0.03 (0.30)	0.54 (2.16)	0.05 (1.01)
p-Xylene	5.12 (19.29)	1.30 (12.77)	5.33 (21.25)	1.05 (20.21)
o-Xylene	1.57 (5.90)	0.37 (3.64)	1.63 (6.49)	0.24 (4.56)
Styrene	-	-	-	0.01 (0.14)
Benzene, 1-ethyl-3-methyl	0.95 (3.59)	0.05 (0.51)	0.61 (2.43)	0.08 (1.44)
Benzene, 1,2,3-trimethyl-	0.70 (2.64)	0.16 (1.58)	0.54 (2.15)	-
Indane	0.23 (0.88)	0.02 (0.21)	0.49 (1.96)	0.02 (0.38)
Indene	0.25 (0.92)	0.02 (0.17)	0.40 (1.58)	0.01 (0.11)
3-Methyl-1H-Indene	0.00 (0.00)	0.00 (0.00)	-	0.04 (0.73)
Naphthalene	0.49 (1.84)	0.06 (0.57)	0.38 (1.52)	-
Naphthalene, 2-methyl-	1.08 (4.05)	0.11 (1.05)	0.70 (2.79)	0.02 (0.42)
1,2-Dimethyl-Napthalene	0.56 (2.12)	0.14 (1.35)	0.55 (2.21)	0.02 (0.35)
Anthracene	-	0.21 (2.04)	-	-
2-Methyl Panthracene	-	-	-	0.01 (0.20)
Aliphatic hydrocarbon C% (selectivity %)				
CH_4	1.60 (2.60)	1.45 (1.78)	3.06 (4.46)	2.14 (2.33)
C_2H_6	2.78 (4.52)	2.70 (3.31)	2.11 (3.08)	1.42 (1.55)
C_3H_8	21.28 (34.66)	1.71 (2.10)	18.85 (27.51)	2.99 (3.25)
C_4H_{10}	11.95 (19.45)	0.54 (0.66)	12.05 (17.58)	2.51 (2.73)
C_2H_4	6.33 (10.31)	20.15 (24.66)	8.87 (12.94)	17.01 (18.52)
C_3H_6	9.64 (15.69)	41.55 (50.84)	13.33 (19.46)	46.88 (51.06)
C_4H_8	5.74 (9.35)	12.26 (15.00)	7.82 (11.41)	18.09 (19.70)
C_5H_{10}	2.09 (3.41)	1.36 (1.66)	2.43 (3.54)	0.79 (0.86)

CHAPTER 6
CONCLUSIONS AND FUTURE WORK

Conclusions

As an economical way to produce chemicals and fuels from sustainable low-cost feedstock, fast co-pyrolysis of biomass and plastic was studied in this PhD work in order to elucidate the underlying chemicals and physical phenomena occurring during pyrolysis. Overall, co-pyrolysis with plastics reduced the formation of oxygenated compounds from biomass, increasing HHV of bio-oil. The catalytic co-pyrolysis of biomass and plastics promotes the production of high-quality liquid products catalyzed by zeolite catalyst. The co-pyrolysis process can be further optimized through conducting feedstock pretreatment, changing reactant-catalyst contact mode and carrier gases during pyrolysis.

First, a continuous co-pyrolysis of HDPE and red oak was successfully implemented in a bench-scale fluidized bed reactor from 525 ºC to 675 ºC. The yield of pyrolysis oil was optimized at 625 ºC. The presence of 20% HDPE in the feedstock promoted the formation of furans and acids from holocellulose and alkylated phenols from lignin. Water was found to increase during co-pyrolysis, possibly due to the enhanced hydrodeoxygenation reaction of red oak derived oxygenates by hydrogen transfer from HDPE. The yield of pyrolysis char from red oak decreased. The difference of char SEM pictures between red oak-only pyrolysis and co-pyrolysis further suggested the interaction among red oak and melted HDPE.

Second, this study focused on unravelling the thermal synergy and catalytic synergy during the co-pyrolysis of biomass and plastic. The thermal synergy manifested in terms of increased production of light oxygenates from cellulose and phenolic monomers from lignin. Reduction of catalytic coke, carbon oxides and enhancement of aromatic hydrocarbons

production constituted the catalytic synergy. Increase of temperature was found to promote the yield of aromatic hydrocarbons. The catalytic synergy was favored at moderate catalyst temperature and became insignificant at higher catalyst temperature.

This study further investigated the possibility of enhancing the synergistic effects between biomass and plastic. Pretreatment of corn stover by sulfuric acid infusion and leaching processes can significant enhancing the cross-reaction between corn stover and polyethylene. The yield of levoglucosan was found to increase with the co-pyrolysis of acid infused corn stover and polyethylene during non-catalytic co-pyrolysis. The neutralized potassium sulfate as well as lignin components in corn stover catalyzed the cracking of polyethylene chain. The catalytic co-pyrolysis of raw/acid leached/acid infused corn stover and polyethylene further confirmed the contribution of Diels-Alder reaction between furans (dehydration products of levoglucosan) and olefins (depolymerization production of PE) to the synergistic effects.

Finally, four main waste plastics were catalytic pyrolyzed to evaluate their potentials for hydrocarbon production. The product species and distribution heavily depended on the feedstock-catalyst contact mode and plastic types. The difference of product outcomes between *in-situ* and *ex-situ* catalytic pyrolysis indicated different reaction mechanisms existing in these two scenarios. By changing the carrier gas of pyrolysis, hydrogen was found to improve the conversion of hydrogen deficient plastics including PS and PET, while played a much less important role in the hydropyrolysis of PE and PP. Further co-pyrolysis of PE and PS/PET confirmed the hydrogen transfer from PE to these hydrogen deficient plastics, thus improving the overall process performance in terms of enhancing hydrocarbon production and inhibition of catalytic coke formation.

Overall, cross reactions between biomass and plastic were proven in both non-catalytic and catalytic fast co-pyrolysis. The co-pyrolysis with plastics can be considered to improve the performance of biomass conversion technologies, such as increasing stabilized products and valuable chemicals. These finds and improvements further prove the concept and feasibility of processing and recycling Municipal Solid Waste through thermochemical technologies to produce advanced products.

Future work

Work in this dissertation has helped the understanding of interaction during fast co-pyrolysis of biomass and plastic and improve the methods for producing fuels and chemicals from co-pyrolysis process. Such a work is believed to be useful in using waste plastics as additives in biomass conversion to improve bio-oil yield and quality.

However, there are still some controversies about the role of pyrolysis heating-rate in promoting the interaction between plastic and biomass (fast pyrolysis VS. slow pyrolysis). Thus, part of the future work can be done to unravel these controversies by both experimental study and kinetic modeling.

Besides, future research will be focused on realizing the successful pyrolysis-oriented conversion of Municipal Solid Waste based on the current findings. Different from the co-pyrolysis of well-defined plastics and biomass performed in this dissertation work, several issues need to be addressed before successful bench-scale and pilot-scale pyrolysis of MSW. To be able to apply the knowledge gained in this work to real world MSW, pyrolysis and catalytic pyrolysis of other waste streams (waste paper, grass clippings, food waste etc.) should also be evaluated.

Although the major pyrolyzable components of MSW are similar, including organic waste (paper, food waste, yard waste) and plastic waste, the seasonal and regional variations of these components require a more robust reactor design which can achieve stable heat and mass transfer as well as operating conditions regardless of the composition difference.

Furthermore, the inorganic elements in MSW are far more complex than AAEMs mentioned in *Chapter* 4. These elements can include sulfur, nitrogen, chloride and heavy metals like iron, copper, cobalt and mercury. Understanding the catalytic effects and evolution of these elements during pyrolysis is important for predicting the product outcomes as well as preventing the pollutants emission. Evaluation is also needed for the possible catalyst poison by these inorganic elements during catalytic pyrolysis process.